Fisheries New Zealand
Tini a Tangaroa

A climate vulnerability framework for New Zealand marine fisheries

New Zealand Aquatic Environment and Biodiversity Report No. 377.

D.G. Boyce,
D.P. Tittensor,
K.E. Schleit,
S. Fuller

ISSN 1179-6480 (online)

ISBN 978-1-997337-91-1 (online)

September 2026



Te Kāwanatanga o Aotearoa
New Zealand Government

Disclaimer

This document is published by Fisheries New Zealand, a business unit of the Ministry for Primary Industries (MPI). The information in this publication is not government policy. While every effort has been made to ensure the information is accurate, the Ministry for Primary Industries does not accept any responsibility or liability for error of fact, omission, interpretation, or opinion that may be present, nor for the consequence of any decisions based on this information. Any view or opinion expressed does not necessarily represent the view of Fisheries New Zealand or the Ministry for Primary Industries.

Enquiries should be directed to:

Fisheries Science Editor
Fisheries New Zealand
Ministry for Primary Industries
PO Box 2526
Wellington 6140
NEW ZEALAND

Email: Fisheries-Science.Editor@mpi.govt.nz
Telephone: 0800 00 83 33

This publication is also available on the Ministry for Primary Industries websites at:
http://www.mpi.govt.nz/news-and-resources/publications
http://fs.fish.govt.nz go to Document library/Research reports

© Crown Copyright – Fisheries New Zealand

Please cite this report as:

Boyce, D.G.; Tittensor, D.P.; Schleit, K.E.; Fuller, S. (2026). A climate vulnerability framework for New Zealand marine fisheries. *New Zealand Aquatic Environment and Biodiversity Report No. 377.* 113 p.

TABLE OF CONTENTS

1 EXECUTIVE SUMMARY 1

2 Introduction 2

3 Climate vulnerability in marine systems and the CRIB: an overview 5

4 CRIB-NZ: A climate vulnerability framework for New Zealand fisheries 8

4.1 CVA priorities 8
4.1.1 A CVA for New Zealand 9
4.1.2 High resolution outputs 9
4.1.3 Scenario-specific outputs 9
4.1.4 The inclusion of bottom-associated species 9
4.1.5 Vulnerability across life stages 11
4.2 Input data layers 12
4.2.1 Species native geographic distribution 13
4.2.2 Species thermal niches 14
4.2.3 Species conservation status 16
4.2.4 Species' maximum body lengths 17
4.2.5 Historical and present-day temperatures 17
4.2.6 Projected temperatures 19
4.2.7 Cumulative impacts 21
4.3 Analyses 22
4.3.1 Climate Sensitivity 26
4.3.2 Climate exposure 33
4.3.3 Adaptive capacity 40
4.3.4 Climate vulnerability 45

5 Results 49

5.1 Climate vulnerability across the New Zealand Exclusive Economic Zone 49
5.2 Climate vulnerability across FMA 5 (Southland) 52
5.3 Contrasted vulnerability for pāua 55
5.4 The importance of distribution to CRIB-NZ 57

6 Interpreting CRIB-NZ outputs 60

6.1 Climate vulnerability 60
6.2 Climate risk 61

7 Acknowledgements 62

8 References 62

Appendix A: Vulnerability across life stages 86

Appendix B: Extended data **87**

B.1 Species geographic distributions 87

Appendix C: Extended methods **88**

C.1 Climate Sensitivity 88
C.1.1 Thermal safety margins 88
C.1.2 Vertical habitat use 88
C.1.3 Cumulative impacts 89
C.2 Climate Exposure 89
C.2.1 Time of climate emergence 89
C.2.2 Ecosystem disruption 89
C.2.3 Loss of suitable thermal habitat 90
C.2.4 Marine heatwaves 90
C.3 Adaptive capacity 91
C.3.1 Geographic range extent 91
C.3.2 Habitat fragmentation 92
C.3.3 Thermal habitat variability and use 92
C.3.4 Maximum body length 93
C.4 Discount rates 93
C.5 Spatially explicit vulnerability 94
C.6 Spatially implicit vulnerability 95

Appendix D: Practical applications of vulnerability from Canada **96**

D.1 Marine fisheries 96
D.2 Conservation and marine spatial planning 97

Appendix E: CRIB-NZ technical workflow **98**

E.1 Data extractions 99
E.1.1 AquaX species traits and distributions 99
E.1.2 GLORYs temperature data 99
E.1.3 CMIP 6 temperature projections 100
E.2 Statistical computing and R code 100

Appendix F: Supplementary Tables **105**

PLAIN LANGUAGE SUMMARY

- Climate change is warming New Zealand's oceans and increasing the frequency and intensity of marine heatwaves, impacting marine species and creating challenges for fisheries management.
- This report presents the Climate Risk Index for Biodiversity-New Zealand (CRIB-NZ), a framework developed to assess the climate vulnerability of New Zealand marine fish and invertebrate species.
- The framework combines information on species biology, climate change exposure, sensitivity, and adaptive capacity to evaluate climate vulnerability.
- CRIB-NZ uses climate projections and spatial data to estimate how marine species vulnerability may vary across different parts of New Zealand's marine environment.
- The framework can assess both surface-dwelling and bottom-dwelling species, making it relevant to a broad range of New Zealand fisheries.
- An end-to-end example using yellowtail kingfish is provided to demonstrate how the framework operates, from data inputs through to vulnerability outputs.
- Eight case-study species were also assessed to illustrate the types of outputs generated by CRIB-NZ and how they can be interpreted and applied.
- Results show that climate vulnerability can vary considerably among species and regions.
- Moving forward, successfully implementing CRIB-NZ will require additional vetting of the input data, specifically the reliability of geographic distribution data for New Zealand species.
- The framework can be applied under different climate scenarios and future time periods to explore how vulnerability may change over time.
- CRIB-NZ provides information that can support fisheries management and climate adaptation planning by identifying species and regions that may be most vulnerable to climate change.

EXECUTIVE SUMMARY

Boyce, D.G.[1]; Tittensor, D.P.[2]; Schleit, K.E. [3]; Fuller, S. [3] (2026). A climate vulnerability framework for New Zealand marine fisheries.

***New Zealand Aquatic Environment and Biodiversity Report No 377.* 113 p.**

Climate change is already affecting marine ecosystems in Aotearoa, New Zealand, and is projected to intensify throughout the twenty-first century. Rising ocean temperatures, marine heatwaves, changing oceanographic conditions, and shifts in species distributions are expected to alter the productivity, resilience, and sustainability of fisheries resources. These changes present important challenges for fisheries management, conservation, and the communities that depend on marine ecosystems. As climate impacts continue to emerge, there is an increasing need for tools to identify which species, stocks, and regions are most vulnerable and which factors drive vulnerability to support fisheries management under climate change.

This report describes the development of CRIB-NZ, a climate vulnerability assessment framework designed for New Zealand fisheries. The framework was developed as part of Fisheries New Zealand project ZBD2024-04 and builds upon the Climate Risk Index for Biodiversity (CRIB), a spatially explicit framework previously applied to marine ecosystems at global and regional scales. Prior to developing CRIB-NZ, an extensive review of international climate vulnerability assessment approaches was undertaken to identify best practices and evaluate existing frameworks for their applicability to New Zealand fisheries. The CRIB framework was selected for this application because of its flexibility, transparency, reproducibility, and ability to generate spatially explicit estimates of vulnerability.

Following consultations with Fisheries New Zealand, several adaptations were made to tailor the framework to New Zealand fisheries. These included the incorporation of New Zealand-specific environmental and biological datasets and projections, the development of high-resolution spatial analyses, and the extension of the framework to evaluate both surface- and bottom-associated species using sea-surface and bottom temperatures. The framework is designed to evaluate vulnerability under alternative greenhouse gas emission scenarios and over past and future time horizons, and to provide outputs relevant to fisheries management scales.

The adapted CVA—CRIB-NZ—evaluates climate vulnerability as the interaction of three dimensions: sensitivity, exposure, and adaptive capacity. These dimensions are captured using twelve standardised climate vulnerability indices that integrate information on species biology, ecology, habitat use, conservation status, anthropogenic pressures, and past and projected climate changes. The indices were selected based on their scientific justification, broad acceptance in previous studies, ability to capture climate impacts across diverse marine taxa, and ability to provide complementary information while minimizing redundancy. For temperature-related indices, CRIB-NZ assumes that climate vulnerability increases continuously with increasing temperature. This assumption is intended to capture the increasing risk of a species approaching or exceeding its upper thermal limits, rather than representing variation in fitness within its thermal niche. Together, they provide a comprehensive and multifaceted representation of the processes through which climate change may affect marine species and fisheries. To demonstrate the implementation of the framework, an end-to-end worked example is presented using yellowtail kingfish (*Seriola lalandi*), illustrating the complete workflow

[1] Wild Ocean Research, Cow Bay, Nova Scotia, Canada

[2] Dalhousie University, Halifax, Nova Scotia, Canada

[3] Oceans North, Halifax, Nova Scotia, Canada

from data inputs and index calculation through to the generation and interpretation of climate vulnerability outputs.

The functionality of the CRIB-NZ framework is demonstrated through eight case-study species spanning a range of taxonomic groups, habitats, and ecological characteristics. The results of these case studies should not be interpreted as final; rather an illustration of how the framework operates, including how input data are processed and how outputs can be visualised, interpreted, and used to assess climate vulnerability in fisheries. The examples show how vulnerability can vary among species, across geographic regions, and under alternative future climate scenarios. Outputs include maps of climate vulnerability, sensitivity, exposure, and adaptive capacity, as well as supporting climate indicators that help explain the mechanisms through which climate change may affect species and fisheries. Together, the case studies highlight the framework's ability to identify vulnerable species, locations, and climate-impact pathways while generating information relevant to fisheries management and adaptation planning. However, additional vetting of the input data is required before the outputs are deemed accurate for use in fisheries management, especially for species' spatial distribution.

CRIB-NZ provides Fisheries New Zealand with a flexible, scientifically defensible, and scalable framework for incorporating climate change considerations into fisheries assessment, management, monitoring, and strategic planning. The framework can support the prioritization of vulnerable species and fisheries, guide climate adaptation efforts, identify research and monitoring needs, and contribute to climate-informed decision-making. CRIB-NZ is not intended to replace traditional fisheries stock assessments or existing management processes. Rather, it is designed to complement these approaches by providing information on climate vulnerability and its underlying drivers, helping to place fisheries status and management decisions within the broader context of climate change. As additional ecological, environmental, and socioeconomic information becomes available, CRIB-NZ can be expanded and refined, providing a foundation for the long-term integration of climate change considerations into the sustainable management of New Zealand's marine fisheries.

1 Introduction

This work is part of a Fisheries New Zealand project (ZBD2024-04) to develop a climate vulnerability assessment (CVA) framework to guide the management of New Zealand's fisheries. This project was created to address Fisheries New Zealand's interest in predicting the impacts of climate change on fisheries and aquatic ecosystems to support adaptation. The outputs provide a framework for prioritizing key species or stocks for further management or research and add to the evidence base for existing management decisions. This represents a first step towards an organised and proactive approach to managing the risk of climate change impacts on our fisheries. The three objectives of this project include:

Objective 1: To review available international approaches to climate change vulnerability assessments for fisheries and identify existing frameworks that could be adapted for use in New Zealand.

Objective 2: To develop a climate vulnerability assessment framework for New Zealand's fisheries that can be applied to any fishery or region, along with a user guide.

Objective 3: To demonstrate the vulnerability framework's operation by applying it to a priority fishery or region.

At the project outset, it was agreed that the vulnerability framework for New Zealand (NZ) would be an adaptation of the Climate Risk Index for Biodiversity (CRIB)—a published framework that evaluates climate vulnerability and risk for marine species and ecosystems in a quantitative, flexible, spatially explicit manner (Boyce et al. 2022, 2023, 2024). Following the review of CVA approaches (objective 1, above) (Boyce et al. 2025), a series of meetings was held with Fisheries New Zealand,

during which participants provided input on adapting the CRIB framework for New Zealand fisheries. Key elements identified as priorities included:

Priority 1: Tailoring the CVA for New Zealand through the identification of nationally, locally, or regionally appropriate input information wherever possible.

Priority 2: The ability to evaluate vulnerability at high spatial resolutions. Previous CRIB implementations estimated vulnerability at intermediate spatial resolutions, including 1° and 0.25°. Following participant input, this adaptation explores new input data layers that could be used to generate high-resolution, spatially resolved vulnerability estimates for New Zealand.

Priority 3: The ability to evaluate vulnerability over medium- and long-term future horizons (e.g. 2050), under middle-of-the-road emission scenarios (SSP2-4.5 and SSP3-7.0).

Priority 4: The ability to include bottom-associated species. Previous CRIB implementations estimated the vulnerability and risk of species that spend significant time in the epipelagic zone (e.g. the upper 200 m) based on sea surface temperatures (Boyce et al. 2022, 2023, 2024; Keen et al. 2023; Lewis et al. 2023; Boyce et al. 2024b). To enhance relevance to fisheries, participants requested that the CVA framework be extended to include bottom-associated species that exclusively inhabit deeper waters, using bottom-temperature measurements or estimates.

Priority 5: Marine heatwaves (MHWs) are an emerging climate hazard in New Zealand (Cook et al. 2025). Participants requested that MHW information be taken into account in the New Zealand CVA.

Priority 6: The participants requested an assessment of the feasibility of evaluating vulnerability across species' life stages. Consistent with virtually all published CVAs, the CRIB evaluates vulnerability only during adulthood.

Additional priorities were discussed, including consideration of social and economic factors and climate stressors beyond temperature. However, additional project funding would be required to sufficiently address these priorities, as they were outside this project's time and budgetary constraints. This report discusses the CRIB-adapted CVA framework for New Zealand's marine fisheries, hereafter referred to as CRIB-NZ, including the revised framework methodology and potential input data sources to incorporate the identified priorities. Meeting participants also discussed how CRIB-NZ would be applied to a priority fishery or region to demonstrate its functioning (objective 3, above). It was requested that it be applied across Fisheries Management Area 5 (Southland) to the following eight case-study species:

1. **Yellowtail kingfish *(Seriola lalandi*):** Yellowtail kingfish, or amberjack, is a large, fast-swimming benthopelagic/pelagic predator associated with reefs, islands, kelp beds, and coastal-to-oceanic waters. It is highly mobile, important to recreational fisheries, and supports commercial and aquaculture interests in parts of its range. FishBase lists it as benthopelagic with a depth range between 3 and 825 m.
2. **Red gurnard *(Chelidonichthys kumu):*** Red gurnard is a medium-sized demersal fish found on sandy and muddy bottoms in coastal New Zealand waters; FishBase lists it as demersal from about 1–200 m, usually 75–150 m. It is commercially important in New Zealand and is often taken in inshore trawl fisheries.
3. **Blue cod *(Parapercis colias):*** Blue cod is a New Zealand endemic, bottom-dwelling demersal fish common on rocky coastal habitats, especially around the South Island and

Chatham Islands; Fisheries New Zealand describes it as occurring to about 150 m depth and growing up to about 60 cm. It is an important recreational and commercial species.

4. **Blue moki *(Latridopsis ciliaris*):** Moki is a coastal benthopelagic fish that occurs primarily over rocky reefs, kelp forests, and adjacent soft-bottom habitats. It is commonly found in shallow to mid-depth waters (approximately 10–150 m). Blue moki are relatively long-lived, slow-growing fishes that form spawning aggregations and undertake seasonal movements between feeding and spawning grounds.
5. **Red cod *(Pseudophycis bachus):*** Red cod is a demersal species usually found on soft muddy or sandy bottoms, and also occurring on rocky bottoms, bays, estuaries, and the continental shelf; FishBase notes that it can exceed 700 m but is abundant around 200–300 m in New Zealand. It is commercially harvested mainly by bottom trawl and is also taken as bycatch in deeper fisheries.
6. **Rock lobster *(Jasus edwardsii*):** Red rock lobster is a benthic spiny lobster found around mainland New Zealand and offshore islands, occupying rocky reef and crevice habitats, commonly in shallow coastal waters but also deeper. It supports one of New Zealand's major high-value invertebrate fisheries, with both ecological and cultural importance.
7. **Blackfoot pāua (*Haliotis iris*):** Pāua is a benthic abalone/gastropod endemic to New Zealand rocky shores, especially shallow subtidal reef habitats. It is benthic, occurring at depths of 0–20 m. It supports important customary, recreational, commercial, and aquaculture sectors, but local populations can be sensitive to harvest pressure and environmental disturbance.
8. **School shark (*Galeorhinus galeus*)**: School shark, also known as tope shark, is a wide-ranging demersal to pelagic coastal shark found around New Zealand's continental shelf and upper slope, from shallow waters to a depth of several hundred metres. It is a mobile predator and scavenger, has slow life-history traits typical of many sharks, and supports commercial fisheries, often as part of mixed inshore and mid-depth fisheries. FishBase notes that it is benthopelagic, with a depth range of 0–1100 m.

This report describes the development of CRIB-NZ, including the revised methodology, potential input data sources, and illustrative examples using the case study species. The report begins with an overview of CVAs in marine systems, including the CRIB framework. Then, it summarises the high-level adaptations made to produce CRIB-NZ, including whether and how the identified priorities were accommodated. Next, the data sources used to generate vulnerability outputs for the eight case-study species are described. Following this, the CRIB-NZ analyses are presented using one of the case study species (yellowtail kingfish, *Seriola lalandi*) as an example to illustrate the workflow and methodology. Next, the CRIB-NZ outputs for the case study species are presented under the two requested emission scenarios (SSP-2.45 and SSP-3.70) to demonstrate how the results can be visualised and interpreted. To keep the main report concise, many of the technical details of the CVA, including mathematical equations, technical data, and code descriptions, are included in an appendix as a user guide (objective 2, above). The appendix also describes efforts to incorporate life-stage analysis into the CVA and provides examples of CVA applications undertaken using the CRIB in Canada. Whereas CRIB-NZ estimates vulnerability, the report also discusses how the CRIB framework can estimate risk, which can complement vulnerability and be useful when actioning CVA outputs.

The work builds on the information summarised in ZBD2014-09 (Cummings et al. 2021) and ZBD2022-02A; (Behrens et al. 2025; Cook et al. 2025), as well as prior work investigating the impacts of climate change on fished populations (ZBD2018-03).

2 Climate vulnerability in marine systems and the CRIB: an overview

CVAs are increasingly seen as a critical component of climate-informed management of species and ecosystems (Busch et al. 2016; Hare et al. 2016; FAO, 2018). Hundreds of CVAs have been developed across different scales and systems, using various approaches (e.g. trait-based, correlative, mechanistic modelled, theoretical) (Pacifici et al. 2015; de los Ríos et al. 2018; Foden et al. 2019). This has led to a broad consensus on what elements define vulnerability. Following an early IPCC definition (IPCC, 2001, 2014) and subsequent adoption (Foden et al. 2013, 2019; Pacifici et al. 2015; Comte & Olden, 2017; de los Ríos et al. 2018; Albouy et al. 2020), a species' climate vulnerability is defined by its sensitivity, exposure, and adaptive capacity (adaptivity) to climate change. Sensitivity refers to the propensity for a species to be adversely affected by its exposure to climate change. Exposure refers to the extent to which species are subjected to hazardous climate change, including the magnitude of the effects. Adaptivity is a species' ability to cope with the adverse effects of climate change. In the aggregate, CVAs aim to address overarching questions about the effects of climate change on species and ecosystems, namely: *which* species and ecosystems are most vulnerable, *where* they are most vulnerable, *when* they become vulnerable, and *why* they are vulnerable, as well as identifying gaps in data and information needed to more completely understand the impacts of climate change on marine life.

Despite the interest in defining and assessing climate vulnerability (de los Ríos et al. 2018; Foden et al. 2019) CVA methods have not been consistently applied across species, locations, geographic scales, or time. Further, climate vulnerability assessments are not yet routinely used in applied marine management settings, such as marine fisheries (Pacifici et al. 2015; Boyce et al. 2024). Vulnerability studies often incorporate qualitative or semi-quantitative expert opinions, such as species rankings, rather than quantitative approaches, have been locally or regionally focused (Pacifici et al. 2015; de los Ríos et al. 2018; Foden et al. 2019), and infrequently incorporate all dimensions that define vulnerability (sensitivity, exposure, and adaptivity). For instance, a review of 743 climate change vulnerability studies (de los Ríos et al. 2018) reported that only 11% had considered all three vulnerability dimensions, while another review (Pacifici et al. 2015) reported that only 4% of assessments were global. CVAs also frequently report vulnerability as relative scores and rankings, which could limit their uptake and application in management settings.

The Climate Risk Index for Biodiversity (CRIB) was developed to integrate the diverse knowledge accumulated in climate impact studies and CVAs (Foden et al. 2013, 2019; Pacifici et al. 2015; de los Ríos et al. 2018) into a unified framework for assessing both relative climate vulnerability and absolute climate risk, helping to fill some of these existing gaps (Boyce et al. 2022, 2024). It enables the vulnerability and risk of marine species to be evaluated at all locations across their geographic distributions in a quantitative, reproducible, consistent, and standardised manner, can be applied at scales from local to global, can incorporate new information as it becomes available, is transparent, and evaluates the statistical uncertainty of estimated vulnerability and risk. The framework provides a method for translating relative vulnerability scores and rankings into definitive risk categories for species and ecosystems, aiding the management and conservation of marine ecosystems under climate change.

To support its ongoing development, use, uptake, and reliability, the CRIB was designed to be generalised, adaptable, and scalable, using climate-vulnerability indicators that operate consistently across species with diverse taxonomies and life histories, while remaining flexible enough to incorporate new climate-relevant information as it becomes available. It uses quantitative, transparent, and reproducible methods to calculate adaptive capacity, sensitivity, and exposure, drawing on multiple complementary indices spanning trait-based, correlative, and mechanistic approaches across species, ecosystem, and climate dimensions. Vulnerability metrics are standardised through consistent statistical transformations and scaling procedures, enabling comparisons across species, ecosystems, and spatial scales, from local to global assessments. The framework emphasises practical, parsimonious, and interpretable methods by integrating publicly available, peer-reviewed data using

information-efficient approaches that maximise insight into climate vulnerability while minimizing unnecessary complexity.

Climate change impacts on species can be complex and synergistic (Scheffers et al. 2016). Therefore, much like the similarly holistic concept of health, climate vulnerability or risk can't be adequately defined by a single index or dimension. CRIB defines vulnerability hierarchically; it is calculated from its three dimensions (sensitivity, exposure, and adaptivity) (IPCC, 2014), each of which is derived from four climate indices (12 total), which in turn are calculated using data layers and ecological theory (Table F1 and Table F2). These climate indices were selected based on pre-defined criteria, prioritizing those grounded in ecological theory, widely accepted, and validated through peer review and publication. Indices were restricted to those where the mechanism of climate change effects was widely accepted and well-documented in existing climate change vulnerability studies (Loarie et al. 2009; Mora et al. 2013; Halpern et al. 2015; Stuart-Smith et al. 2015; Henson et al. 2017; Pinsky et al. 2019; Trisos et al. 2020; IUCN, 2021). Indices were also chosen to maximise their unique information content and minimise redundancy; their uniqueness was evaluated by assessing collinearity and conducting sensitivity analyses. Indices that were easy to interpret and calculate (e.g. parsimonious) were prioritised. The CRIB is a 'combined approach' to CVA (Pacifici et al. 2015; de los Ríos et al. 2018; Foden et al. 2019); it incorporates abiotic, biotic, and human pressures across multiple biological organisation levels (species to ecosystems). Following most previous CVAs (Foden et al. 2013, 2019; Pacifici et al. 2015; Stortini et al. 2015; Comte & Olden, 2017; de los Ríos et al. 2018; Greenan et al. 2019; Albouy et al. 2020), the CRIB uses temperature as the primary indicator of climate change, even though it may not capture all climate impact pathways (McHenry et al. 2019). Temperature is widely available across historical and future periods at high spatiotemporal resolution, and there is a greater understanding of its effects on species than of other climate variables (Scheffers et al. 2016; Boyce et al. 2020a).

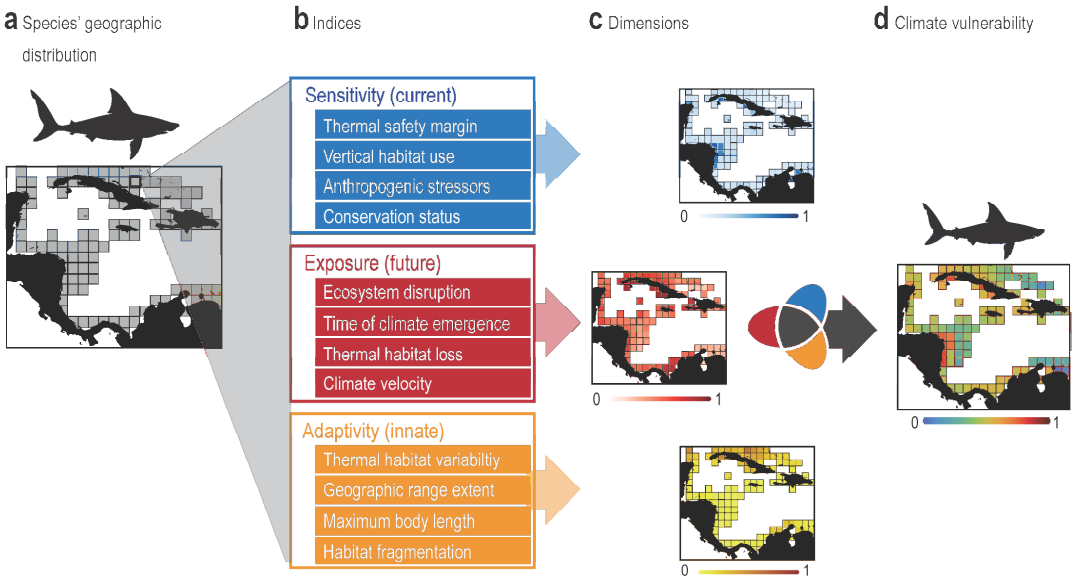


Figure 1*:* Spatially explicit CRIB framework. Within each grid cell across the native geographic distribution of a species (a), 12 standardised climate indices are calculated (b) and used to define the three dimensions of climate vulnerability (c): present-day sensitivity (blue), projected future exposure (red), and innate adaptivity (yellow). The dimensions are used to calculate the species' climate vulnerability (d). Figure taken from (Boyce et al. 2022)**.**

The flow of input data into the CRIB index calculation is depicted in Figure 2 and the 12 standardised indices used are in Table F1 and the input data used are in Table F2. The input data for the first global CRIB analysis are fully described by Boyce et al. (2022, 2024). All analyses to calculate the CRIB were undertaken using the R statistical computing platform (version 4.5 (R Core Team & R Team, 2024) and are available through a publicly available GitHub repository[4].

[4] https://github.com/danielgboyce/DFO-NCR-Climate-Risk-2024

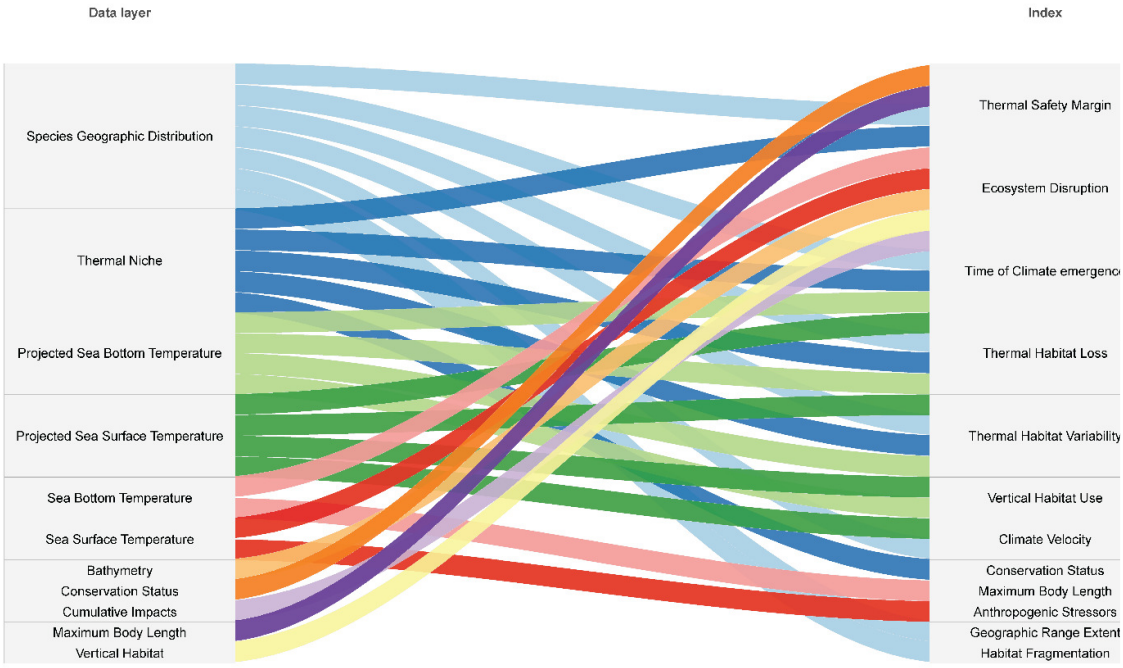


Figure 2*:* Flow of input data into index calculation. Visual depiction of which of the 11 input data layers (left) are used to calculate each of the 12 standardised climate indices (right). Colours depict the type of input data layer.

The CRIB has assessed climate risk for approximately 25 000 species globally (Boyce et al. 2022), for fish stocks across the northwest Atlantic (Boyce et al. 2024), for spatial planning across the Canadian exclusive economic zone (Lewis et al. 2023; Keen et al. 2024), harvested species within the Northwest Atlantic Fisheries Organization convention area (Boyce et al. 2026) and for freshwater species in the Canadian Maritimes (Shin, 2023) and has been cited as an emerging approach to CVA in marine fisheries (Braun et al. 2026; Farchadi et al. 2026). Together, these studies demonstrate that the CRIB can draw on diverse input data sources and be flexibly tailored to different situations and users.

3 CRIB-NZ: A climate vulnerability framework for New Zealand fisheries

3.1 CVA priorities

The CRIB was adapted for New Zealand based on six key elements identified by participants as priorities. The elements and their outcomes are listed in Table 1 and are discussed below.

Table 1: Overview of identified CVA priorities and their outcomes for the New Zealand application.

N	CVA Priority	Outcomes
1	NZ-specific data and information	Successful: included regional New Zealand earth system model projections and national stock assessment information.
2	High-resolution spatially explicit outputs	Successful: increased spatial resolution from 0.25° to 0.083°.
3	Scenario-specific outputs	Successful: CVA can be run under any user-specified emission scenario.
4	Inclusion of surface- and bottom-associated species	Successful: revised methods and input data to accommodate bottom-associated species.
5	Inclusion of marine heatwave information	Successful: developed a new indicator of marine heatwave duration and intensity.
6	Vulnerability across life stages	Unsuccessful: input data and information required to assess early life stage vulnerability were lacking. Refer to the appendix for further information.

3.1.1 A CVA for New Zealand

As much as possible, input data layers were replaced with those more suitable to the New Zealand context. This included projections from regional climate models and nationally developed estimates of species conservation status (see input data layers section, below). The feasibility of using additional data sources from within New Zealand, such as species distribution models, was also explored.

3.1.2 High resolution outputs

Previous CRIB implementations estimated vulnerability at intermediate spatial resolutions, including 1° and 0.25°. To produce high-resolution CVA outputs, all spatial data layers, including species geographic distributions, historical and projected sea surface and bottom temperatures, bathymetry, and cumulative impacts, were replaced with high-resolution sources (see input data layers section, below), enabling geographic patterns in vulnerability to be better resolved.

The CRIB-NZ case study analysis was conducted at 1/12° (0.083°) resolution, to match the native resolution of the historical bottom temperature data (Table 2). Whereas surface temperatures have longer decorrelation scales (e.g. the distance over which observations remain significantly correlated with one another) and are relatively straightforward to regrid, bottom temperatures have shorter decorrelation scales and are therefore much more challenging to regrid reliably. To avoid regridding bottom temperature data and potentially introducing bias, the analysis of case-study species was conducted at the native resolution of the bottom temperature data.

3.1.3 Scenario-specific outputs

The ability to evaluate vulnerability over different future horizons and emission pathways. In the case studies presented here, vulnerability is evaluated to 2100 under two middle-of-the-road emission scenarios (SSP2-4.5 and SSP3-7.0). To achieve this, temperature projections from an ensemble of two global and one regional Earth System Models were used (see the input data layers section below).

3.1.4 The inclusion of bottom-associated species

Previous CRIB implementations estimated the vulnerability and risk of species that spend significant time in the epipelagic zone based on sea surface temperatures (Boyce et al. 2022, 2023, 2024; Keen et al. 2023; Lewis et al. 2023; Boyce et al. 2024b). To enhance relevance to fisheries, participants requested that the analyses be extended to include species that exclusively inhabit deeper waters. To achieve this, high-resolution time series of surface and bottom temperatures, as well as projections, were sourced. Following this, species are separated into those that reside exclusively on the seafloor

('bottom-dependent') and those that depend on the upper ocean (upper 50 m) for some portion of their life— for instance, diel migrations, seasonal shoaling, spawning events, feeding, or other upward vertical movements ('surface-dependent'). Climate vulnerability of bottom-dependent species was assessed using seafloor temperatures, and that of surface-dependent species using sea surface temperatures. Species were categorised as either surface- or bottom-associated using logic rules based on their full taxonomies, minimum and maximum depths of occurrence, and vertical habitat classifications extracted from FishBase and SeaLifeBase as follows:

Surface-associated:

1. Any species with a vertical habitat categorised as pelagic, pelagic-neritic, or pelagic-oceanic. or
2. Any non-sessile species with a vertical habitat categorised as benthic, demersal, bathydemersal, benthopelagic, reef-associated, or bathypelagic that has a minimum depth of occurrence of less than 50 m.

Bottom associated:

1. Any species with a vertical habitat that is categorised as sessile.
2. Any species with a vertical habitat categorised as benthic, demersal, bathydemersal, or reef-associated that has a minimum depth of occurrence of greater than 50 m.
3. Any taxonomic group (e.g. phyla, class, order, species) that can be reliably identified as living entirely on or in the seafloor with limited vertical mobility, including:
    i. Any species in the following phyla: Porifera, Placozoa, Gnathostomulida, Entoprocta, Phoronida, Brachiopoda, Siphuncula, Priapulida, Kinorhyncha, Loriciferan, Xenacoelomorpha, Echinodermata.
    ii. Any species in the following classes: Anthozoa, Staurozoa, Polyplacophora, Scaphopoda, Caudofoveata, Solenogastres, Enteropneusta, Pterobranchia, Ascidiacea, and Pycnogonida.
    iii. Any species in the following order: Platyctenida, Tanaidacea, Cumacea.
    iv. Any species whose common name contained the following text strings: lobster, crab, clam, starfish, seastar, urchin, worm, cucumber, dollar, pāua, abalone, cockle, scallop, chiton, hare, limpet, oyster, mussel, conch, geoduck, anemone, quahog, crayfish, snail, mud shrimp, barnacle, stargazer, whelk, slug, frogfish.

The application of this classification system to the eight case study species is illustrated in Figure 3. Under these rules, many species that are primarily bottom-dwelling (e.g. benthic, demersal) are categorised as surface-associated if they are vertically mobile and range into the upper 50 m. This might at first seem counterintuitive. For instance, species distribution models (SDMs), including those used here, commonly estimate the distribution of benthic and demersal species using seafloor temperatures. However, this is a key difference between SDMs and CVAs. Species distribution models rightly focus on where species spend *most* of their time, whereas CVAs focus on where species spend *any* part of their time. Understanding where species spend most of their time is useful for predicting where they are most likely to be found, but it would produce biased estimates of climate vulnerability. For instance, while school sharks (*Galeorhinus galeus*) are demersal, spending most of their time near the seafloor, they also migrate to surface waters to feed on pelagic prey, where they are exposed to different, often more extreme, climate conditions. Assessing school shark vulnerability to seabed temperatures alone would underestimate it, as it would fail to account for their exposure to warming during vertical migrations. To avoid this bias, CVAs must assess the vulnerability of marine species to the most acute climate conditions they experience, rather than those they most commonly experience. For this reason, the logic rules outlined previously allow the vulnerability of species that spend any portion of their time in the uppermost pelagic zone to be assessed against surface temperatures, while those spending the totality of their lives at the seabed are assessed against seabed

temperatures. Those that did not exclusively inhabit the seabed and did not inhabit any portion of the pelagic zone (e.g. vertically migrating mesopelagic species, such as lanternfishes) are excluded.

Practically, the difference between being assessed as surface- versus bottom-associated would diminish along the bathymetric gradient. For instance, in shallow benthic systems, the difference between surface and bottom temperatures is generally much smaller than in abyssal ones.

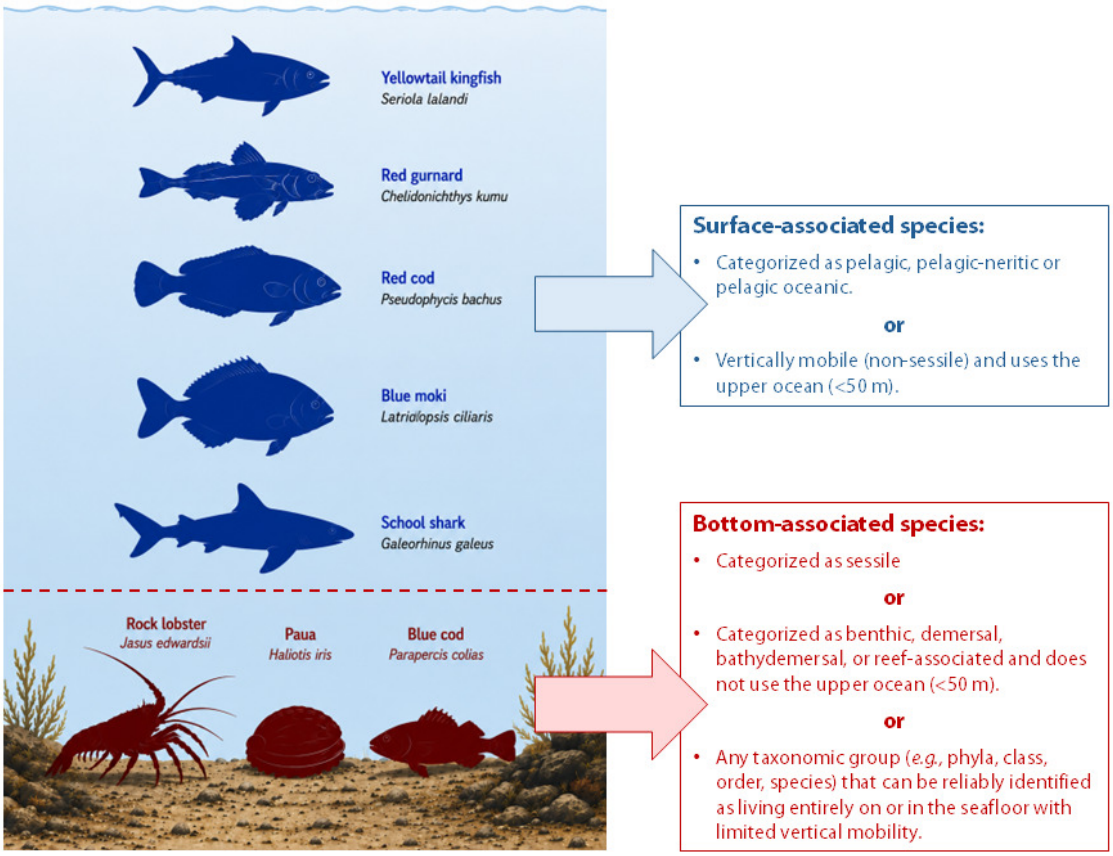


Figure 3: Vertical habitat categorization of marine species. Case study species are categorised as surface- (blue) or bottom- (red) associated, based on their habitat, depth distribution, and vertical mobility. Surface-associated species vulnerability is assessed relative to surface conditions, and bottom-associated species vulnerability is assessed relative to bottom conditions.

3.1.5 Vulnerability across life stages

Consistent with virtually all published CVAs, the CRIB evaluates vulnerability only during adulthood. However, because early-life-stage dynamics are critical to fisheries assessment, Fisheries New Zealand requested an assessment of the feasibility of evaluating vulnerability across species' life stages. The vulnerability during juvenile life stages is a known uncertainty in CVAs. Adults are more frequently studied than larvae or juveniles, and thus their geographic distributions, trait information, and overall responses to environmental and climate variability are far better understood. The paucity of data and peer-reviewed studies on the climate vulnerability of species' early life stages has impeded the development of CVAs for these stages. This is unfortunate, as early life stages can sometimes be more climate-vulnerable than adults, creating 'thermal bottlenecks' (Dahlke et al. 2020). Seeking to address this gap, two approaches to evaluating the vulnerability of early life stages within an adapted CRIB framework for New Zealand were explored (refer to Appendix A: Vulnerability across life stages).

3.2 Input data layers

CRIB-NZ relies on 11 input data layers that can be flexibly sourced. To demonstrate the CRIB-NZ for the case study species, we sourced input data that met the requested criteria (e.g. Section 3.1: CVA priorities), and were readily available and feasible to implement within the time and budgetary constraints of this project (Table 2). As the CRIB-NZ is a flexible framework, these input data layers could feasibly be replaced with alternative sources.

Table 2: Data sources used in the New Zealand-adapted CRIB run (CRIB-NZ).

N	Variable	Type	Source	Temporal	Spatial	References
1	Species native geographic distribution	Taxonomic, spatial	AquaX		0.05°	(Reygondeau et al. 2026)
2	Conservation status	Taxonomic	MPI probability of overfishing	-	-	Fisheries New Zealand
3	Vertical habitat use	Taxonomic	FishBase, SeaLifeBase, AquaX	-	-	(Pauly et al. 2000; Palomares & Pauly, 2022; Reygondeau et al. 2026)
4	Maximum body length	Taxonomic	Marine Organism Body Size Database (MOBS)	-	-	(McClain et al. 2025)
5	Thermal niche	Taxonomic	AquaX		-	(Reygondeau et al. 2026)
6	Bathymetry	Spatial	Copernicus GLORYS static fields	-	~0.08°	(Jean-Michel et al. 2021)
7	Sea surface temperature	Spatiotemporal	Global Ocean Reanalysis (GLORYS)	Monthly; 1993-2025	~0.08°	(Jean-Michel et al. 2021; Copernicus Marine Service, 2023; Drevillon & Gues, 2023)
8	Projected sea surface temperature	Spatiotemporal	Coupled Model Intercomparison Project Phase 6 (CMIP6)	1850-2100	0.25°	(Eyring et al. 2016; Sein et al. 2018; Voldoire et al. 2019)
			New Zealand Earth System Model (NZESM)	Monthly; 2015-2100	~0.08°	(Williams et al. 2016; Behrens et al. 2020)
9	Sea bottom temperature	Spatiotemporal	Global Ocean Reanalysis (GLORYS)	Monthly; 1993-2025	~0.08°	(Jean-Michel et al. 2021; Copernicus Marine Service, 2023; Drevillon & Gues, 2023)
10	Projected sea bottom temperature	Spatiotemporal	Coupled Model Intercomparison Project Phase 6 (CMIP6)	1850-2100	0.25°	(Eyring et al. 2016)

			New Zealand Earth System Model (NZESM)	Monthly; 2015-2100	~0.08°	(Williams et al. 2016; Behrens et al. 2020)
11	Cumulative impacts	Spatial	Cumulative human impact index	-	1km^2	(Halpern et al. 2008, 2012, 2015)

3.2.1 Species native geographic distribution

In previous CRIB iterations (Boyce et al. 2022, 2024), the native geographic distributions of each species were acquired from the AquaMaps (Kaschner et al. 2019) on a native global 0.5° grid. To generate high-resolution vulnerability outputs, an alternative is needed that produces robust, high-resolution estimates of species distributions for many marine species.

The AquaX framework is a next-generation ensemble species distribution modelling approach that builds off of AquaMaps (Reygondeau et al. 2026). It predicts present-day marine species distributions using an integrated ecological niche modelling pipeline that combines standardised taxonomic information, cleaned occurrence records, ecological and biogeographical traits, and a high-resolution suite of environmental predictors. Species occurrence records are drawn from AquaMaps, OBIS, and GBIF, and taxonomies are standardised using WoRMS AphiaIDs to ensure taxonomic consistency. Of critical value to the CRIB, the AquaX process can empirically determine species presence/absence using species-specific thresholds calculated within the modelling framework. Refer to the Appendix (section B.1) for an extended description of the AquaX analysis pipeline.

Present-day species distribution estimates from AquaX were extracted at their native 0.05° resolution globally, re-gridded to 0.08°, converted to binary presence/absence using the empirically derived threshold, and clipped to the New Zealand exclusive economic zone (EEZ); this resulted in 8912 species distributed within the New Zealand EEZ (Figure 4).

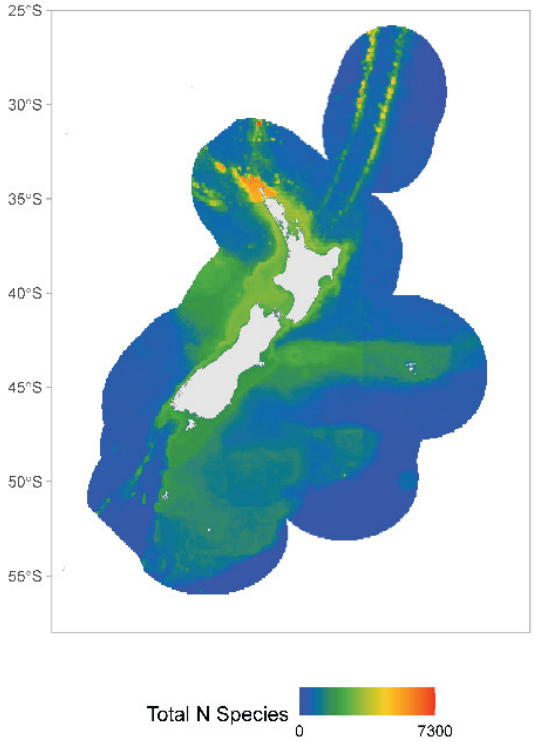


Figure 4*:* Total number of species estimated with the AquaX framework across the New Zealand EEZ.

3.2.2 Species thermal niches

The realised thermal niche of marine species was derived from the AquaX global species distribution modeling framework (Reygondeau et al. 2026), which is an update to the widely used AquaMaps platform (Kaschner et al. 2019).

Within AquaX, each species was assigned to a habitat category (pelagic vs. benthic/demersal/reef-associated) using their FishBase or SeaLifeBase information. Species classified as pelagic (including pelagic-oceanic, bathypelagic and pelagic-neritic) were associated with a global gridded field of baseline seawater temperature representative of the surface water column. Species classified as benthic or demersal (including reef-associated, benthopelagic, bathydemersal and sessile forms) were associated instead with a global gridded field of baseline temperature representative of conditions near the seafloor.

The native-range map for each species was overlaid with its habitat-specific temperature fields on the same spatial grid. The native range map identified all grid cells where the species is present. Temperature fields were restricted to grid cells where the species was present, ensuring that subsequent calculations represent the thermal conditions experienced within the species' modelled native range. From this restricted set of temperature values, the distribution of temperatures across the occupied cells was used to calculate the mean, minimum, maximum, and the 1st, 5th, 25th, 50th, 75th, 95th, and 99th percentiles, which represent the thermal niche. These calculations were conducted separately for each dataset (pelagic occurrence-based, pel_occ; seafloor occurrence-based, seaf_occ) and for each temperature metric (e.g. max and long-term maximum, ltmax). We explored how the lower and upper thermal limits and the range varied across methods. To determine which approach most closely approximates previously used thermal niche estimates, we compared all candidate lower

and upper limits, as well as resulting niche widths, against AquaMaps-derived thermal tolerances across species.

Agreement with AquaMaps was quantified using mean absolute error (MAE), root mean square error (RMSE), bias, and correlation. Across all datasets and variables, thermal limits defined by the 5th and 95th percentiles (q05 and q95) consistently showed the strongest agreement with AquaMaps, yielding the lowest MAE and RMSE and minimal bias relative to alternative definitions. In contrast, extreme-based limits (min, max, q01, q99) systematically overestimated niche breadth, while intermediate quantiles (q025–q975) produced moderately wider niches but did not improve agreement with AquaMaps. On average, the q025–q975 method increased estimated niche width by approximately 15–25% (~1–3 °C) relative to q05–q95, whereas min–max approaches resulted in substantially larger overestimates.

Dataset choice had a much larger influence on inferred niche width than the quantile definition did. Thermal niches derived from seafloor occurrence data (seaf_occ) were consistently broader than those from pelagic occurrences (pel_occ), with mean niche widths approximately 50–100% larger (~4–10 °C wider), possibly reflecting greater environmental variability in benthic habitats and greater vertical habitat range of bottom-associated species. Differences among temperature metrics were comparatively small: using long-term maximum temperature instead of instantaneous maximum increased niche width by approximately 5–15% (~0.5–2 °C). Despite these differences, the relative performance of quantile-based methods was consistent across datasets and variables.

Based on these analyses, we defined species thermal niches using the q05–q95 range derived from occurrence-based datasets, which provided the closest match to AquaMaps estimates while avoiding the inflation associated with extreme values. Upper thermal limits were therefore defined as the 95th percentile (q95) and lower limits as the 5th percentile (q05) of the species-specific temperature distributions. This approach captures the central realised thermal niche while minimizing the influence of outliers and sampling artifacts, and is consistent with independently derived global niche estimates.

The validity of the AquaX upper thermal tolerances was checked by comparing them against experimentally determined critical thermal maxima (CTmax) for species documented in published sources (Comte & Olden, 2017; Bennett et al. 2018; Pinsky et al. 2019). AquaX realised upper thermal tolerances were evaluated against the fundamental thermal tolerances for 62 species in the GlobTherm database (Bennett et al. 2018) 63 species reported by Pinsky et al. (2019), and 784 species in Comte & Olden 2017. These comparisons revealed a strong positive correlation between the realised upper thermal niches in AquaX and the fundamental upper thermal niches reported in these databases (r = 0.89–0.9); (Figure 5). However, as expected, fundamental tolerances were typically higher than the realised tolerances from AquaX. This difference is partly due to differences in the duration of thermal exposure considered in the assessments. Realised tolerances are based on time-averaged sea temperatures, whereas fundamental tolerances are determined through experiments that measure responses to acute heat exposure (e.g. over minutes, hours, or days). If we were to use the hottest hourly or daily temperatures within a year, the realised and fundamental tolerances would be expected to align more closely.

While CTmax values that represent fundamental thermal limits are higher than realised thermal tolerances, realised thermal tolerance may be a more suitable metric for assessing climate vulnerability or risk. Whereas the fundamental thermal limit denotes mortality, the realised limit is likely to denote the onset of thermal stress and declining productivity. Thermal stress onset is more closely aligned with the concept of climate vulnerability (e.g. susceptibility to the effects of climate change) and is likely to provide advance warning of climate-driven mortality, which is one of the primary goals of most CVAs, including CRIB.

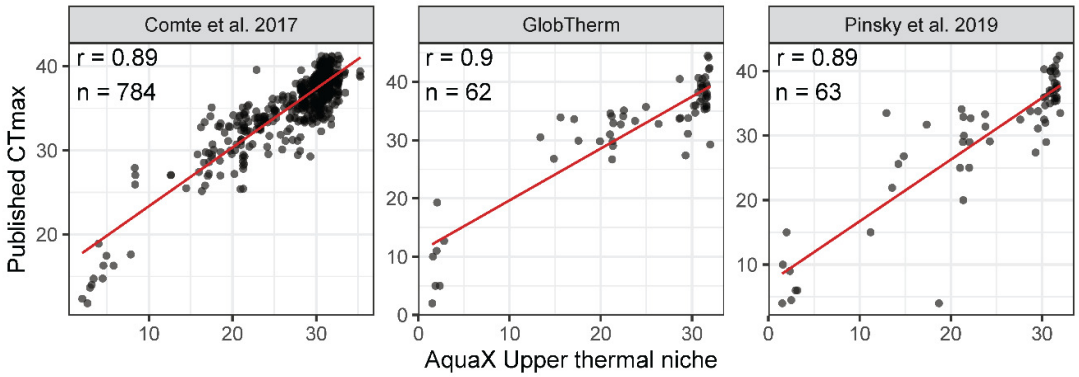


Figure 5*:* Relationships between realised upper thermal niches of species in AquaX and in the scientific literature. Points show the upper thermal tolerances (95th percentile of the distribution) of species reported in AquaX, matched to species in Comte & Olden (2017), the GlobTherm database (Bennett et al. 2018)**, and Pinsky** et al. **(2019).**

3.2.3 Species conservation status

Stock status information is summarised annually in Fisheries New Zealand's "Status of the Stocks" tables, which draw on assessments reviewed by species-specific Fisheries Assessment Working Groups (FAWGs) and endorsed in the national Plenary. These groups include government scientists, industry analysts, university researchers, and invited experts who jointly review data, models, and uncertainty. For data-rich stocks, age- or length-structured stock assessment models integrate catch histories, standardised CPUE, survey indices, and biological composition data to estimate current biomass and fishing mortality. Posterior distributions from these assessments are compared with reference points to derive the probability that biomass exceeds targets and limits, and whether fishing mortality exceeds the overfishing threshold. These probabilities are translated into 7 likelihood categories ("Exceptionally Unlikely", "Very Unlikely", "Unlikely", "About as Likely as Not", "Likely", "Very Likely", and "Virtually Certain") for reporting. For partially assessed stocks, simpler analyses using CPUE trends, survey indices, or production-model indicators inform qualitative estimates of biomass status and the risk of overfishing. For low-information stocks, FAWGs rely primarily on trends in catch, effort, size composition, and life-history traits to provide expert-based likelihood statements. In all cases, uncertainty is explicitly communicated through the likelihood scale.

Each stock's evaluation includes a summary of the data used, data quality, and any key omissions. The Working Groups determine base-case models, evaluate sensitivity analyses, and agree on the most plausible assessment outcomes. The Plenary then reviews these conclusions for consistency with national standards and may revise probability statements. Finalised assessments are subsequently compiled into a public stock-status table. The resulting probability-based classifications determine whether stocks are above or below biomass targets and whether overfishing is occurring or likely to occur under current removals. The approach provides a transparent, reference-point-based framework for evaluating stock condition. It also enables consistent communication of uncertainty across fisheries.

To assign species conservation statuses spatially, quota management areas were used. The quota management areas for each harvested marine species were obtained from the MPI Geospatial Management web portal (Quota Management Areas: Ministry for Primary Industries Open Data Site). The Quota Management Areas (FMAs) are based on the fisheries management area boundary definitions (first schedule of the Fisheries Act, 1996) and are either a combination of FMAs or correspond directly to an FMA. Legal definitions of the boundaries of the FMAs and some individual stocks are contained within the first schedule of the Fisheries Act, 1996. Remaining stock definitions were sourced from the notices of Declaration of New Stocks Subject to Quota Management System.

The areas were extracted as polygon shapefiles for 677 stocks, 643 of which are managed under New Zealand's quota management system.

3.2.4 Species' maximum body lengths

Species maximum body lengths were obtained from the Marine Organismal Body Size (MOBS) Database (McClain et al. 2025). MOBS compiles standardised measurements of maximum linear dimensions—length, height, width, and diameter—for 85 204 marine animal species across 30 phyla representing 40% of valid marine animal species listed in the World Register of Marine Species (WoRMS). The dataset is built on the World Register of Marine Species (WoRMS) taxonomy (WoRMS Editorial Board 2020), with each record linked to an AphiaID to ensure consistency in species names, synonymies, and higher classification. MOBS gathers body size data from multiple sources, beginning with online taxonomic databases and then drawing on published species descriptions, taxonomic monographs, and museum specimen records, particularly holotypes and paratypes. All measurements reflect the largest reported size for each species, extracted from source materials rather than calculated or inferred. Because different publications sometimes report different maxima, the database retains multiple values when available, enabling users to assess variability in reported size estimates. Linear dimensions are used instead of mass because they are more widely available for marine invertebrates and scale predictably with body mass at higher taxonomic levels. For species with indeterminate growth, the largest individuals likely approximate maximum adult size, and log-transformed analyses reduce the influence of intra-specific variation. Each entry includes measurement notes, data sources, and indicators of the biological unit measured (e.g. colony vs. individual). Quality control involved verifying online measurements against original sources to prevent the propagation of data-entry errors. As of release 1.0, the database contains 170 214 measurements representing 85 204 species—approximately 40% of all valid marine animal species in WoRMS—with seven phyla exceeding 75% coverage. The database is global in taxonomic scope but contains no geographic data; however, integration with OBIS allows spatial analyses. MOBS is distributed as a publicly accessible CSV file hosted on GitHub, with clear versioning and guidance for reconciling records with updated WoRMS taxonomy.

3.2.5 Historical and present-day temperatures

Surface and bottom temperatures with the requisite geographic and temporal coverage were obtained from a Global Ocean Physics Reanalysis produced by the Copernicus Marine Service Global Monitoring and Forecasting Centre (GLORYS). Previous regional iterations of CRIB used daily SST estimates from the NOAA 0.25° daily Optimum Interpolation Sea Surface Temperature dataset (OISST) (Reynolds et al. 2007). However, using surface temperatures from the Reynolds dataset and bottom temperatures from GLORYS could create biased risk estimates for pelagic versus demersal species. To avoid this and ensure strict comparability of the surface and bottom temperature datasets, surface and bottom temperatures were extracted from the same GLORYS dataset.

The GLOBAL_MULTIYEAR_PHY_001_030 dataset is a global physical-ocean reanalysis produced by the Copernicus Marine Service in partnership with Mercator Ocean International, designed to provide consistent three-dimensional fields of potential temperature, salinity, currents, sea surface height, mixed-layer thickness and sea-ice parameters globally (±80° S to 90° N, 180° W–180° E) on a regular 1/12° (~0.083°) horizontal grid and 50 standard vertical levels. The model is derived from the NEMO ocean model (Arakawa C-grid) coupled to the LIM2 sea-ice component, forced by ECMWF atmospheric reanalyses (ERA-Interim historically and ERA5 more recently) and incorporating data assimilation via a reduced-order Kalman filter/scheme (SAM2/SEEK) that ingests satellite SST, altimeter sea-level anomalies, in-situ T/S profiles and sea-ice concentration. Temporal coverage

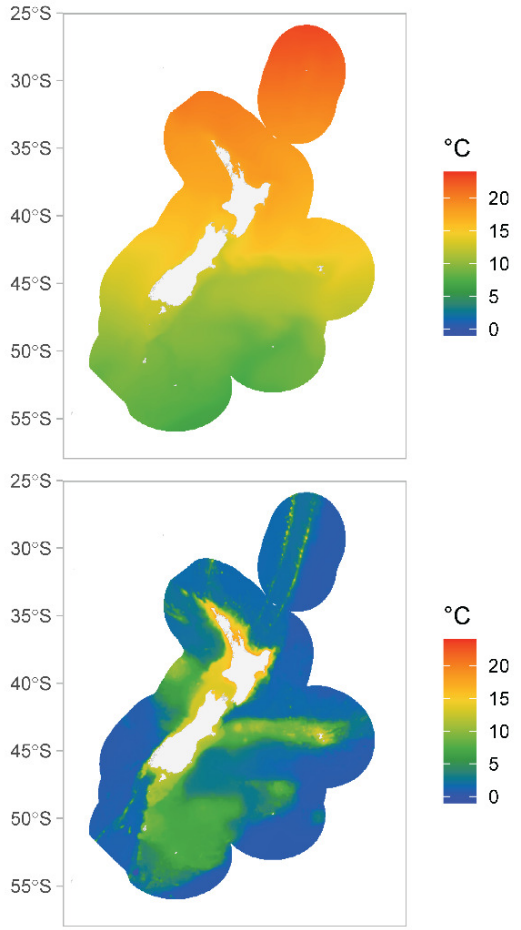


Figure 6: Average surface (top) and bottom (bottom) sea temperature between 1993 and 2025.

begins on 1 January 1993 (daily and monthly means) and continues into the near-real-time interim stream[5]. The horizontal grid (~4320×2041 grid points globally) resolves mesoscale features at ~8 km resolution in mid-latitudes. Data are delivered in CF-compliant NetCDF format (Level 4) and include auxiliary static fields (masking, bathymetry, cell metrics) to support volume integrations. Because the product is observation-constrained and globally consistent, it has been used widely for studies of ocean temperature variability, trend detection, and extremes across space and depth. Its high resolution and long record make it suitable for exploring subsurface warming and regional climate change impacts. For example, the dataset permits investigation of three-dimensional thermal structure rather than surface-only fields. The user manual documents the production system, resolution, assimilation strategy and quality assessment. In total, the product offers a robust, freely available reference for long-term and near-real-time physical ocean state, including full-depth temperature fields at 0.083° horizontal resolution and daily/monthly temporal resolution. These reanalyses are as close as possible to the observations and in agreement with the model physics.

For the case studies presented here, monthly surface and bottom temperatures were extracted at their native ~0.08° across the New Zealand EEZ (Figure 6).

[5]https://data.marine.copernicus.eu/product/GLOBAL_MULTIYEAR_PHY_001_030/services?utm_source=chatgpt.com

3.2.6 Projected temperatures

Monthly surface and bottom temperature projections were extracted between 2015 and 2100 from global and regional Earth System Models (ESMs; Table 3). All temperature projections (°C) were made under the IPCC's shared socioeconomic pathway (SSP) scenarios SSP2-4.5, representing a "middle of the road" fossil fuel pathway, and SSP3-7.0, representing a higher emissions "rocky road' socioeconomic pathway (Riahi et al. 2017; Meinshausen et al. 2020). Under SSP2-4.5, the global mean surface temperature is anticipated to increase by ~2.1–3.5°C by 2100 relative to pre-industrial levels, whereas under SSP3-7.0, a ~3–3.6°C increase is projected.

Table 3: Earth System Models used.

N	Model	Modeling Center (or Group)	References
1	CNRM-CM6-1-HR	Centre National de Recherches Meteorologiques	(Voldoire et al. 2019)
2	AWI-CM-1-1-MR	Helmholtz Centre for Polar and Marine Research	(Sein et al. 2018)
3	NZESM	Several, led by Earth Sciences New Zealand (ESNZ)	(Williams et al. 2016; Behrens et al. 2020)

3.2.6.1 CMIP 6 projections

Projected monthly surface (SST) and bottom temperature time series were obtained from the Coupled Model Intercomparison Project phase 6 (CMIP6) between 1850 and 2100. All temperature projections were extracted onto a regular 0.25° grid. An ensemble of temperature projections was obtained from three published Global Climate Models (GCMs) or Earth System Models (ESMs) in the CMIP6 archive. These models span a broad range of temperature projections within the CMIP6 model set. All CMIP6 surface and bottom temperature projections were interpolated to the template 0.08° grid across the New Zealand EEZ using nearest neighbour interpolation (Figure 7 and Figure 8).

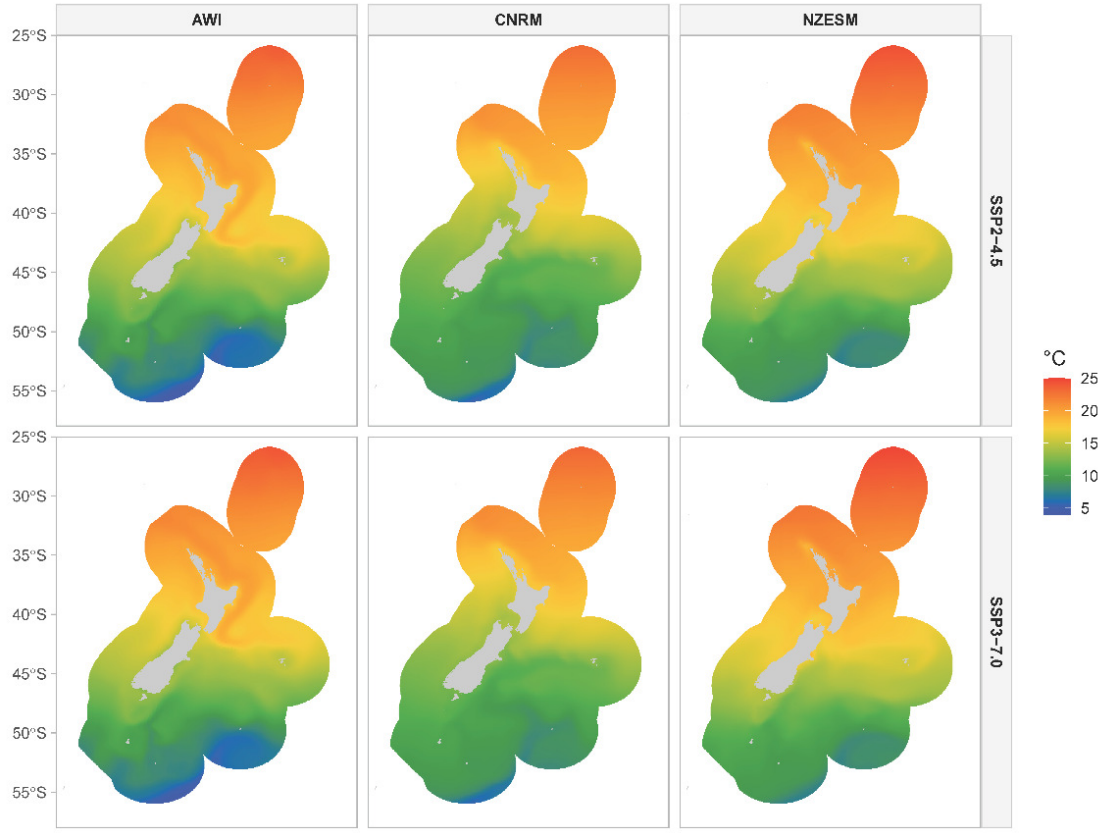


Figure 7: Average projected surface temperature under SSP2-4.5 (top row) and SSP3-7.0 (bottom row) from three ESM models (Table 3) to 2100.

3.2.6.2 New Zealand Earth System Model (NZESM) projections

The New Zealand Earth System Model (NZESM) is a fully coupled Earth system model based on UKESM, which uses NEMO (Madec, 2015) and MEUSA (Yool et al. 2013) to simulate ocean physics and biogeochemistry. It uses the Unified Model and Jules (Walters et al. 2019) for the atmosphere and land processes and CICE (Rae et al. 2015; Hunke et al. 2017) for sea ice. NZESM captures ocean circulation in the New Zealand region better than its parent model by embedding a 1/5° resolution nested region in the ocean around New Zealand (Behrens et al. 2020) and by incorporating a solar-cycle-dependent photolysis rate (Dennison et al. 2019). NZESM has reduced model biases in temperature around New Zealand by resolving small-scale processes and improving boundary current transport. All NZESM surface and bottom temperature projections were interpolated to a template 0.08° grid across the New Zealand EEZ using nearest neighbour interpolation (Figure 7 and Figure 8).

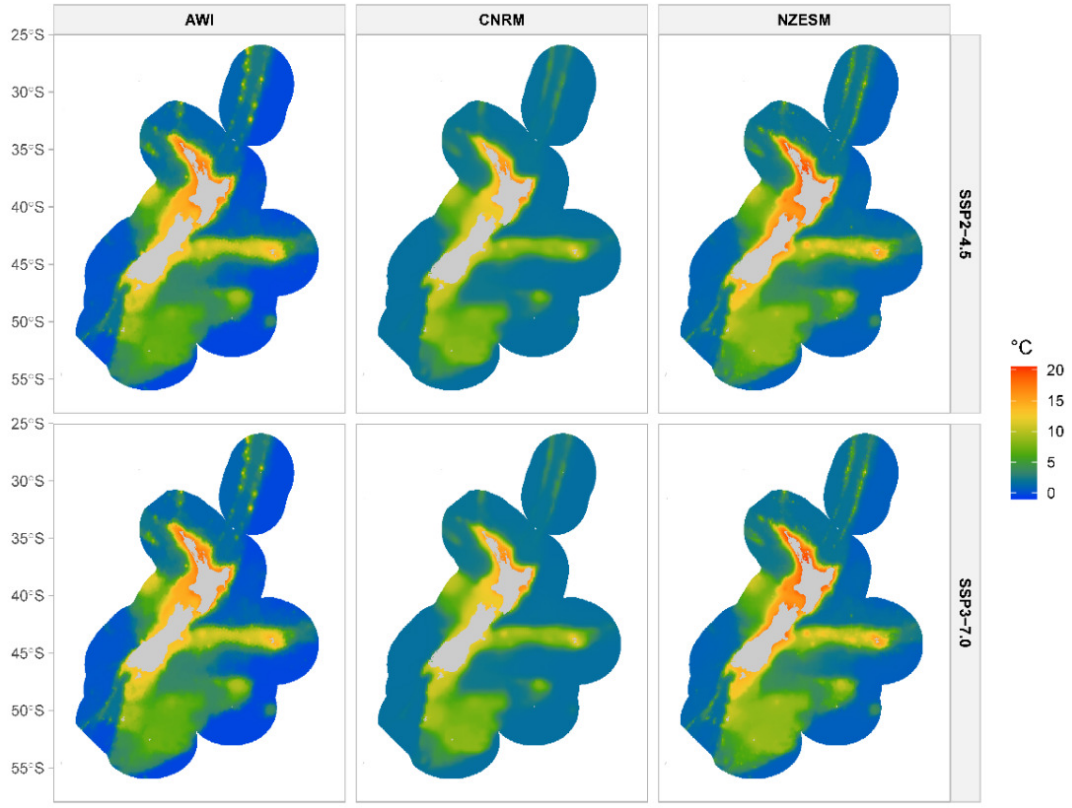


Figure 8*:* Average projected bottom temperature under SSP-2.45 (top row) and SSP-3.70 (bottom row) from three ESM models (Table 3) to 2100.

3.2.7 Cumulative impacts

A multivariate index of cumulative human impacts (Human Impacts Index; HII) on ocean ecosystems was developed by Halpern et al. (2008, 2015). The HII index integrates 17 global anthropogenic drivers of ecological change, including fishing pressure, pollution, invasive species, eutrophication, and climate change. Temperature change is a factor in the HII; however, since there are 16 additional indices, its collinearity with the CRIB indices is likely to be minor. The HII estimates were available at a global 1km^2 native resolution. These values were rescaled to a 0.8° grid around the New Zealand EEZ using bilinear interpolation (Figure 9).

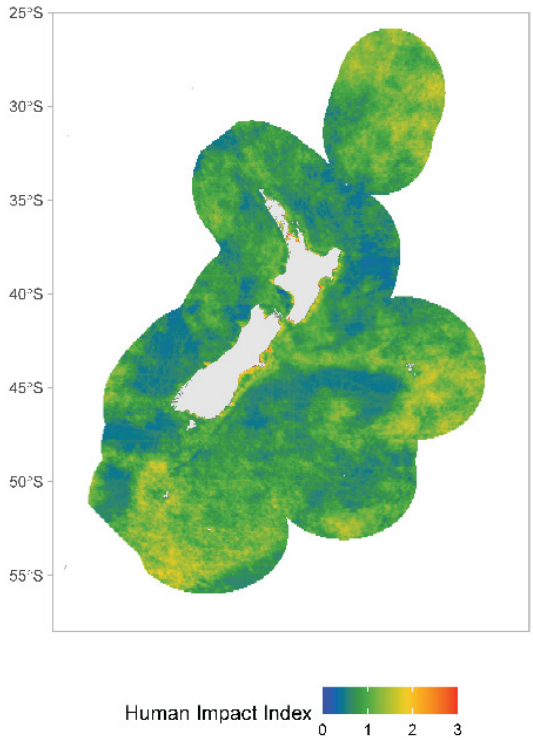


Figure 9*:* Cumulative human impact index from Halpern et al. **2015.**

3.3 Analyses

Like the CRIB, CRIB-NZ climate indices are calculated or obtained in their native units. Each index is defined by the focal species' traits, calculated from environmental or ecological data on a geographic grid across the geographic distribution of the focal species and/or a combination of the two. This leads to indices that are taxonomically and geographically explicit. Each index is transformed to map to a standardised 0–1 scale using hyperbolic functions (see Boyce et al. (2022) for details). This step ensures that indices with different units can be compared and combined. It also enables vulnerability to be re-estimated at different spatial resolutions or at different points in time without information loss.

To adapt the CRIB framework to the New Zealand fisheries context, some indices were modified. The vertical habitat variability and use index (climate sensitivity) was modified to accommodate bottom-associated species, and the climate velocity index (climate exposure) was replaced entirely to incorporate the impacts of marine heat waves in New Zealand waters. The 12 climate indices used in the CRIB-NZ adaptation—the original 10 and the newly developed ones—are listed in Table 4 and described below. All of the edits made to the CRIB to develop CRIB-NZ are listed in Table 5.

Table 4: Indices used in the CRIB-NZ framework.

Index	Description	Data	Rationale	References
Sensitivity (S)				
Thermal safety margin	The difference between the maximum environmental temperature and the species' upper temperature tolerance.	AquaX, Global Ocean Reanalysis (GLORYS) surface and bottom temperature	Species inhabiting waters at their upper thermal limits are more vulnerable to further warming. The thermal safety margin has been extensively used in climate vulnerability assessments to measure species sensitivity and tolerance to further warming.	(Deutsch et al. 2008; Sunday et al. 2012; Sunday et al. 2014; Pearson et al. 2014; Stuart-Smith et al. 2015; Comte & Olden, 2017; Walters et al. 2018; Vinagre et al. 2019; Gallagher et al. 2019; Pinsky et al. 2019, 2021; Dahlke et al. 2020; Payne et al. 2021; Molina et al. 2025; Storm, 2025)
Conservation status	Assessed probability of stock overfishing (categorical).	MPI stock table	Climate effects on species can be more severe when species are or have been impacted by additional stressors (e.g. fishing, pollution, and nutrient loading) and are at low conservation status.	(Ohlemüller et al. 2008; IUCN, 2012; Berry et al. 2013; Pearson et al. 2014; KEITH et al. 2014; Stanton et al. 2015; Morrison et al. 2016; Hare et al. 2016; Foden et al. 2019; Bateman et al. 2020; McClure et al. 2023; Craig et al. 2025; Frawley et al. 2025; Lettrich et al. 2025)
Cumulative impacts	Multivariate index of human impacts.	Human impact index	Species exposed to multiple impacts are more sensitive to additional stressors, tipping points, and synergistic impacts.	(Worm et al. 2002, 2006; Worm & Duffy, 2003; Ottersen et al. 2006; Crain et al. 2008; Darling & Côté 2008; Halpern et al. 2008, 2012, 2015; Carilli et al. 2009; Ban et al. 2010; Stelzenmüller et al. 2010; Maxwell et al. 2013; Kroeker et al. 2013; Le Bris et al. 2018; Rogers-Bennett & Catton, 2019; Sumaila & Tai, 2020; Butt et al. 2022; Gove et al. 2023)
Vertical habitat variability and use	A bivariate function of the minimum depth distance of occupancy from the surface or bottom and the vertical range of species.	AquaX, FishBase, SeaLifeBase	Habitat generalist species are more adapted to climate variability and change than are specialist species due to their ability to occupy a greater variety of habitats. Species inhabiting the upper ocean and having narrow vertical habitat ranges are more sensitive to upper-ocean warming.	(Peters, 1985; Natori et al. 2006; Laidre et al. 2008; Rosset & Oertli, 2011; Guest et al. 2012; Garcia et al. 2014; Spencer et al. 2019; Firth et al. 2021; Lettrich et al. 2023; McClure et al. 2023; Moll et al. 2024)
Adaptivity (AC)				
Geographic range extent	A bivariate function of the global present-day geographic habitat area and the latitude span	AquaX	Broadly distributed species are less susceptible to adverse climate change events over parts of their geographic distributions. Greater opportunity for favourable habitat (e.g. climate refugia) within larger distributions.	(Cheung et al. 2007; Burek et al. 2008; Laidre et al. 2008; Ohlemüller et al. 2008; Ficetola & Denoel, 2009; Davidson et al. 2012; Gonzalez-Suarez et al. 2013; Pearson et al. 2014; Dickinson

Index	Description	Data	Rationale	References
	occupied by the species.			et al. 2014; Garcia et al. 2014; Runge et al. 2015; Ofori et al. 2017; Ducatez & Shine, 2017; Chichorro et al. 2019; Albouy et al. 2020; Staude et al. 2020; Chase et al. 2020)
Geographic habitat fragmentation	The proportion of species native geographic distribution that is fragmented.	AquaX	Species with less fragmented habitat ranges have greater access to potentially favourable habitats (e.g. climate refugia), migration corridors, and larval dispersal. Consequently, studies in terrestrial and marine systems have reported that species with fragmented geographic ranges are more sensitive to and less resilient to climate change impacts	(Brown & Kodric-Brown, 1977; Lehtinen et al. 1999; Warren et al. 2001; Fahrig, 2002; Kaschner et al. 2006; Moore & Huntington, 2008; Rueda et al. 2013; Gonzalez-Suarez, Gomez and Revilla, 2013; Pearson et al. 2014; MacLean & Beissinger, 2017; Crooks et al. 2017; Rogan & Lacher, 2018; Rogers et al. 2018; Albouy et al. 2020; Brauer & Beheregaray, 2020; Palmeirim et al. 2020; Chase et al. 2020; Fordham, 2024)
Maximum body length	The maximum body length reached globally.	MOBS database	The maximum size is a predictor of several life-history traits (e.g. generation length, time to maturity, intrinsic rate of population increase) that cumulatively define a species' potential reproductive capacity and population growth rate. The maximum size (length or mass) reached by species has been commonly used as a proxy of extinction risks and vulnerability of species to climate change. Smaller species that tend to be r-selected are viewed as more resilient than larger, K-selected ones.	(Fenchel, 1974; Blueweiss et al. 1978; Cheung et al. 2007; Davidson et al. 2012; Gonzalez-Suarez, Gomez and Revilla, 2013; Chessman, 2013; Cheung et al. 2013; Healy et al. 2014; Pearson et al. 2014; Dulvy et al. 2014; Ripple et al. 2017; Cheung and Oyinlola, 2018; Foden et al. 2019; Donner & Carilli, 2019; Albouy et al. 2020; Kuo et al. 2022; Bak et al. 2023; Fordham, 2024)
Thermal habitat variability and use	A bivariate function of the fraction of species' thermal niche covered by its historical temperature habitat and the total temperature range experienced by the species across its global present-day geographic range.	AquaX, Global Ocean Reanalysis (GLORYS) surface and bottom temperature	Species inhabiting more variable thermal environments, such as at the range-edges of their geographic distributions, are thought to have a greater capacity to adapt to climate change and are believed to be less sensitive to it	(Morley et al. 2009; Sunday et al. 2011; Carilli et al. 2012; Guest et al. 2012; Cole et al. 2014; Mora et al. 2014; Rehm et al. 2015; Xu et al. 2016; Shah et al. 2017; Nadeau et al. 2017; Safaie et al. 2018; Donner & Carilli, 2019; Albouy et al. 2020; Bennett et al. 2021)
Exposure (E)				

Index	Description	Data	Rationale	References
Projected marine heatwave duration and magnitude	Bivariate function of the proportion of months the temperature exceeds the species thermal niche, and the magnitude of its exceedance.	AquaX, projected monthly SST and bottom temperature	The velocity of climate change (VoCC) represents climatic isotherms' geographic movement over time and is a widely used measure of climate exposure	(Loarie et al. 2009; Burrows et al. 2011; IPCC, 2014; Garciá Molinos et al. 2016; Brito-Morales et al. 2018, 2020; Li et al. 2018; English et al. 2022)
Projected ecosystem disruption	For each grid cell across the focal species' native geographic distribution, the proportion of all species projected to exceed their thermal tolerances.	AquaX, Projected monthly SST and bottom temperature	Individual species will be impacted by climate-driven ecosystem restructuring via altered predation, prey availability, and competition.	(Frank et al. 2006; Frank et al. 2018; Cardinale et al. 2012; Boyce et al. 2015; Boyce et al. 2015a; Martin & Watson, 2016; Hillebrand et al. 2018; du Pontavice et al. 2020; Trisos et al. 2020; Irvine et al. 2025)
Projected time of climate emergence from species' thermal niche	The year when the projected temperature first exceeds the thermal tolerance of the focal species for at least three years in a row.	AquaX Projected monthly SST and bottom temperature	The timing of climate emergence from pre-industrial temperature variability has been widely used as a proxy for the timing of climate change. The time of climate emergence from a species' thermal tolerance range has recently been developed as an index of when a species is exposed to dangerous climate conditions.	(Mora et al. 2013; Henson et al. 2017; Bruno et al. 2018; Turk et al. 2019; Xu et al. 2020; Trisos et al. 2020; Jenouvrier et al. 2022; Lewis et al. 2023; Pigot et al. 2023; Meyer et al. 2024; Barrier et al. 2025)
Projected loss of suitable thermal habitat	For each focal species, the proportion of its native geographic distribution is lost due to projected climate change.	AquaX Projected monthly SST and bottom temperature	Species that are projected to lose more of their thermal habitat are more vulnerable.	(Cheung et al. 2009, 2015; Pinsky et al. 2013; Hazen et al. 2013; Shackell et al. 2014; MacKenzie et al. 2014; Ochoa-Quintero et al. 2015; Pacifici et al. 2015; Stortini et al. 2015; Davies et al. 2017; Foden et al. 2019; McHenry et al. 2019; Lavender et al. 2021; Reddin et al. 2022; Hodapp et al. 2023; Meyer et al. 2024)

To illustrate the CRIB-NZ workflow and facilitate understanding of how the raw climate indices are calculated and used to define climate vulnerability, yellowtail kingfish (*Seriola lalandi*) is discussed as a case study species. Kingfish is a large, highly mobile, fast-swimming pelagic predator found in temperate and subtropical oceans. Adults are active predators that feed primarily on small schooling fishes and squid. Kingfish can reach a maximum length of 250 cm and are relatively fast-growing, which may give them greater resilience than slower-growing species. They are classified as benthopelagic and FishBase reports their global occupancy depth as 825 m (Hureau, 1991), but frequently inhabit surface waters to feed, migrate, and spawn. In CRIB-NZ, they are categorised as 'surface-associated'. They are broadcast spawners, and studies suggest they can tolerate temperatures between 12 and 29°C.



Figure 10: Yellowtail kingfish (*Seriola lalandi*). Source: MPI (https://tinyurl.com/pw457syw).

3.3.1 Climate Sensitivity

3.3.1.1 Thermal safety margins

The thermal safety margin (TSM) has been frequently and extensively used in climate vulnerability assessments to measure species sensitivity and tolerance to further warming (Deutsch et al. 2008; Sunday et al. 2012; Sunday et al. 2014; Pearson et al. 2014; Stuart-Smith et al. 2015; Comte & Olden, 2017; Walters et al. 2018; Vinagre et al. 2019; Gallagher et al. 2019; Pinsky et al. 2019, 2021; Dahlke et al. 2020; Payne et al. 2021; Molina et al. 2025; Storm, 2025). Species inhabiting thermal environments close to their upper temperature limit (narrow thermal safety margin) are more vulnerable to climate warming than those further away.

For each species within each grid cell across its estimated geographic distribution, a thermal safety margin was calculated as the difference between the species' estimated upper thermal tolerance and the maximum temperature observed between 2015 and 2025. Equation 1 and Figure 11 describe how climate sensitivity varies with TSM. The equation standardises the index (0–1), normalises its distribution, and allows most of the change in sensitivity to occur for TSMs below 10°C, with sensitivity becoming increasingly uniform as TSM exceeds 10°C. There should be little difference in the sensitivity of species inhabiting ocean temperatures that are >10°C from their upper thermal maximum. This definition of sensitivity (Figure 11) specifies that risk declines with thermal distance from the species' upper thermal tolerance. In general, thermal performance is strongly warm-skewed, with fitness increasing gradually toward the thermal optima before rapidly declining to zero as the species' upper thermal tolerance limit is approached. The assumption that risk increases continuously with temperature thus captures the risk of the species' upper thermal tolerance being exceeded rather than representing variation in fitness within the thermal niche. Refer to Boyce et al. (2022) for an evaluation of how the vulnerability calculations are affected by the specification of λ.

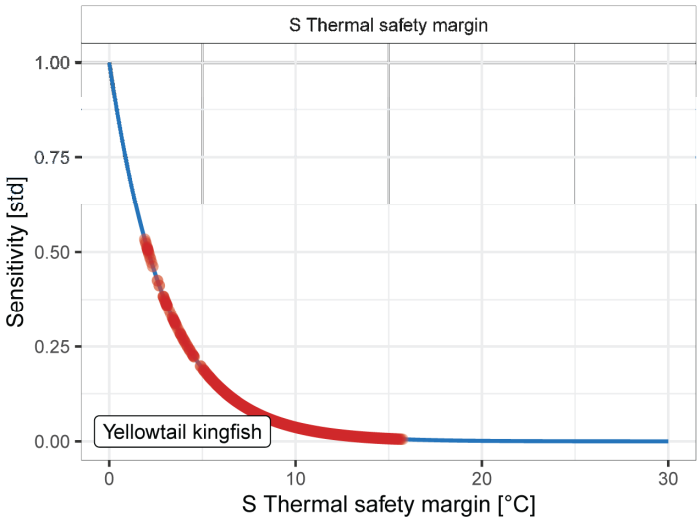


Figure 11: TSM standardization. The blue trend line depicts how Equation 1 maps thermal safety margins (°C) to standardised sensitivity scores (0–1). Maximum sensitivity (index=1) occurs when the TSM is 0. Red points are the values for yellowtail kingfish across the New Zealand EEZ.

In the case of yellowtail kingfish, its broad thermal niche (~12 to ~29°C) results in TSMs that are variable, but generally large, leading to modest sensitivity scores across most of the New Zealand EEZ (Figure 12).

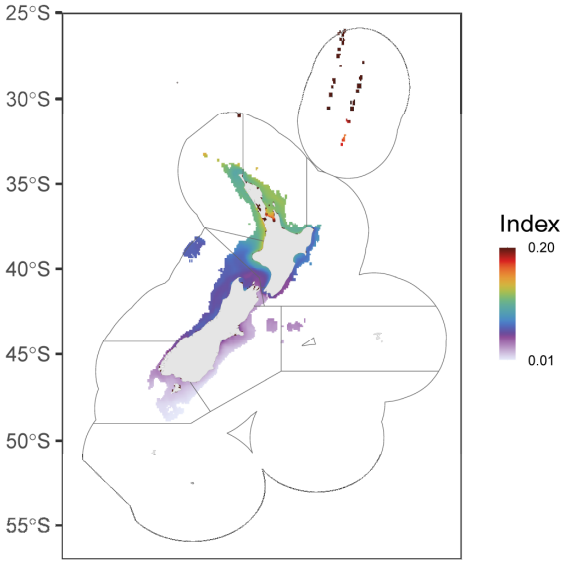


Figure 12: Sensitivity as a function of thermal safety margins for yellowtail kingfish across its geographic distribution. Light purple depicts areas of low sensitivity, while orange and red show areas of high sensitivity.

3.3.1.2 Vertical habitat use

Vertical habitat specialization, the depth of species' occupancy, and the ability to occupy different vertical habitats play a significant role in determining species' sensitivity to climate change. Species restricted to the uppermost epipelagic layers of the ocean are expected to be more sensitive to climate changes occurring at the sea surface, whereas those constrained to the seafloor are expected to be more sensitive to climate changes at the sea bottom (e.g. Albouy et al. 2020). Similarly, species that occupy a narrow range of vertical habitats are less able to avoid unfavourable climate conditions and are more climate-sensitive. As such, a vertical habitat index was calculated for each species according to its vertical habitat occupancy and range depth.

Equation 2 and Equation 3 and Figure 13 describe how climate sensitivity varies with the maximum distance of species occupancy from the surface (for surface-associated species) or bottom (for bottom-associated species), respectively, and the vertical range of each species. The equation standardises the index (0–1), normalises its distribution, and allows sensitivity to scale between 0 and 1, with most of the change occurring between the sea surface or bottom and 200 m depth or range, with sensitivity being very similar below (surface associated) or above (bottom associated) 200 m (Figure 13). Maximum sensitivity occurs for species with narrow vertical ranges that exist in close proximity to the sea surface or bottom.

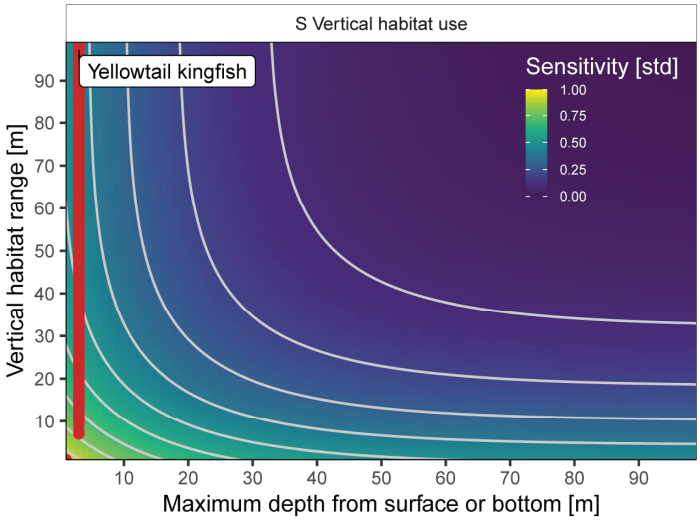


Figure 13: Vertical habitat standardizations. The dark blue to yellow colours depict how Equation 2 and Equation 3 map vertical habitat range and maximum depth from the surface or bottom (m) to standardised sensitivity scores (0–1). Red points are the values for yellowtail kingfish across New Zealand waters.

In the case of yellowtail kingfish, its broad global depth range between shallow (0 m) and deeper (up to 825 m) waters (Hureau, 1991) results in sensitivity scores that are variable, but generally low across most of the New Zealand EEZ (Figure 14).

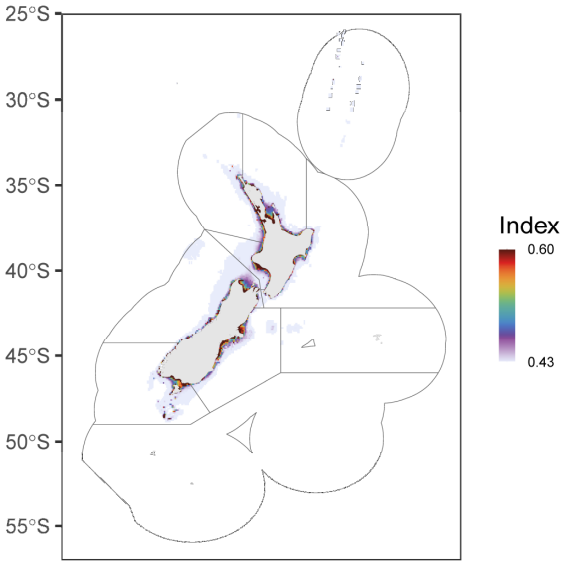


Figure 14: Sensitivity as a function of vertical habitat use for yellowtail kingfish across its geographic distribution. Light purple depicts low sensitivity, while orange and red show areas of high sensitivity.

3.3.1.3 Conservation status

The conservation status of species, populations, or fish stocks is a widely used indicator of climate sensitivity, adaptability, and overall vulnerability. Species with low conservation status (e.g. reduced abundance, reduced fitness, reduced range size) have often been found to be more sensitive and less resilient to additional stressors and perturbations, such as climate change, and conservation status is frequently used in CVAs for species and fisheries (Ohlemüller et al. 2008; IUCN, 2012; Berry et al. 2013; Pearson et al. 2014; Keith et al. 2014; Stanton et al. 2015; Morrison et al. 2016; Hare et al. 2016; Foden et al. 2019; Bateman et al. 2020; McClure et al. 2023; Craig et al. 2025; Frawley et al. 2025; Lettrich et al. 2025).

The estimated conservation status of individual stocks was obtained as the probability that each stock is overfished, as reported in the Fisheries New Zealand stock status table. The probability of overfishing is given as seven categories: ("Exceptionally Unlikely", "Very Unlikely", "Unlikely", "About as Likely as Not", "Likely", "Very Likely", and "Virtually Certain". Stocks where the overfished status was entered as "Uncertain" and those that were unassessed were set to "Likely" to ensure that the assessment was precautionary, as assuming a higher overfishing probability (lower conservation status) leads to a higher risk category, relative to assuming equivalence ("About as Likely as Not"). Because the probability of overfishing is updated annually, the climate sensitivity of species can vary slightly from year to year, and the CRIB-NZ could, conceivably, be updated to reflect any changes in conservation status.

The probability of overfishing levels was linearly transformed to numeric values between 0 and 1 as follows:

1. Exceptionally Unlikely: 0
2. Very Unlikely: 0.167
3. Unlikely: 0.333
4. About as Likely as Not: 0.5
5. Likely: 0.667
6. Very Likely: 0.833
7. Virtually Certain: 1.

In the case of yellowtail kingfish, a moderate probability of being overfished ("Likely" to "Exceptionally Unlikely") across all assessed stocks results in sensitivity scores that are spatially variable but generally low across the New Zealand EEZ (Figure 15, Figure 16, and Figure 17). Where there was more than one probability of overfishing per QMA area (e.g. kingfish QMA KIN 1 had four sub-stock areas), numeric overfishing levels were averaged across the QMA.

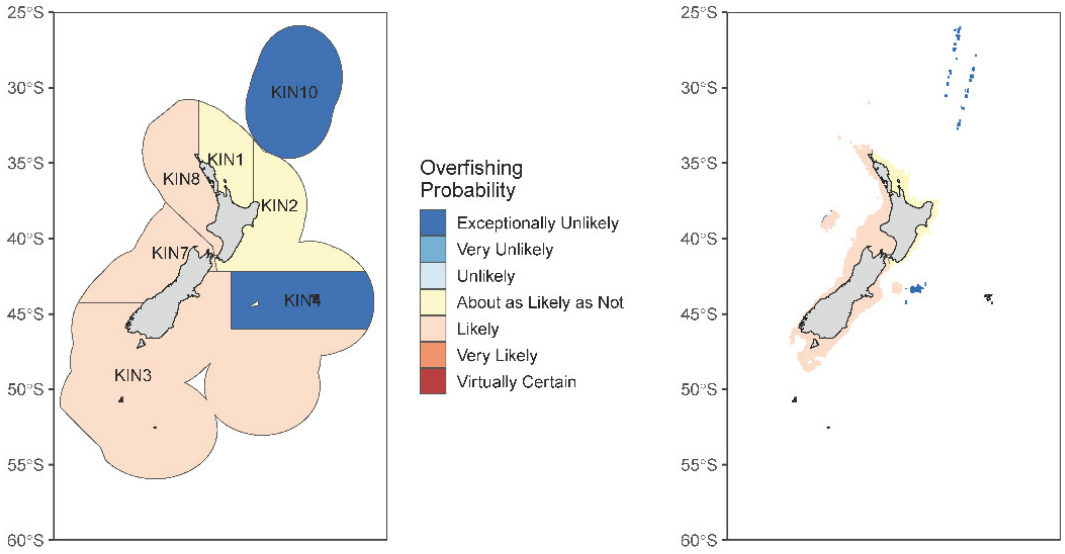


Figure 15: Conservation status represented as the probability of stock overfishing for yellowtail kingfish. Probability of overfishing at the scale of kingfish stock quota management areas (left) and clipped to the species' native geographic range (right).

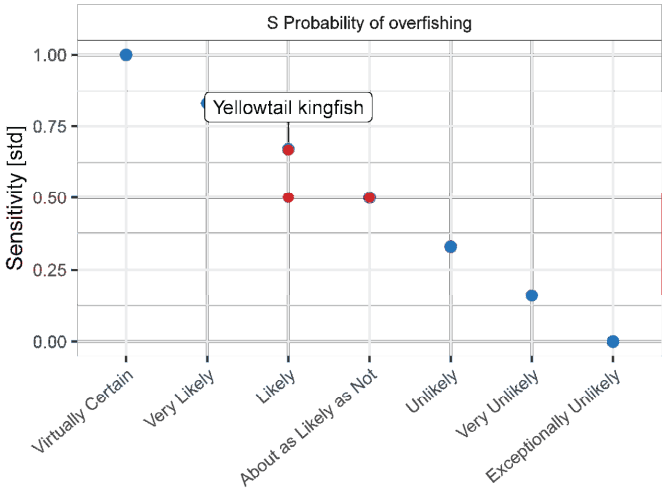


Figure 16: Conservation status standardization. The blue points depict how equation 4 maps conservation status (here, the probability that a stock is being overfished) to standardised sensitivity scores (0–1). Red points are the values for yellowtail kingfish across the New Zealand EEZ.

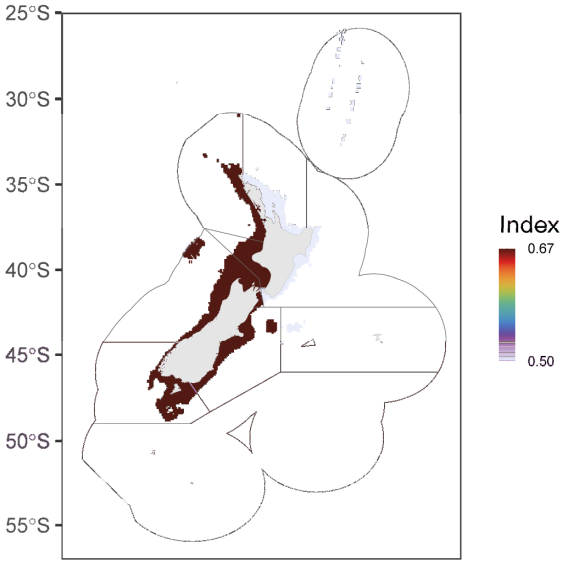


Figure 17: Sensitivity as a function of conservation status (e.g. the probability of overfishing) for yellowtail kingfish across its geographic distribution. Light purple depicts low sensitivity, while orange and red show areas of high sensitivity.

3.3.1.4 Cumulative impacts

Climate effects on ecosystems and species are often more severe when intersected with additional stressors, such as fishing, pollution, and nutrient loading (Worm et al. 2002, 2006; Worm & Duffy, 2003; Ottersen et al. 2006; Crain et al. 2008; Darling & Côté 2008; Halpern et al. 2008, 2012, 2015; Carilli et al. 2009; Ban et al. 2010; Stelzenmüller et al. 2010; Maxwell et al. 2013; Kroeker et al. 2013; Le Bris et al. 2018; Rogers-Bennett & Catton, 2019; Sumaila & Tai, 2020; Butt et al. 2022; Gove et al. 2023).

Studies have shown that habitat degradation, pollution, exploitation and coastal development can diminish population size and genetic diversity, thereby weakening species' capacity to resist the adverse effects of warming, acidification, and deoxygenation (Halpern et al. 2008; McLeod et al. 2009). When species are simultaneously exposed to multiple stressors, they often interact synergistically rather than additively, meaning that populations already negatively affected by anthropogenic impacts experience disproportionately stronger responses to climate stress (Crain, et al. 2008; Gunderson et al. 2016). Organisms subjected to chronic disturbances typically exhibit reduced thermal tolerance, impaired immune function, and diminished reproductive output, all of which increase sensitivity to climate-driven changes (Portner & Farrell, 2008; Sunday et al. 2014). Additionally, cumulative impacts often undermine key ecosystem functions—such as structural habitat provision and trophic regulation—thereby reducing the stability of ecological networks under climate stress (Bruno et al. 2021).

Species experiencing high cumulative impacts frequently occupy altered or degraded environments where climate-related extremes (e.g. heatwaves, hypoxia events) have intensified effects (Smale et al. 2019). Meta-analyses demonstrate that biodiversity loss from non-climatic stressors lowers ecosystem resilience, magnifying the ecological consequences of warming and acidification (Isbell et al. 2015; Oliver et al. 2015). For example, Ottersen et al. (2006) reported that extensive fishing could render fish populations less resistant to the harmful effects of short-term climate variability on occasional low year classes. Alternatively, studies have reported that species and ecosystems protected from such stressors may be more resistant and resilient to stressors such as climate change (Worm et al. 2002, 2006; Worm & Duffy, 2003). Le Bris et al. 2018 found that management initiatives to protect large

female lobsters in the Gulf of Maine led to higher resilience to ocean warming and productivity of the lobster population there when compared to populations where large individuals were less strictly conserved (Le Bris et al. 2018). Without conservation measures to protect large lobsters and female reproductive lobsters, lobster abundance would have increased by 242% rather than 515%, as oceans warmed between 1985 and 2014 (Le Bris et al. 2018).

These results contribute to a growing body of research suggesting that protecting species, and predators, in particular, can enhance the resilience of populations to stressors, such as climate change(Britten et al. 2014; Le Bris et al. 2015, 2018). In this context, cumulative impacts act as a preconditioning factor, leaving species closer to physiological and ecological limits and therefore more vulnerable to additional climate forcing (IPCC, 2022). For these reasons, incorporating cumulative human impacts into assessments of climate-change sensitivity provides a more realistic measure of species' vulnerability and better reflects the compounded pressures shaping future marine biodiversity trajectories.

The multivariate index of cumulative human impacts (HII) on ocean ecosystems developed in Halpern et al. (2008, 2015) was used to assess cumulative impacts on marine ecosystems. The HII index integrates 17 global anthropogenic drivers of ecological change, including fishing pressure, pollution, invasive species, eutrophication, and climate change. The 1 km^2 HII values were re-interpolated using nearest-neighbour methods to the template 0.08° grid. This interpolation changed the HII scale: whereas the global native 1 km^2 HII ranged from 0 to 12, the interpolated values across the New Zealand EEZ ranged from ~0 to ~5. Equation 4 and Figure 18 describes how climate sensitivity varies with the HII. The equation standardises the index (0–1), normalises its distribution, and allows sensitivity to scale between 0 and 1.

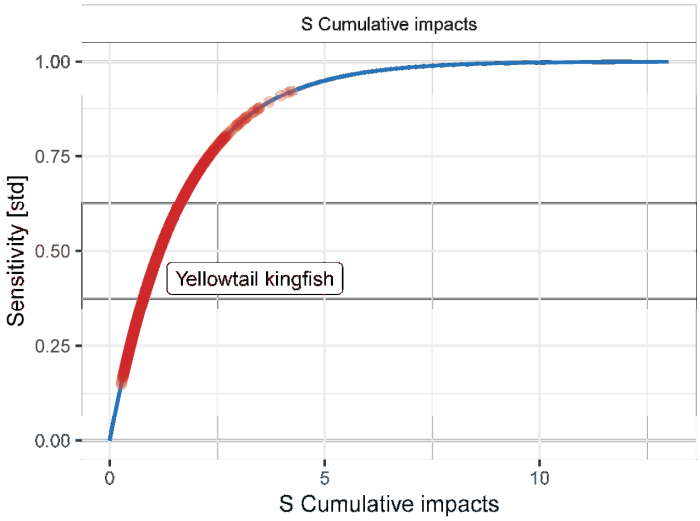


Figure 18: Cumulative impacts standardization. The blue trend line depicts how Equation 4 maps cumulative human impacts to standardised sensitivity scores (0–1). Red points are the values for yellowtail kingfish across the New Zealand EEZ.

Yellowtail kingfish is a coastal neritic species primarily inhabiting waters where cumulative impacts are often higher, leading to sensitivity scores that are spatially variable, ranging from low to high across the New Zealand EEZ (Figure 18 and Figure 19).

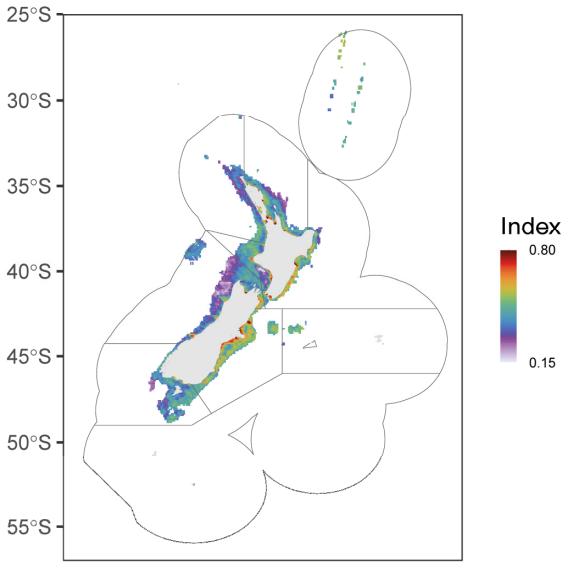


Figure 19: Sensitivity as a function of cumulative impacts for yellowtail kingfish across its geographic distribution. Light purple depicts low sensitivity, while orange and red show areas of high sensitivity.

3.3.2 Climate exposure

3.3.2.1 Time of climate emergence

The time of climate emergence from pre-industrial temperature variability has been widely used as a proxy for climate change timing (Mora et al. 2013a; Henson et al. 2017; Bruno et al. 2018). In the same vein, the time of climate emergence from a species' thermal tolerance range has recently been developed as an index of the timing of species exposure to dangerous climate conditions (Trisos et al. 2020; Xu et al. 2020; Meyer et al. 2024). This index provides a means of assessing whether exposure to hazardous climate change is an imminent or distant threat.

The time of initial climate emergence (ToE) for each species was estimated as the year in which the projected maximum annual temperature emerges from the species' thermal tolerance niche for two consecutive years. ToE calculations were made using the methods described in Trisos et al. (2020) for each species within each grid cell across its native geographic distribution. Whereas Trisos et al. (2020) used projections of mean annual temperature and an exceedance run length of 5 years, we used the hottest-month temperature and a run length of 2 years. In doing so, our ToE index quantifies the onset of thermal stress in species rather than mortality to inform climate risk. We used climate projections for the period 2025 to 2100. ToEs for species that did not exceed their thermal tolerances within this projection window were set at the maximum year of the projection. The ToE for each species and grid cell was estimated individually for each ESM and then averaged across all ensemble models. Equation 5 describes how climate exposure varies with the ToE. The equation ensures that ToE ranges between 0 and 1, and increases more rapidly as it approaches 0 and declines more slowly as it increases (Figure 20).

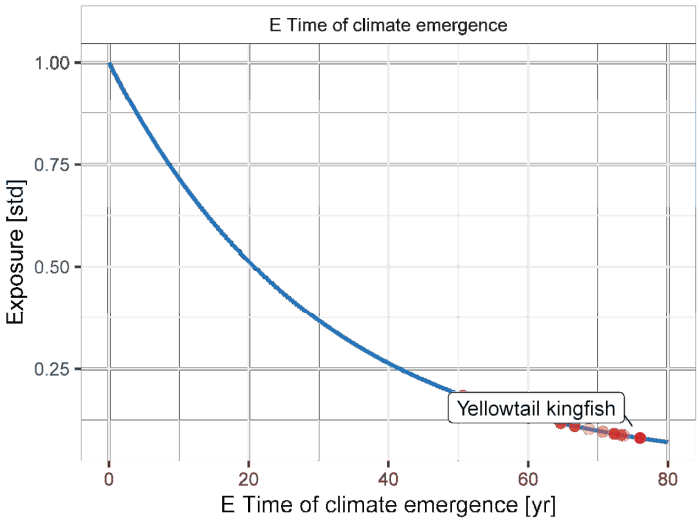


Figure 20: ToE standardization. The blue trend line depicts how Equation 5 maps the projected time of climate emergence (ToE; yrs) to standardised sensitivity scores (0–1). Red points are the ToEs and their standardised scores for yellowtail kingfish across the New Zealand EEZ.

In the case of yellowtail kingfish, projected temperatures are often within its broad thermal niche (~12 to ~29°C), leading to later times of climate emergence and lower sensitivity scores across the New Zealand EEZ (Figure 20 and Figure 21).

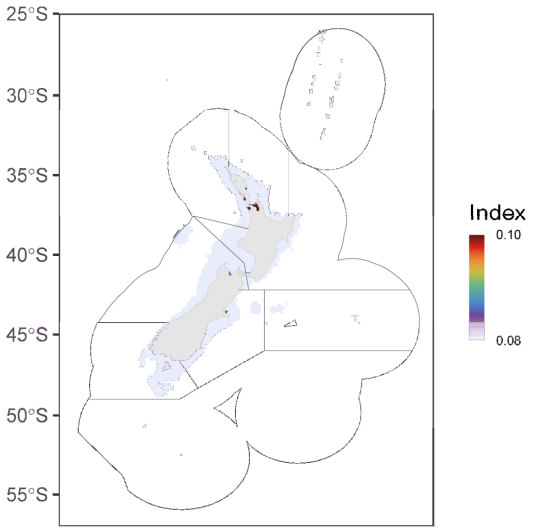


Figure 21: Exposure as a function of time of climate emergence for yellowtail kingfish across its geographic distribution. Light purple depicts low sensitivity, while orange and red show areas of high sensitivity.

3.3.2.2 Ecosystem disruption

Healthy, intact ecosystems are more resilient and resistant to stressors, including climate change (Frank et al. 2006; Frank et al. 2018; Cardinale et al. 2012; Boyce et al. 2015; Boyce et al. 2015a; Martin & Watson, 2016; Hillebrand et al. 2018; du Pontavice et al. 2020; Trisos et al. 2020; Irvine et

al. 2025). In contrast, less intact ecosystems are less resistant and resilient to stressors, including climate change. In addition to the direct effects of temperature on species via their physiological tolerances, climate change can also indirectly affect species by altering their predators, prey, and competitors (Frank et al. 2006; Frank et al. 2018; Boyce et al. 2015; Boyce et al. 2015a). Such ecologically mediated climate change effects on species are notoriously challenging to assess and understand *in situ* due to lagged predator-prey interactions, high collinearity among non-interacting species, and the scarcity of requisite data to disentangle these effects. Notwithstanding this, studies suggest that changes in the abundance or distribution of species can trigger cascading ecosystem effects, ecological regime shifts, and alternative stable states, thereby modifying ecosystem structure and function (Estes et al. 1998; Frank et al. 2005, 2011). Studies also indicate that these ecological effects tend to be more significant when the abundance of several species changes in concert. Research on biodiversity and ecosystem functioning also suggests an increased risk to ecosystem functioning as more species are removed (Worm et al. 2006).

To quantify the magnitude of ecological disruption resulting from an ecosystem's exposure to climate change, we calculated, for each location (grid cell), the fraction of all species that are thermally exposed before the maximum year in the projection window (2100). This index quantifies the risk of secondary ecological effects (e.g. changes in predation, prey availability, competition) due to climate change that species may be exposed to; it does not assume all species interact but instead captures the risk that a species will be impacted by the loss of other species in the system, which will increase with the fraction of species that are exposed.

Equation 6 describes how climate exposure varies with ecosystem disruption (Figure **22**). The equation standardises the index (0–1), normalises its distribution, and ensures that a species' exposure increases asymptotically with the fraction of species lost in its ecosystem, with the greatest exposure occurring for species inhabiting ecosystems with the greatest loss of species. This assumes that individual species are most affected when the ecosystem initially undergoes climate-driven restructuring (species loss); thus, exposure increases most rapidly for species loss up to ~50%. However, as climate-driven ecosystem disruption becomes sufficiently large, additional species losses are likely redundant; for example, losing 80% of species is functionally equivalent to losing 90%.

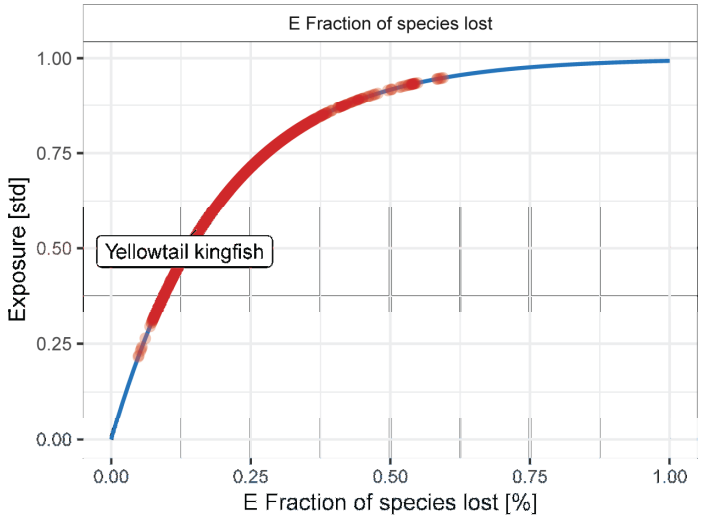


Figure 22: Ecological disruption standardization. The blue trend line depicts how Equation 6 maps ecological disruption to standardised sensitivity scores (0–1). Red points represent the ecological disruption values and their standardised scores for yellowtail kingfish across NZ.

In the case of yellowtail kingfish, the proportion of the species projected to be lost or redistributed due to climate change within the kingfish's ecosystem varies between ~5 and 60%, leading to spatially variable exposure scores across the New Zealand EEZ (Figure 22 and Figure 23).

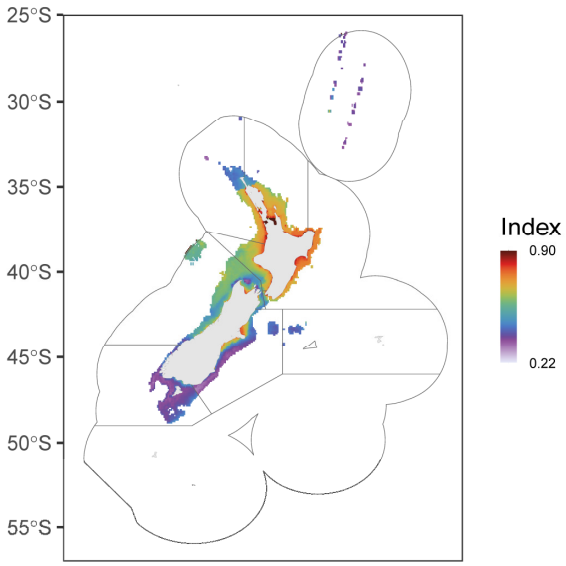


Figure 23: Exposure as a function of climate driven ecological disruption for yellowtail kingfish across its geographic distribution. Light purple depicts low sensitivity, while orange and red show areas of high sensitivity.

3.3.2.3 Loss of suitable thermal habitat

Temperature changes have caused, and are expected to continue to cause, geographic range expansions, contractions, and redistributions in marine species (Pinsky et al. 2013; MacKenzie et al.

2014; Shackell et al. 2014; Davies et al. 2017). Accordingly, changes in species' geographic ranges predicted by temperature shifts are frequently used to define their vulnerability to climate change (Cheung et al. 2009, 2015; Pinsky et al. 2013; Hazen et al. 2013; Shackell et al. 2014; MacKenzie et al. 2014; Ochoa-Quintero et al. 2015; Pacifici et al. 2015; Stortini et al. 2015; Davies et al. 2017; Foden et al. 2019; McHenry et al. 2019; Lavender et al. 2021; Reddin et al. 2022; Hodapp et al. 2023; Meyer et al. 2024). The nature and magnitude of such geographic range shifts will primarily depend on the correspondence between local temperature changes and the species' thermal-tolerance niche. Accordingly, we evaluated the extent of each species' estimated native geographic distribution that would be lost due to projected ocean warming. We did not assess the net change in the geographic distribution of species (e.g. the difference between habitat gained and habitat lost due to climate change) for several reasons. While range contractions can be driven by a single variable (*i* temperature), species expansions into new habitats depend on the favorability of several environmental and biotic factors that we did not evaluate (e.g. bathymetry, oxygen, acidity, ocean mixing, predators, prey, competition, dispersal). Evaluating species range expansions would require future projections in many of these environmental and biotic factors, which are, in many cases, unavailable. Even if such projections were available, using them to forecast species range expansions would introduce considerable uncertainty into our analysis. Further, this study aims to assess risk to current marine biodiversity rather than trying to project how biodiversity may shift in the future, which has been the focus of other studies (Garciá Molinos et al. 2016). Whereas many factors are needed to determine range expansions, the lethality of temperature alone can mediate range contractions. Therefore, our approach is conservative yet potentially simplistic for some species, as it predicts that most species will lose habitat but none will expand their range. Nonetheless, this index provides a valuable assessment of how the native geographic distribution of species could contract in response to climate change, while avoiding the assumptions, complexities, and data requirements involved in evaluating net distributional responses. Finally, because our framework does not evaluate the potential for geographic range expansions, it should be interpreted as the climate risk to the *in situ* persistence of species.

Projected changes in species geographic distributions that are attributable to temperature were estimated from the time of climate emergence from the thermal niche calculations described above. The number of grid cells in each species' native geographic distribution is projected to reflect its thermal niche by the end of the climate projection window (the year 2100) and was standardised to the total number of grid cells in that distribution using Equation 7. The equation standardises the index (0–1) and specifies that a species' exposure increases asymptotically with the fraction of thermal habitat loss, with the most significant exposure occurring for species that lose all of their present-day suitable thermal habitat (Figure 24).

The broad thermal niche of yellowtail kingfish ensured that projected temperatures were often within the preference range, resulting in very little thermal habitat loss, and low exposure (Figure 24 and Figure 24).

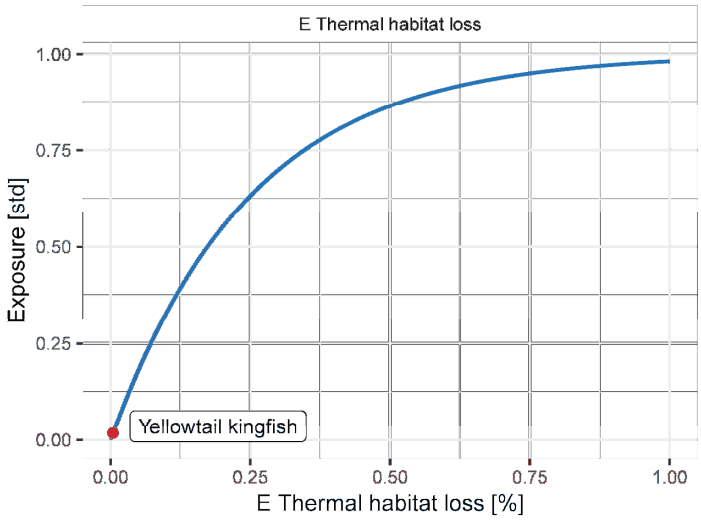


Figure 24: Thermal habitat loss standardization. The blue trend line shows how Equation 7 maps thermal habitat loss (as a fraction) to standardised exposure scores (0–1). Red points are the thermal habitat loss values and their standardised scores for yellowtail kingfish across the New Zealand EEZ.

3.3.2.4 Marine heatwaves

Globally, marine heatwaves (MHWs)—discrete, prolonged periods of anomalously warm ocean temperatures—have become markedly more common and persistent over the last century. From 1925–2016, their average frequency rose ~34% and duration ~17%, yielding ~54% more MHW days per year—clear, attributable signals of a warming climate superimposed on natural variability (Oliver et al. 2018). The biological consequences span from individual physiology to whole-ecosystem reconfiguration, including mass mortalities, recruitment failure, disease outbreaks, range shifts, and the loss of habitat-forming "foundation" species (kelps, corals, seagrasses), which, in turn, undermine fisheries productivity and coastal ecosystem services (Smale et al. 2019). Because MHWs integrate both the warming trend and short-term circulation/air-sea flux anomalies into extreme thermal exposures that organisms actually experience, they serve as powerful indicators of climate vulnerability (Hobday et al. 2016). For climate-risk applications, MHW metrics (e.g. frequency, duration and intensity) provide exposure measures that align closely with observed impacts, supporting species- and habitat-level vulnerability assessments and informing spatial planning (Frölicher et al. 2018; Smale et al. 2019; Benthuysen et al. 2020; Cheung & Frolicher, 2020; Jacox et al. 2020; Capotondi et al. 2024; Deser et al. 2024; Kajtar et al. 2024; Aitkenhead et al. 2025).

MHWs are particularly relevant in Aotearoa, New Zealand. Recent summers have featured several large MHWs, including the extreme 2017/18 Tasman Sea event that persisted for 138 days over millions of square kilometres, with a maximum intensity of 2.9°C, creating widespread ecological and sectoral impacts and the 2022/23 event that persisted for 289 days with a maximum intensity of 2.1°C (Salinger et al. 2024; Cook et al. 2025). Synthesis for New Zealand fisheries highlights observed and plausible effects on species of high value (e.g. mussels, salmon, snapper) via direct thermal stress, shifts in prey fields, altered biogenic habitats, and disease pathways that translate anomalous heat into measurable stock performance and economic outcomes (Cook et al. 2025). Economic analyses also link intense MHWs to future reductions in commercial catch, reinforcing their relevance to risk assessments and adaptation planning for the seafood sector (Lacheheb et al. 2024). In light of this, the CRIB was adapted for the New Zealand fisheries context to include an MHW exposure index.

Equations 8, 9, and 10 describe how climate exposure varies with the duration and magnitude of marine heatwave disruption (Figure 25). The equations standardise the index (0–1), normalise its distribution, and ensure that exposure increases asymptotically with exposure to hazardous marine heatwaves, with the greatest exposure occurring for species exposed to long-duration, high-magnitude warming events. Instead of calculating heatwave-specific events, these metrics aim to capture broad spatial patterns in the duration and intensity of a species' exposure to hazardous temperatures.

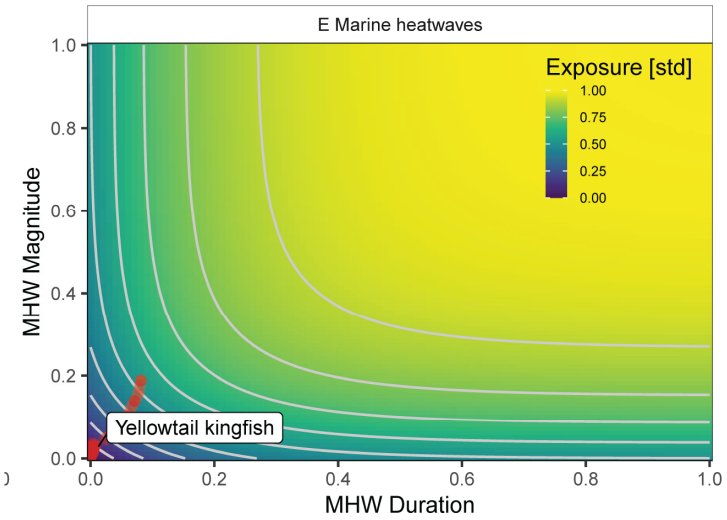


Figure 25: MHW standardization. The colours (blue to yellow) show how Equations 8, 9, and 10 map marine heatwave duration and magnitude to standardised exposure scores (0–1). Red points are the values for yellowtail kingfish across the New Zealand EEZ.

Yellowtail kingfish's broad thermal niche resulted in low MHW duration and magnitude, leading to low exposure (Figure 25 and Figure 26).

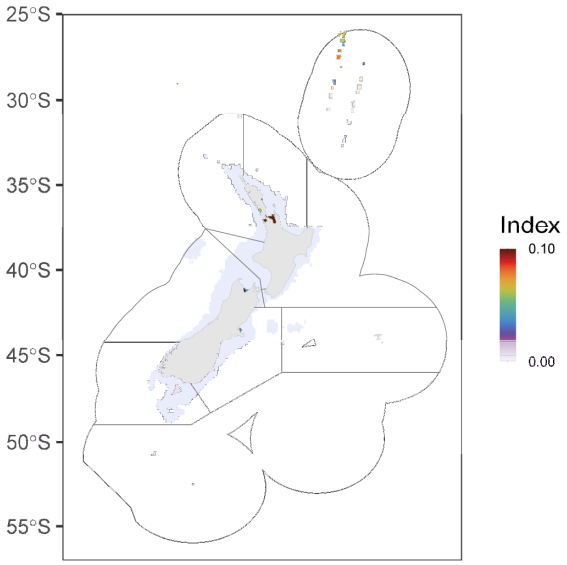


Figure 26: Exposure as a function of marine heatwave duration and exposure for yellowtail kingfish across its geographic distribution. Light purple depicts low sensitivity, while orange and red show areas of high sensitivity.

3.3.3 Adaptive capacity

3.3.3.1 Geographic range extent

Species distributed broadly are thought to have a greater adaptivity to climate changes; there is a greater breadth of suitable climatic and habitat conditions (e.g. climate refugia) within their geographic distributions, buffering them against adverse climate changes (Burek et al. 2008; Laidre et al. 2008; Ficetola & Denoel, 2009; Pearson et al. 2014; Staude et al. 2020). Alternatively, range-restricted species are more likely to depend on specific habitat types and thus vulnerable to climate-driven habitat alteration. The latitude spanned by species is significant to their climate vulnerability, as temperature and climate change impacts have consistently varied by latitude (Loarie et al. 2009; Boyce et al. 2010; Mora et al. 2013; Poloczanska et al. 2016; Boyce et al. 2020a). The total geographic range area (km^2)(Cheung et al. 2007; Davidson et al. 2012; Garcia et al. 2014; Albouy et al. 2020) and the latitude range of species(Cheung et al. 2007; Gonzalez-Suarez et al. 2013; Albouy et al. 2020) are frequently used in climate vulnerability analyses to index their adaptability or sensitivity to climate change.

An index of the adaptivity of each species was calculated as a bivariate function of the geographic range area (km^2) and the latitude spanned by their native geographic distributions over the spatial domain of our CCRA analysis (*i.e.* global). The geographic range (km^2) occupied by each species was calculated from its native geographic distribution at a 0.08° resolution and standardised to the maximum possible occupancy area for any marine species across the spatial domain of the analysis. Equation 11 and Equation 12 standardise the index (0–1), normalise its distribution, and ensure that adaptivity increases asymptotically with geographic range area and latitude spanned, with the greatest adaptivity occurring for species with the largest geographic range areas (Figure 27). Adaptivity was virtually uniformly high among species inhabiting >20% of the total area.

Yellowtail kingfish inhabits roughly 10% of the New Zealand EEZ spanning roughly 25 degrees of latitude, resulting in a moderate adaptivity value across the New Zealand EEZ (Figure 27).

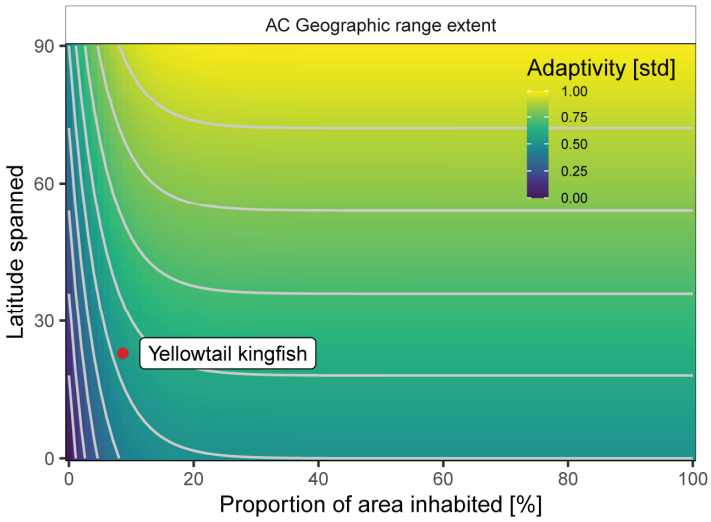


Figure 27: Geographic range extent standardization. The colours (blue to yellow) show how Equation 11 and Equation 12 map the area inhabited (%), and latitude spanned (°; truncated to 90) to standardised adaptivity scores (0–1). Red points are the values for yellowtail kingfish across the New Zealand EEZ.

3.3.3.2 Habitat fragmentation

Range fragmentation refers to the number of distinct habitat patches that a species occupies across its native geographic distribution. Marine species may exhibit fragmented habitats when suitable environmental conditions occur in discrete patches separated by unsuitable areas. It can result from habitat specialization, narrow environmental tolerances, oceanographic barriers, limited dispersal, or metapopulation structures characterised by multiple partially connected subpopulations. As a result, species distributions may comprise isolated or weakly connected habitat patches, potentially reducing connectivity and increasing vulnerability to environmental change.

Species with less fragmented habitat ranges have greater access to potentially favourable habitats (e.g. climate refugia), migration corridors, and larval dispersal. Alternatively, greater habitat fragmentation increases the isolation of habitat patches, reducing the probability that they can be recolonised following local extinctions (e.g. the 'rescue effect' (Brown & Kodric-Brown, 1977)) and increases the amount of edge habitat in those patches. Consequently, studies in terrestrial and marine systems have reported that species with fragmented geographic ranges are more sensitive to and less resilient to climate change impacts (Kaschner et al. 2006; Moore & Huntington, 2008; Gonzalez-Suarez et al. 2013; Pearson et al. 2014; Crooks et al. 2017; Rogan & Lacher, 2018; Albouy et al. 2020), primarily by affecting their extinction and colonization (e.g. Warren et al. 2001). Habitat fragmentation is also known to exacerbate the negative impacts of habitat loss on populations (Lehtinen et al. 1999; Fahrig, 2002; Rueda et al. 2013; Palmeirim 2020).

The extent of geographic habitat fragmentation for each species across the spatial domain here (*i.e.* the New Zealand EEZ) was calculated from their native geographic distribution. Whereas the original CRIB calculated habitat fragmentation as the number of patches standardised by the number of grid cells across the species' total geographic range, CRIB-NZ calculates it using the widely known largest patch index (LPI; Equation 13). This change was made because it was noted that, when migrating to a higher spatial resolution, the original fragmentation calculation was sensitive to the number of grid cells; under the previous formulation, a higher-resolution geographic range could lead to lower fragmentation even though the number of patches and total geographic range remained constant. Alternatively, the LPI correlates with related fragmentation indices, such as patch density and the

number of effective patches, but is less scale-sensitive to changes in grid resolution and fragment size. LPI is weakly sensitive to total range size or tiny fragments and is widely used in landscape ecology (Gao & Yu, 2014; Ojoyi et al. 2016; Chen et al. 2023; Jiang et al. 2023). Accordingly, the LPI will be incorporated into the original CRIB framework as well. After calculation, the LPI was standardised via Equation 14. The equation standardises the index (0–1), normalises its distribution and specifies that adaptivity due to habitat fragmentation declines asymptotically with geographic range fragmentation, with the lowest adaptivity occurring for species with highly fragmented habitats (Figure 28). Adaptivity was uniformly low across species in which a single large patch comprised <50% of their present-day distribution.

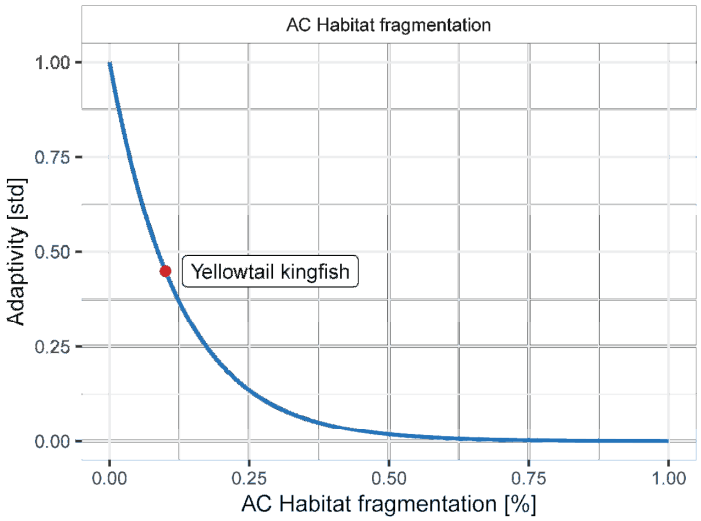


Figure 28: Habitat fragmentation standardization. The blue trend line depicts how Equation 13 to Equation 14 map habitat fragmentation (fraction) to standardised adaptivity scores (0–1). Red point is the value for yellowtail kingfish across the New Zealand EEZ.

In the case of yellowtail kingfish, the largest patch comprised over 80% of its native geographic range, leading to moderate adaptivity scores across the New Zealand EEZ (Figure **28**).

3.3.3.3 Thermal habitat variability and use

Ecological disturbance theory suggests that species and ecosystems that experience high natural variability are better adapted to cope with climate change (Nadeau et al. 2017); empirical analyses have supported this theory (Cole et al. 2014; Mora et al. 2015). Species inhabiting more variable thermal environments, such as at the range edges of their geographic distributions, are more resilient to climate change (Carilli et al. 2012; Guest et al. 2012; Donner & Carilli, 2019) and are believed to be less sensitive to it (Albouy et al. 2020). Continued exposure to temperatures near the species' thermal limits is thought to 'stretch' their thermal niche and pre-adapt them to temperatures outside their thermal preferences. Through this mechanism, species can exhibit varying levels of plasticity in their thermal sensitivity in response to variability in their thermal environment (Rehm et al. 2015).

Existing approaches to quantifying thermal pre-adaptation often rely on measures of environmental inclusion (i.e. the proportion of local environmental temperatures that fall within a species' thermal niche). These approaches may overestimate adaptive capacity in environments where thermal conditions are consistently within the species' niche but occupy only a narrow portion of it. In such cases, the species is not exposed to the full breadth of its potential thermal niche, limiting opportunities for physiological or ecological "stretching" that may promote adaptation.

To address this limitation, we quantified weighted thermal niche coverage, defined as the effective breadth and evenness of temperatures experienced by a species within its thermal niche. This approach builds on established methods in ecological diversity theory, in which Shannon entropy and its exponential transformation (Hill numbers) are used to quantify the effective number of categories occupied by a distribution. These metrics have been widely used to characterise diversity, evenness, and functional breadth in ecological systems (Hill, 1973; Jost, 2006; Chao et al. 2014) and are extended here to temperature distributions to quantify the effective breadth of thermal exposure.

Thermal niche coverage and thermal habitat range are calculated using Equation 15 to Equation 17 and were standardised via Equation 18 to Equation 19. The equations specify that adaptivity due to thermal habitat pre-adaptation increases with the proportion of the thermal niche covered by the environment, the evenness of that coverage, and the breadth of thermal habitats inhabited. Species that inhabit broader thermal habitats that occupy a greater proportion of their thermal niche have a higher adaptivity than those that inhabit a narrower range.

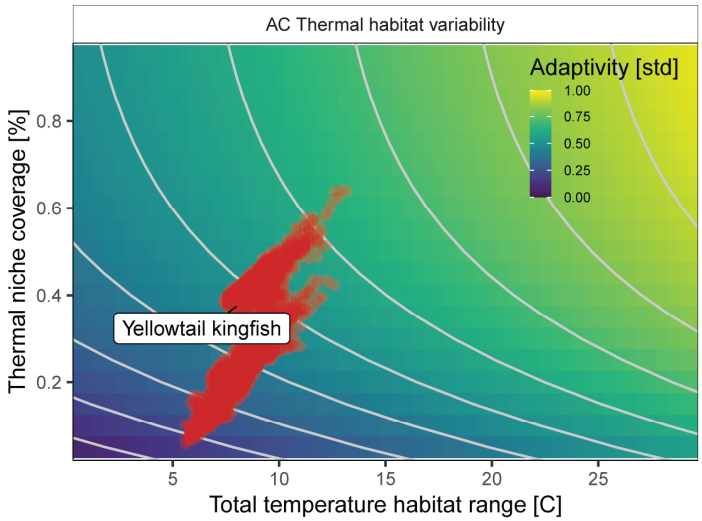


Figure 29: Thermal habitat use standardization. The colours (blue to yellow) show how Equation 17, Equation 18, and Equation 19 map thermal niche coverage (fraction) and total temperature range (°C) to standardised adaptivity scores (0–1). Red points are the scores for yellowtail kingfish across the New Zealand EEZ.

In the case of yellowtail kingfish, the wide range of its thermal habitat and broad thermal coverage resulted in moderate adaptivity scores across the New Zealand EEZ (Figure 29 and Figure 30).

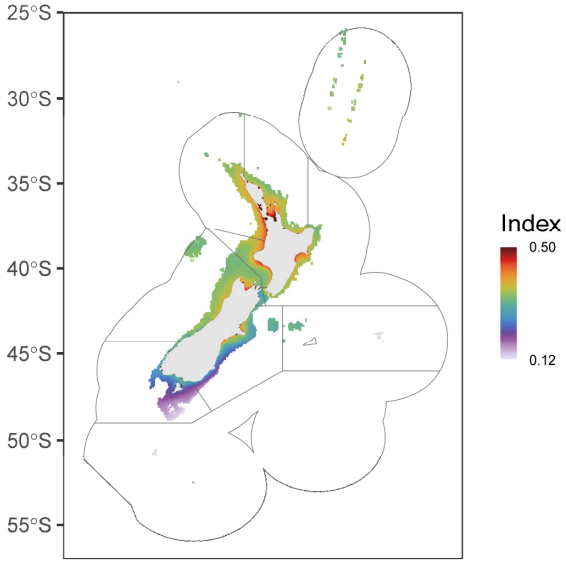


Figure 30: Adaptivity as a function of thermal habitat variability and use for yellowtail kingfish across its geographic distribution. Light purple depicts low sensitivity, while orange and red show areas of high sensitivity.

3.3.3.4 Maximum body length

The maximum size (length or mass) reached by species has been commonly used as a proxy of extinction risks, susceptibility to exploitation, and vulnerability to climate change (Cheung et al. 2007; Davidson et al. 2012; Chessman, 2013; Cheung et al. 2013; Gonzalez-Suarez et al. 2013; Cheung & Oyinlola, 2018; Foden et al. 2019; Albouy et al. 2020). The maximum size is a predictor of several life-history traits (e.g. generation length, time to maturity, intrinsic rate of population increase) that cumulatively define species' potential reproductive capacity and population growth rate (Fenchel, 1974; Blueweiss et al. 1978; Cheung et al. 2007; Healy et al. 2014; Cheung & Oyinlola, 2018). Ecologically, body size has been used to classify species as *r*- (produce many offspring, high growth rates and mortality) or *K*-selected (produce fewer offspring, low growth rates and mortality). For these reasons, the maximum body length was used as an indicator of species' resilience or adaptivity to the potential adverse effects of climate change, whereby smaller species that grow and reproduce faster have a higher adaptivity(Cheung et al. 2007; Davidson et al. 2012; Chessman, 2013; Cheung et al. 2013; Gonzalez-Suarez et al. 2013; Pearson et al. 2014; Cheung & Oyinlola, 2018; Foden et al. 2019; Albouy et al. 2020). The maximum body length of species (cm) was obtained from the Marine Organismal Body Size (MOBS) Database (McClain et al. 2025).

Equation 20 and Equation 21 describes how climate adaptivity varies with maximum body length. The equation standardises the index (0–1). Through this approach, much of the change in adaptivity occurs with changes in maximum body length ranges between 0 and 100 cm, which seems biologically plausible considering the dramatic differences that exist in population doubling time between the smallest plankton (days) to fish that can reach 100 cm (e.g. Shortfin mako; ~24–yrs). The equations predict that a species' adaptivity declines asymptotically with its maximum possible length, with the lowest adaptivity occurring for species with larger body sizes that have slower growth rates, population doubling times, and lower mortality rates (Figure 31). The most rapid changes in $AC\ Mlen_s$ occur for small-bodied species, such as those with body lengths between 0 and 5 m and decline more moderately thereafter.



Figure 31: Maximum body length standardization. The blue trend line depicts how Equation 20 and Equation 21 map maximum body length (cm) to standardised climate adaptivity scores (0–1). Red points are the values for yellowtail kingfish across the New Zealand EEZ.

Yellowtail kingfish reach maximum sizes of 250 cm, conferring them as moderately r-selected, resulting in a moderate climate adaptivity score across the New Zealand EEZ (Figure 31).

3.3.4 Climate vulnerability

CRIB produces spatially explicit outputs (e.g. estimates for each species at each location across its geographic range) that can also be summarised taxonomically (e.g. estimates for each species averaged across its geographic range). Vulnerability can also be estimated using both reliability-weighted and unweighted approaches. Unweighted vulnerability offers the benefit of a simple, straightforward interpretation. Weighting allows the variability across the climate indices to be statistically accounted for in the final vulnerability estimate. Weighting offers a means of propagating the statistical reliability of the dimensions forward in the analysis, but can sometimes produce counterintuitive results. For instance, vulnerability under high-emission scenarios can, at times, be lower than under low-emission scenarios if their climate projections diverge more (higher variance = lower weighting). Both weighted and unweighted approaches are presented here, with unweighted vulnerability presented for the case study species.

3.3.4.1 Spatially explicit vulnerability

For each species within each grid cell that comprises its native geographic distribution, sensitivity, exposure, and adaptivity were calculated as the average of the four indices that define them. The standard deviation of these vulnerability dimensions provided an estimate of their statistical uncertainty and can be propagated forward through all subsequent vulnerability calculations using variance weighting (see below).

Because sensitivity analyses suggested that omitting any of the 12 climate indices from a grid cell could affect vulnerability scores (Boyce et al. 2022), the analysis was restricted to cells that contained all 12 indices. Sensitivity analyses indicated that species could have upwards of 10% of grid cells across their native geographic distribution missing (e.g. one or more of the 12 indices could not be calculated due to missing data), with minimal effect on the vulnerability scores, so 10% was used as a threshold for acceptable geographic missingness.

Climate sensitivity, exposure, and adaptivity are calculated from the standardised climate indices that define them, resulting in spatially explicit estimates across the species' geographic distribution (Figure 32).

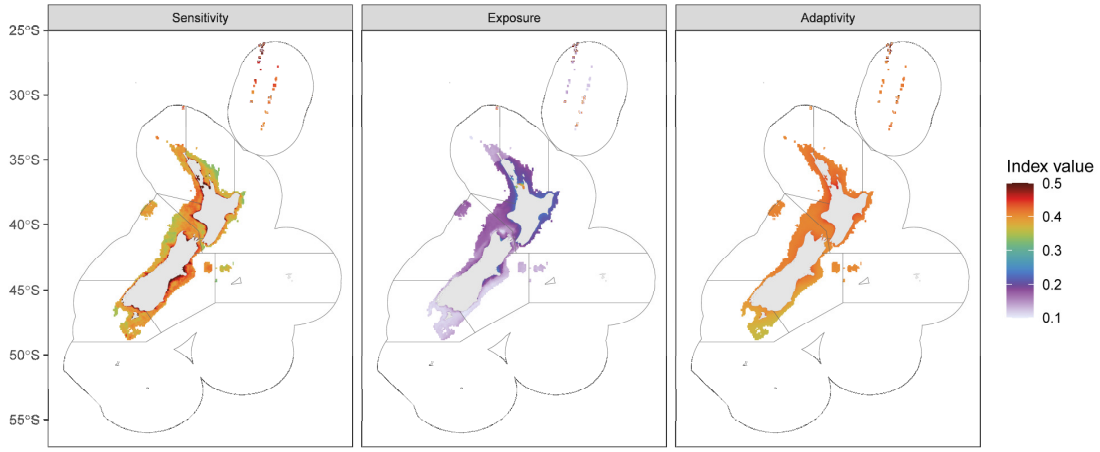


Figure 32: Dimensions of vulnerability for yellowfin kingfish. The sensitivity (left), exposure (middle) and adaptivity (right) of kingfish are calculated from the 12 indices across its native geographic distribution.

For each species, s, and grid cell, c, across their native geographic distribution, vulnerability ($V_{s,c}$) is calculated from sensitivity, exposure, and adaptivity, while accounting for the statistical uncertainty associated with indices of climate exposure derived from ensemble climate projections using discounting. Discounting is common in economics and has also been used in ecological studies (e.g. Halpern et al. 2012) to account for the greater uncertainty associated with unknown future states. Its use in vulnerability analyses is analogous: the projected future exposure of species to climate change, estimated from ESM projections, is less well resolved than their sensitivities or adaptive capacities, which are primarily based on current and historical conditions, respectively. Confidence in the veracity of the projected exposure indices is affected primarily by the length of the climate projection and the number of ensemble projections, and as such, defines a discount rate ∂. With all else being equal, exposure indices derived from single ESMs that make longer-term climate projections are less reliable (Mora et al. 2013; Eyring et al. 2019; Lotze et al. 2019; Boyce et al. 2020a) and are thus more heavily discounted. Those derived from a larger ensemble of ESMs that make shorter-term projections are perceived as more reliable and are discounted less.

Equation 22 to Equation 24 describe the discount rate calculation and Figure 33 illustrates it. Under this calculation, a maximum discount rate of 5% applies when projections are made for ≥100 years from a single projection, and are 0% when projections are made for <5 years from >19 projections. A discount rate of 5% was adopted because it falls within the range commonly used in environmental and public-policy analyses and reflects a moderate weighting of near-term versus long-term climate impacts (Groom et al. 2022). The case study presented here evaluated climate projections from 3 models over 80 years, yielding a discount rate of 4.1%. To conserve the vulnerability scaling to between zero and one, discounts applied to exposure are credited to sensitivity (e.g. the current state), such that the maximum total adjustment across aggregate exposure and sensitivity is 10%.

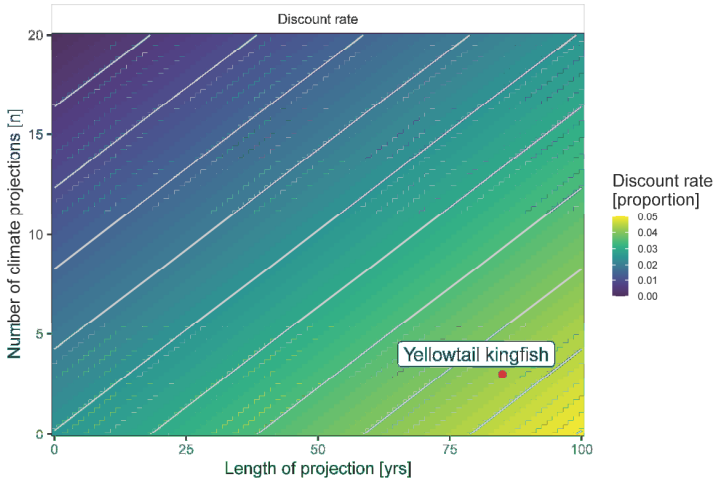


Figure 33: Discount rates. The discount rate on future exposure, credited to the present state, is a function of the length of the climate projection(s) and the size of the ensemble.

Unweighted vulnerability is calculated as the average of adaptivity, discounted exposure and credited sensitivity. Alternatively, weighted climate vulnerability can be calculated from adaptivity, discounted exposure and credited exposure via Equation 25 to Equation 28.

Spatially explicit vulnerability for kingfish across the totality of its geographic distribution under contrasting emission scenarios is shown in Figure 34.

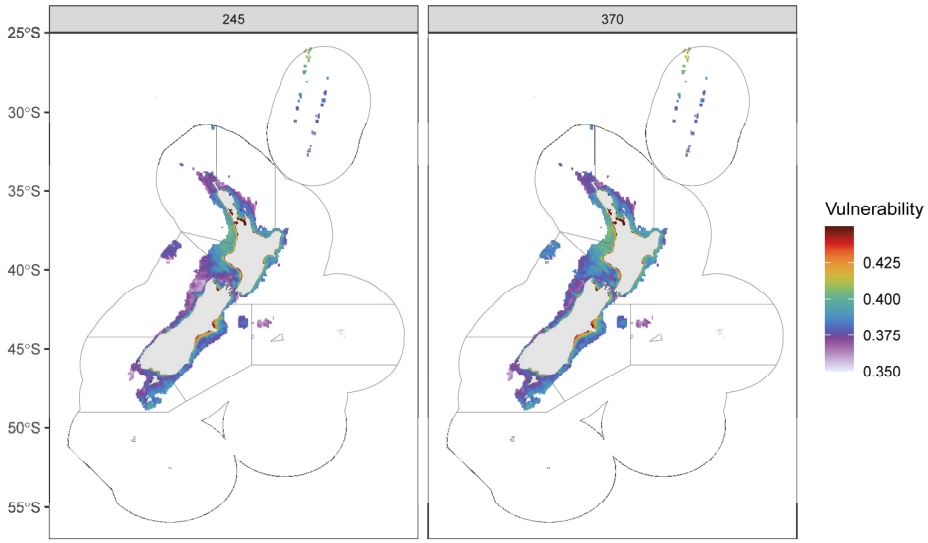


Figure 34: Geographic patterns of climate vulnerability for yellowtail kingfish. The vulnerability of kingfish across its native geographic distribution was calculated from the 12 indices using Equation 25. Vulnerability is displayed under SSP2-4.5 (left) and SSP3-7.0 (right).

3.3.4.2 Spatially implicit vulnerability

For each species under each emission scenario, unweighted vulnerability is calculated as the average vulnerability across the species' geographic distribution, providing a more straightforward interpretation. The standard deviation provides an estimate of statistical uncertainty.

Alternatively, weighted vulnerability for each species was calculated as a variance-weighted mean of the vulnerabilities in each grid cell across its geographic distribution via Equation 29 to Equation 33. Under these formulations, greater statistical weight is given to vulnerability estimates in grid cells where their variance (e.g. across the indices used to calculate them) is lower, and vice versa. Species vulnerability estimates will be more variable when vulnerability differs more across the grid cells that comprise its geographic distribution, and vice versa.

Table 5: Summary of the significant edits made to develop the CRIB-NZ CVA.

Element	Edits
Data: high-resolution outputs	All input data layers were harmonised (regridded) to match the resolution of the GLORYS temperature dataset (0.083°).
Data: temperature projections	Surface and bottom temperature projections were sourced from two high-resolution global ESM models and one high-resolution regional ESM.
Data: historical temperatures	High-resolution monthly surface and bottom temperatures were sourced from a Global Ocean Physics Reanalysis produced by the Copernicus Marine Service Global Monitoring and Forecasting Centre (GLORYS).
Data: maximum body lengths	Maximum species body lengths were sourced from the Marine Organismal Body Size (MOBS) Database for 85 204 marine animal species across 30 phyla representing 40% of valid marine animal species listed in the World Register of Marine Species (WoRMS); (McClain et al. 2025).
Data: species distributions	To obtain estimates of geographic distribution for as many New Zealand marine species as possible (e.g. not only exploited ones), high-resolution species distribution estimates from AquaX were used. New Zealand-specific SDMs from NIWA (ESNZ) and DOC were also explored (Reygondeau et al. 2026).
Data: conservation status	To provide nationally- and fisheries-specific estimates of species conservation status, the assessed probability of stock overfishing was used based on New Zealand's annual report on the status of New Zealand's fish stocks.
Index: marine heatwaves	The climate velocity index was replaced with an index of marine heatwave duration and magnitude. Marine heatwaves are species-specific, depending on each species individual thermal niche, and have been identified as an important climate impact in New Zealand.
Index: conservation status	The MPI assessed probability of a stock being overfished was used as an index of the species' conservation status. Previous CRIB iterations specified a spatially implicit conservation status, whereas the probability of overfishing is spatially explicit.
Index: vertical habitat variability and use	The index definition was expanded to include both bottom- and surface-associated species, defined by their vertical habitat depth and mobility.
Index: habitat fragmentation	The metric used to denote habitat fragmentation was changed from patch density to the largest patch index (LPI). The LPI is conceptually similar to and correlated with patch density, but is less sensitive to changes in the analysis grid resolution and range size, thereby providing a more robust metric of fragmentation.
Index: thermal habitat use	The area under the thermal niche index was replaced with a weighted niche coverage metric. This new metric more robustly captures the extent to which a species' thermal niche is covered by temperature fluctuations in its habitat.

4 Results

To illustrate the CRIB-NZ, vulnerability estimates are provided for eight case study species under two emission scenarios (SSP2.45 and SSP3.70) to 2100, first across the entire study area (e.g. the New Zealand EEZ) and then within FMA 5 (Southland).

4.1 Climate vulnerability across the New Zealand Exclusive Economic Zone

The CRIB-NZ framework was applied to the eight case study species to demonstrate its implementation, show the outputs that can be generated, and explain how they can be viewed and interpreted. For any species with sufficient input data, the CRIB-NZ framework produces geographically explicit, standardised climate vulnerability outputs for all locations where they occur under differing emission scenarios (Figure 35). For the eight case study species, climate vulnerability exhibits significant variability both across species and across their native geographic distributions. Consistent with previous CVA analyses, vulnerability for most species varied by latitude, often being elevated at lower latitudes and declining towards the southern extent of their distribution. Vulnerability was generally higher in nearshore waters, where warming is often more intense, cumulative impacts such as fishing and eutrophication are elevated, and shallower ocean depths limit vertical migration (increasing climate sensitivity).

The CRIB-NZ framework enables ranking the climate vulnerability of candidate species from most to least vulnerable, as well as providing the 12 indices and their geographic variation (Figure 36). It also provides diverse information on climate impacts for each species, including its present-day sensitivity, projected exposure, and inherent resilience to climate change (Figure 37). For those seeking to understand how climate vulnerability for each stock arises, the 12 indices provide detailed information on the components that define it, including where it is highest, when it is expected to first emerge, why it arises, and how it could be reduced. Across the New Zealand EEZ, much of the variation in vulnerability across species is evident in the projected thermal habitat loss, present-day thermal safety margin (TSM), and vertical habitat. Other indices, such as cumulative impacts, vary little because these species occupy broadly similar geographic areas, particularly along coastlines where cumulative impacts are highest, and are therefore exposed to a similar range of cumulative impacts.

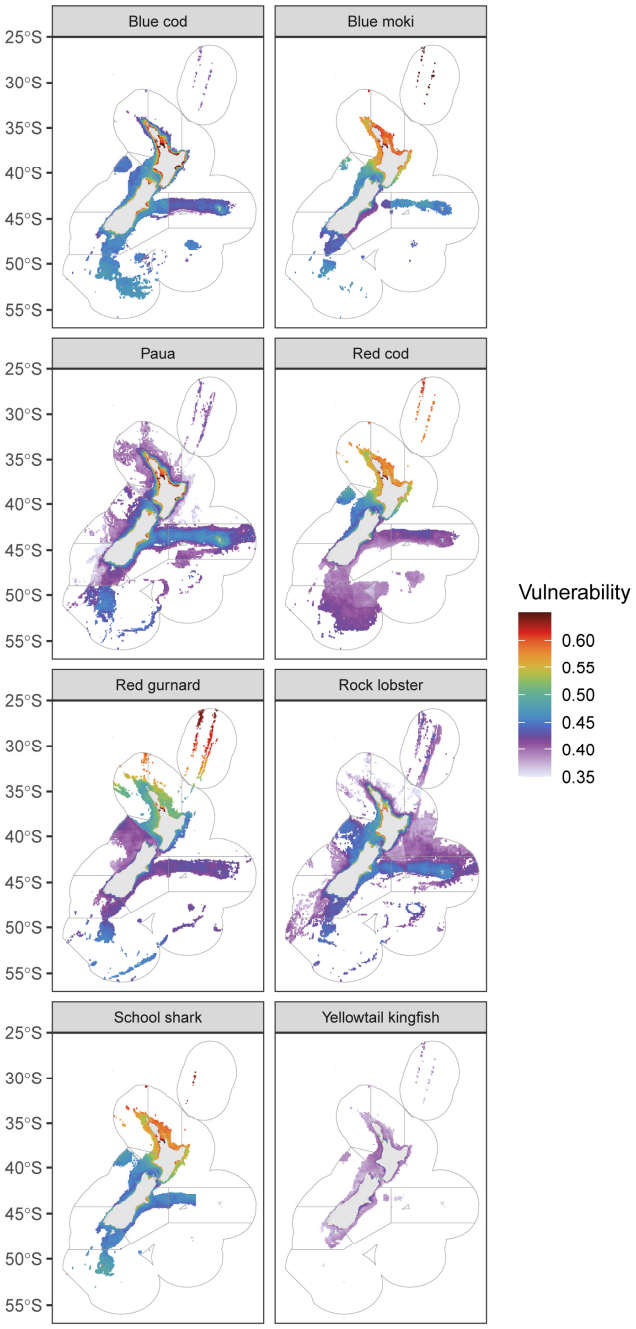


Figure 35: Geographic patterns of climate vulnerability across the New Zealand EEZ under SSP-3.70 to 2100. Note: these outputs should be interpreted as illustrative. Final vulnerability scores using the CRIB-NZ require additional vetting of input data sets on spatial distribution.

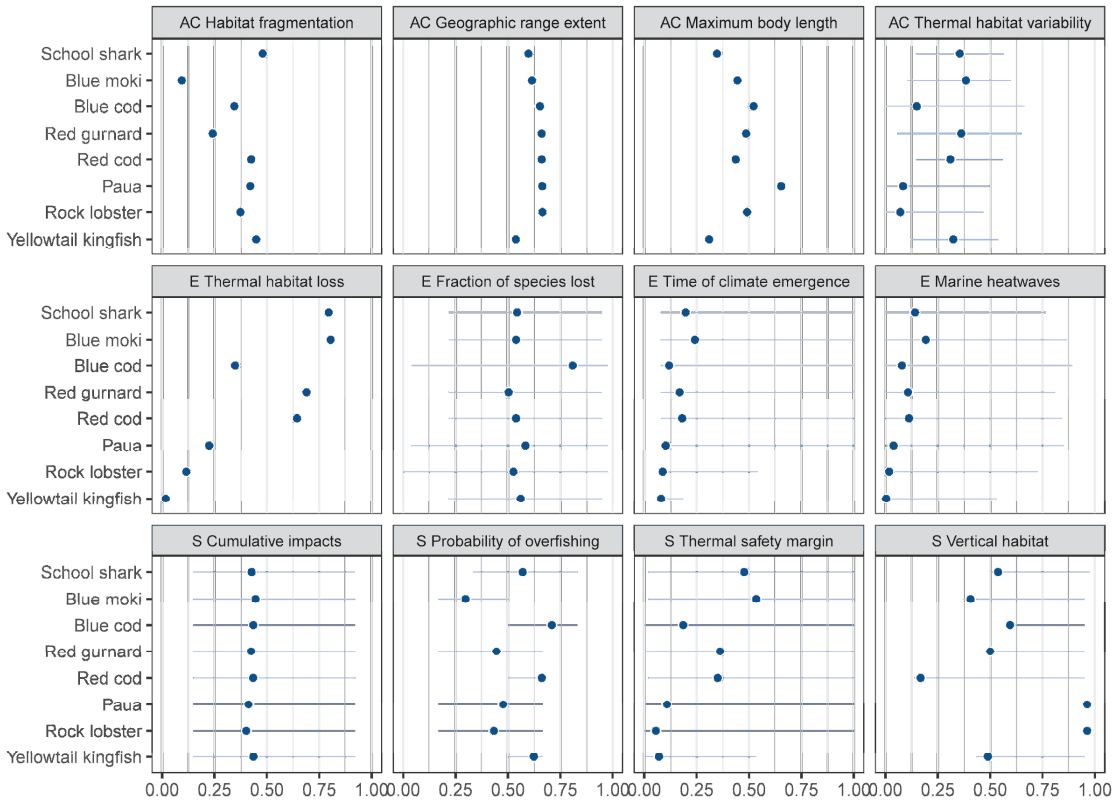


Figure 36: Taxonomic variation in the 12 CRIB-NZ indices across FMA5. Note: these outputs should be interpreted as illustrative. Final vulnerability scores using the CRIB-NZ require additional vetting of input data sets on spatial distribution.

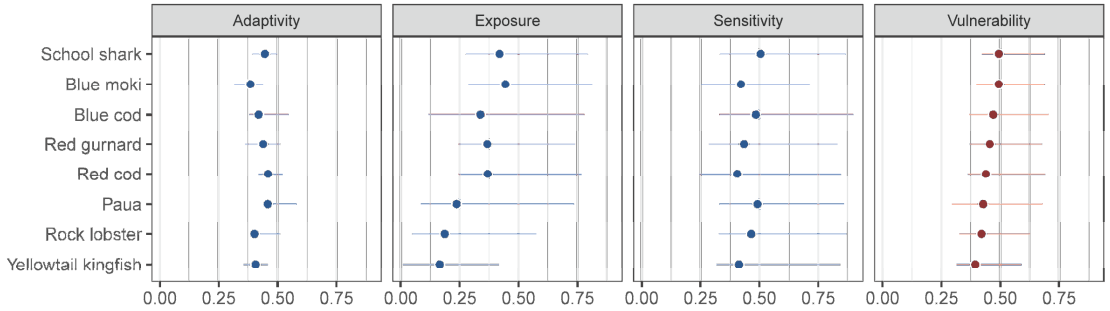


Figure 37: Taxonomic variation in the 3 CRIB-NZ dimensions and vulnerability across FMA5. Blue depicts the three dimensions that are used to calculate climate vulnerability (red). Note: these outputs should be interpreted as illustrative. Final vulnerability scores using the CRIB-NZ require additional vetting of input data sets on spatial distribution.

All indicators, dimensions and vulnerability within the New Zealand EEZ for all species can also be visualised in a stoplight plot (Figure 38), providing a synoptic overview. With this approach, broad-scale patterns and outlying results are more easily seen, which can be helpful in diagnosing interesting findings and quality-checking the outputs. For instance, it can be seen that pāua and rock lobster have the highest climate sensitivity via vertical habitat, by virtue of their close proximity to the seafloor and inability to range vertically. It's also apparent that two of the climate exposure indices—time of thermal emergence and marine heatwaves—are positively correlated. While collinearity runs counter to the design principles of the CRIB, which prioritise indices that provide unique information, the marine heatwave index was requested and therefore retained in CRIB-NZ.

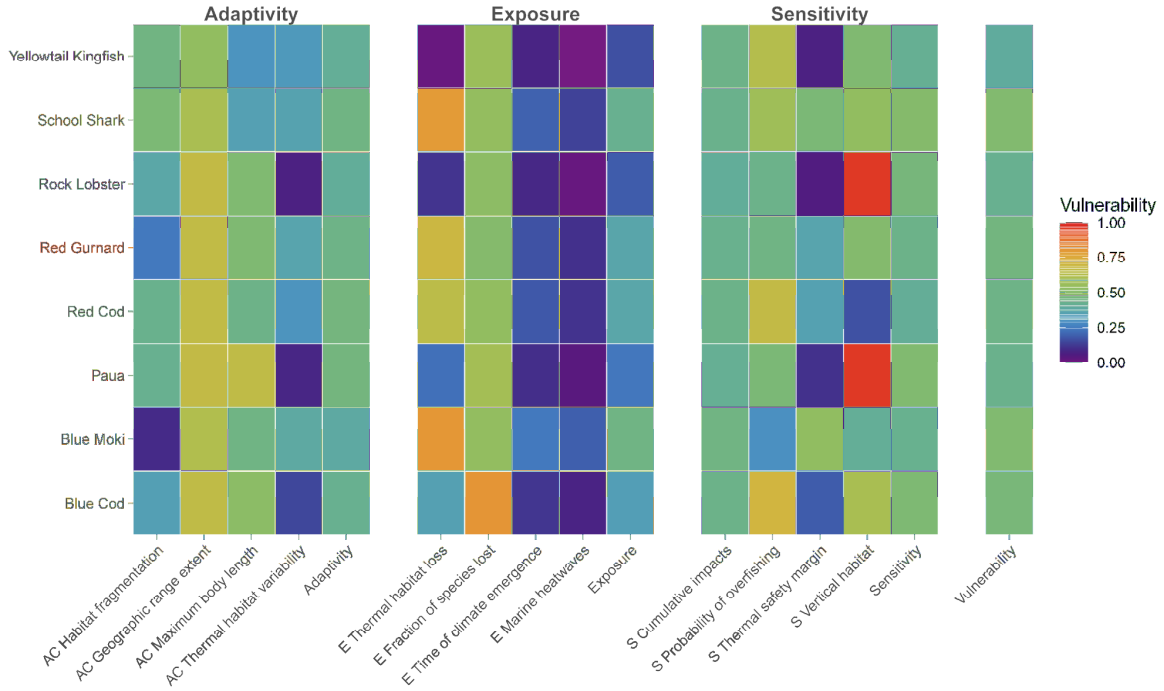


Figure 38: Stoplight plot of climate vulnerability in FMA 5. Colours depict scores for climate indices, dimensions and vulnerability for the case study species across FMA 5 under SSP-3.70 to 2100. Note: these outputs should be interpreted as illustrative. Final outputs require additional vetting of input data sets on spatial distribution.

4.2 Climate vulnerability across FMA 5 (Southland)

Since the CRIB-NZ framework is spatially explicit, its outputs can be flexibly spatially aggregated to evaluate vulnerability at different spatial resolutions. To demonstrate this, the national-scale vulnerability outputs were overlaid with Fisheries Management Area 5, and average vulnerability, its dimensions, and indices, along with their variances, were calculated for each species. This procedure captures the geographic and taxonomic variability in climate vulnerability within New Zealand's Fisheries Management Area 5 (Figure 39). Climate vulnerability scores across FMA 5 were lower than in other New Zealand areas, particularly those in the far north. While lower, areas of elevated vulnerability along the southernmost coastline were still apparent for several species—for instance, blue cod, paua, school shark, blue moki, rock lobster and red gurnard.

Within FMA 5 and under SSP-3.70, the highest vulnerability was observed for blue cod, school shark and blue moki, species with relatively narrow thermal niches (range: 11–15°C). The higher vulnerability of these species was in part due to lower thermal tolerances, leading to greater projected thermal habitat loss, earlier climate emergence, longer durations, greater-magnitude exposure to marine heatwaves, and narrower thermal safety margins. For instance, the most climate-vulnerable species in FMA 5 was blue cod, which had the narrowest thermal niche (11°C) and the second-lowest thermal limit (19°C) among the case study species. Blue cod and school shark also had higher-than-average probabilities of being overfished. Alternatively, yellowtail kingfish exhibited a broad thermal tolerance (range: ~17°C) and had the highest thermal tolerance (~29°C), thereby conferring lower exposure, sensitivity, and overall vulnerability relative to the other case study species.

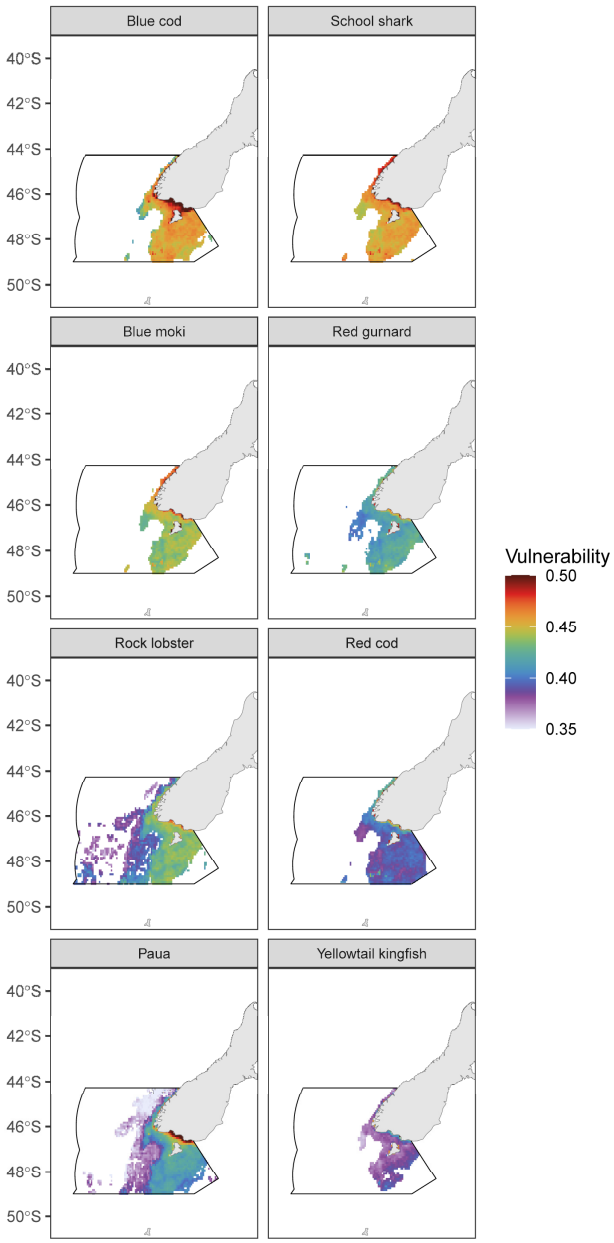


Figure 39: Geographic patterns of climate vulnerability across FMA 5 under SSP-3.70 to 2100. Note: these outputs should be interpreted as illustrative. Final outputs require additional vetting of input data sets on spatial distribution.

Whereas the standardised CRIB outputs are helpful for integrating and comparing vulnerability, the individual raw (e.g. unstandardised) indices can also provide specific information that is sometimes easier to interpret. For instance, TSM provides easy-to-interpret information about the climate

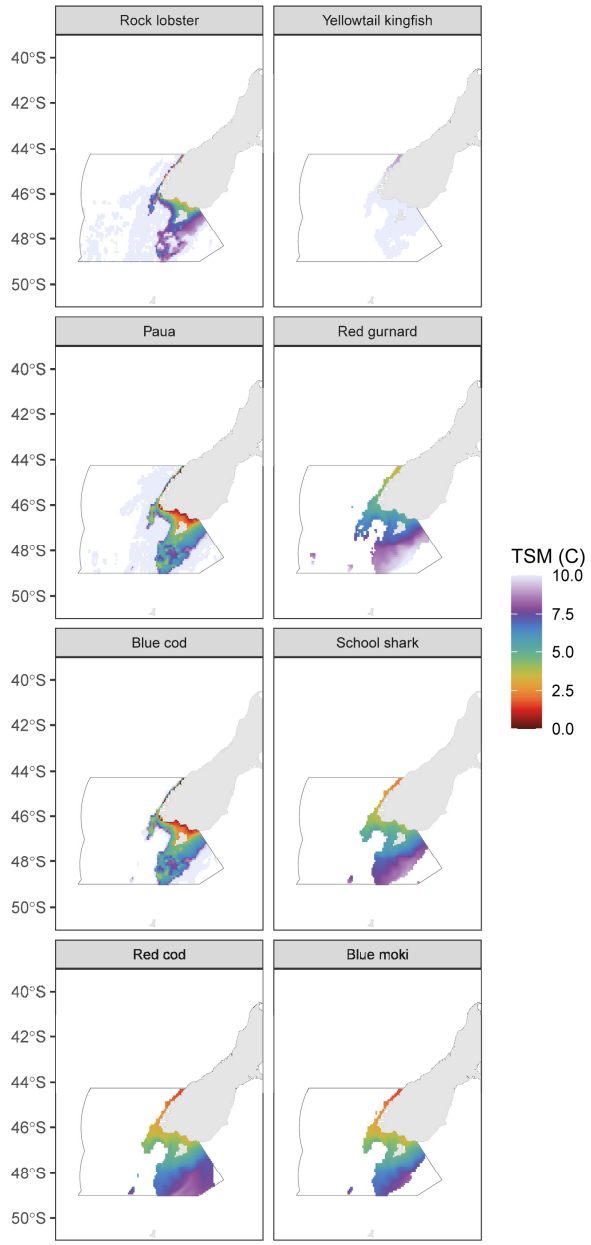


Figure 40: Geographic patterns in the thermal safety margin (°C) across FMA 5. Yellow and red depict areas where the TSM is small (<3°C), and blue and purple depict areas where it is larger (>6°C). Note: these outputs should be interpreted as illustrative. Final outputs require additional vetting of input data sets on spatial distribution.

sensitivity of species and how it varies spatially (Figure 40) while the year of climate emergence can be helpful in understanding the projected timing of hazardous climate changes on species. Such focused analyses can be helpful when viewed jointly; for instance, whereas the TSM evaluates how

close species are to thermal stress (°C), the ToE assesses whether this climate sensitivity will materialise and whether it will occur imminently or in the distant future (yrs). Such information can provide more nuanced insights into climate impacts on species, which could inform climate narratives for individual species and locations.

The ability to spatially aggregate CRIB-NZ vulnerability outputs offers advantages for fisheries, which are assessed and managed spatially. For instance, vulnerabilities could be aggregated at the scale of Quota Management Areas (QMAs), which denote the geographic boundaries for fisheries stock assessments. Figure 41 illustrates this, demonstrating how rock lobster climate vulnerability varies across and within its fisheries management boundaries. This feature means that climate vulnerability could feasibly be estimated for all marine stocks, and the resulting information could be included in stock assessment reports and used when making quota decisions. Because the CRIB-NZ vulnerability scores do not depend on available evidence (e.g, published studies, assessments, or reports), vulnerability can, in theory, be estimated for any stock, even data-limited stocks for which assessments do not exist.

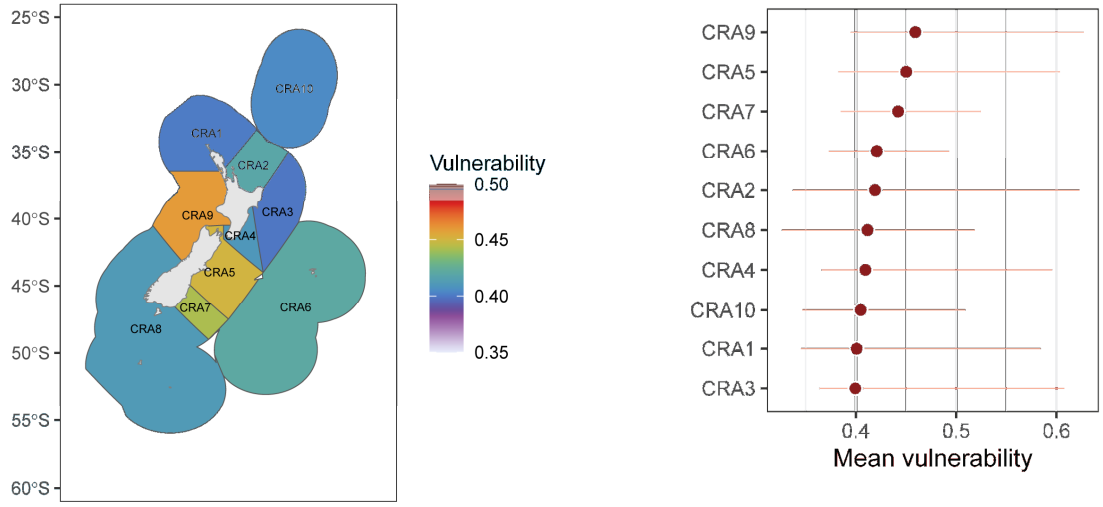


Figure 41: Geographic patterns in the vulnerability of rock lobster across its stock management boundary areas (QMAs). Left: Yellow and red depict areas of high vulnerability, and blue and purple depict areas of lower vulnerability. Right: points depict the average vulnerability within lobster QMAs, and the lines are the minimum and maximum values in each QMA.

4.3 Contrasted vulnerability for pāua

The estimates from CVAs are exceedingly challenging to empirically validate. In many cases, only a single CVA exists within a given spatial domain or species, and independent studies of climate impacts for comparison may be entirely lacking. Where different CVAs exist, methodological differences can obscure comparisons between them. For instance, CVAs can be carried out across slightly different spatial domains, evaluate different impact drivers, draw on different information sources, and assess different dimensions of vulnerability using different approaches. For these reasons, CVA validations are exceedingly rare.

Notwithstanding these issues, we sought to compare the output from CRIB-NZ to independent analyses. Whereas the case studies presented here are primarily intended to illustrate the CRIB-NZ framework's functioning rather than to provide final, fully quality-checked vulnerability estimates, such a comparison can still be valuable for investigating strengths and limitations of different CVA approaches and identifying input data that may require further investigation. We could locate only a single report that provided a semi-quantitative trait-based climate evaluation based on the NOAA rapid vulnerability assessment approach (Morrison et al. 2015; Hare et al. 2016), combining literature

reviews with environmental projections, species summaries, and expert workshops, of three New Zealand species: pāua, snapper and hoki (Cummings et al. 2021). Of these, only pāua was a case study species.

Of the eight case study species in the CRIB-NZ analysis across the New Zealand EEZ, pāua was ranked the 6th most vulnerable (Figure 35). Evaluating pāua's upper thermal niche (19°C) against historical, present-day, and projected temperatures suggested minimal projected thermal range loss, interaction with marine heatwaves, ecological disruption, and more distant years of climate emergence, along with larger thermal safety margins—all suggestive of lower climate exposure (Figure 35). Pāua also scored relatively high in climate adaptation, primarily due to its broad, contiguous geographic distribution and r-selected life-history strategy. However, pāua was also ranked higher in climate sensitivity, primarily due to its relative inability to range vertically.

In contrast, Cummings et al. (2021) assessed pāua vulnerability as "very high" based primarily on its traits: limited mobility, habitat specificity, calcification, short dispersal, and high-temperature exposure. The study reported an upper thermal niche of 21°C for pāua, slightly higher but still comparable to the value in the CRIB-NZ analysis (19°C). How, then, can we explain these differences in pāua vulnerability between the CRIB-NZ CVA and Cummings et al. (2021) assessment? Part of the difference is undoubtedly methodological, given the significant differences between the two CVAs (Table 6).

CRIB-NZ is a data-driven assessment that defines vulnerability using 12 standardised indicators averaged so that each contributes equally to vulnerability. Alternatively, the NOAA rapid climate vulnerability assessment (Morrison et al. 2015; Hare et al. 2016), hereafter rCVA, is an evidence-based assessment that applies logic rules to 22 expert-scored indicators to provide semi-quantitative vulnerability scores. CRIB-NZ assumes that all 12 indices define vulnerability equally, whereas in the rCVA, vulnerability can be defined by 2–3 of the 22 indicators, with the rest having no contribution. Beyond these fundamental differences, the rCVA assesses vulnerability based on sensitivity and exposure, but not adaptivity, a defining component of climate vulnerability (IPCC, 2001, 2014; Foden et al. 2013, 2019; Pacifici et al. 2015). This is significant because, while it does not consider it when scoring vulnerability, Cummings et al. (2021) note, narratively, that pāua's climate adaptability is quite high due to its wide distribution, broad diet, high levels of genetic variation, and high socioeconomic value, among other factors.

Another significant difference is how the CVAs consider vertical habitat. The rCVA evaluates vulnerability for pāua—a species that lives on the sea bottom—against environmental conditions at the sea surface. This contrasts with CRIB-NZ, which categorises pāua as a bottom-associated species with limited vertical mobility and, therefore, assesses its vulnerability against seabed conditions. However, the rCVA employed in Cummings et al. (2021) considers a broader array of surface environmental drivers, some of which are not included in CRIB-NZ (e.g. calcification), which primarily focuses on temperature-related pathways.

The rCVA evaluates species-level features that statistically classify them as more or less vulnerable, but does not consider how these traits interact dynamically with the environment, which CRIB-NZ does. Because of this, the rCVA summarises vulnerability across pāua's distribution, while CRIB-NZ provides spatially-explicit estimates that reflect the dynamic geographic complexity of climate change. The spatial explicitness of CRIB-NZ is a major difference from the rCVA, and emphasises the importance and benefits of using reliable estimates of species' geographic distributions.

Table 6: Summary of the methodological differences between CRIB-NZ and the NOAA Rapid Vulnerability Assessment (Morrison et al. 2015; Hare et al. 2016) employed in Cummings et al. (2021).

CVA element	CRIB-NZ	NOAA Rapid Vulnerability Assessment
Vulnerability dimensions	3	2 (lacks adaptivity)
Assessment type	Quantitative	Semi-quantitative
Spatially explicit	Yes	No
Primary environmental impact driver	Temperature	Multiple
Scoring system	Averaging	Logic rules
Considers how traits interact with the environment?	Yes	No
Uncertainty estimation	Yes	Limited
Output type	Continuous vulnerability estimates, maps, rankings, and indicators	Narrative summaries and species rankings
Information type	Data-driven	Evidence-based
Considers surface and bottom conditions?	Yes	No (surface only)

4.4 The importance of distribution to CRIB-NZ

When averaged across its range, pāua's vulnerability estimated in the case study is moderate (Figure 37), yet a closer look reveals significant geographic variation both within FMA 5 and the New Zealand EEZ. Pāua vulnerability appears far higher in some nearshore waters, particularly at the northern extent of NZ, and much lower in deeper offshore waters. This geographic variation emphasises the critical importance of using reliable estimates of species occurrence. Due to significant geographic variation in vulnerability, assessing it at locations where species don't occur could bias the assessment. The SDMs used in CRIB-NZ show pāua occurring broadly across the New Zealand EEZ, including in waters far deeper than their preferred depth range (~4–20m) and more offshore than indicated by MPI estimates of pāua distribution (Figure 42). It's possible that pāua's lower vulnerability in CRIB-NZ could be driven by the lower vulnerability scores in deeper offshore waters, where its occurrence could be more uncertain. If we were to restrict our vulnerability analysis to outputs within pāua's preferred depth distribution (20 m), the average vulnerability would increase from 0.43 to 0.56, making it the most vulnerable species in the case study. This illustrates the critical importance of using reliable estimates of species distribution when applying the CRIB-NZ framework and highlights the need for MPI to further validate the input data before finalizing the framework outputs.

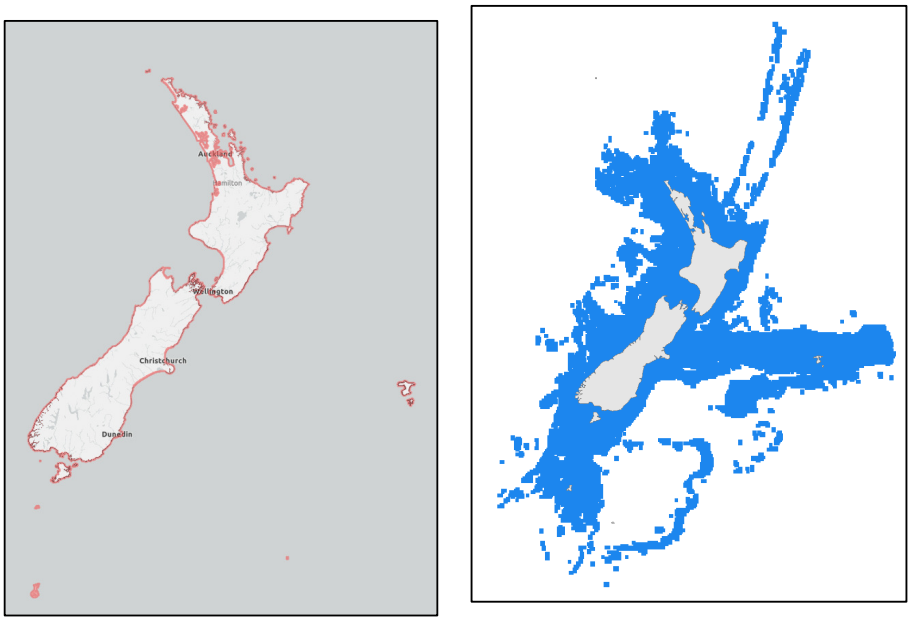


Figure 42: Annual distribution of pāua from MPI (left) and AquaX (right). Left: Shaded orange depicts the pāua's full range as estimated based on published and unpublished reports, museum holdings and expert discussion (source: https://tinyurl.com/2s389duk). Right: Blue depicts pāua's presence based on the AquaX ensemble SDM framework (Reygondeau et al. 2026)**.**

AquaX is a state-of-the-art SDM modelling pipeline, offering a statistically rigorous means of estimating the distributions of more than 30 000 marine species at unprecedented geographic resolution. Yet, as a global framework, it is infeasible to rigorously validate species distributions across all locations or to customise the data and inputs for every situation. In short, the benefit of broad geographic and taxonomic coverage also means that AquaX may produce less reliable distributions for some species at some locations. Alternatively, estimates of species distribution for some New Zealand marine species are available from MPI and the Department of Conservation (DoC).

The MPI distributions are available for hundreds of marine species as individually downloadable shapefiles. These are presence-absence expert-range maps rather than data-driven estimates. Many of the species distribution maps from MPI appeared inconsistent with those from AquaX; for instance, while pāua has a maximum depth range of 20 m, its distribution maps suggested it occurred throughout New Zealand territorial waters, ranging into offshore waters several hundred metres deep.

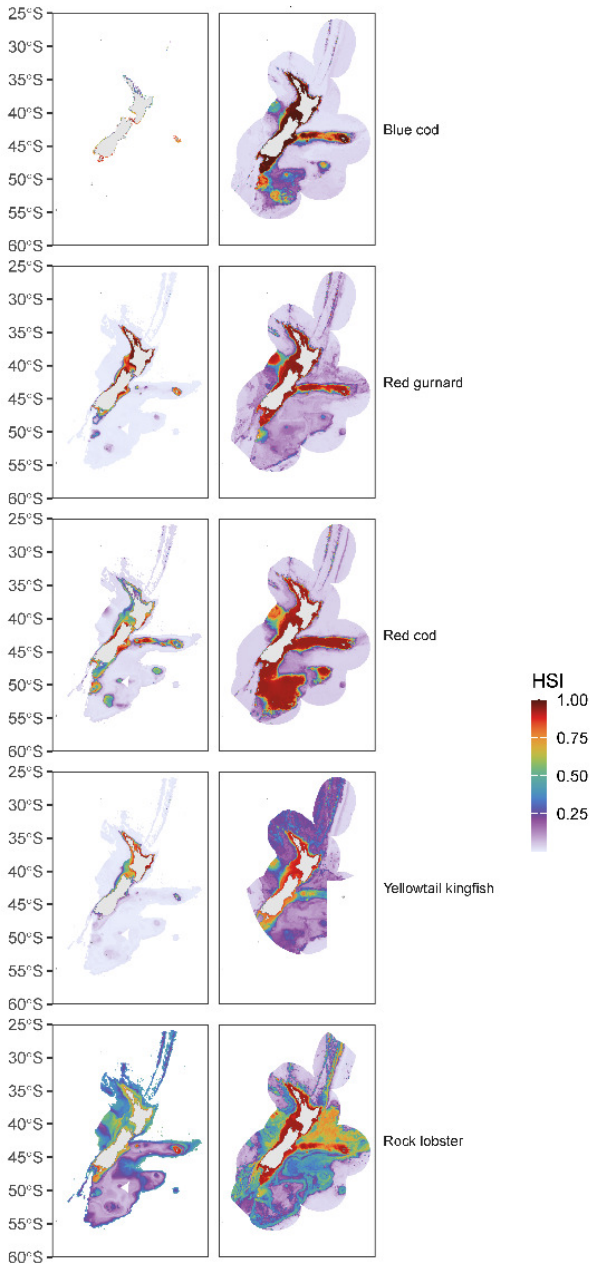


Figure 43: Estimated geographic distributions for five of the eight case study species across the New Zealand EEZ. Left panels show probabilities of occurrence from the DoC models; right panels show standardised habitat suitability indices (HSIs) from AquaX. Note: whereas AquaX provides HSI cutoff values to denote species presence, all HSI values are plotted here.

The DoC distributions are available for six of the eight case study species. Species distributions are estimated using environmental niche models fitted to georeferenced occurrence records and environmental predictor variables across New Zealand waters (Lundquist et al. 2020). Taxon-specific ensemble species distribution models are developed for demersal fishes, reef fishes, benthic invertebrates, macroalgae, and cetaceans, with model uncertainty quantified using bootstrapping. The distributions are available as probabilities of occurrence, but do not provide a threshold to denote species presence as AquaX does.

Comparing DoC distributions with those of AquaX for the five corresponding species revealed broad patterns of agreement, alongside some rather stark differences (Figure 43). Distributions for most species were positively correlated, suggesting that occurrence probabilities generally agree. A notable exception was blue cod, where the DoC indicated a restricted coastal distribution, and AquaX suggested a much broader distribution. In general, AquaX predicted broader geographic distributions than suggested by the DoC methods. However, while AquaX provide a means of assessing species presence, the DoC methods do not, making it difficult to assess the correspondence in species presence.

The case studies presented here suggest some variability between the species distributions provided by AquaX and those available from the DoC and MPI. Considering the inherent challenges and uncertainty in reliably estimating species occurrences, this is perhaps unsurprising (Robinson et al. 2017; Davies et al. 2023). Before implementing the CRIB-NZ framework in New Zealand, it is advisable to conduct analyses to assess the reliability of species distribution models from MPI, DoC, and AquaX, and to determine the optimal approach for reliably estimating species distribution.

With three independent sources of distributional information in New Zealand, there are several avenues for achieving this. AquaX is a rigorous, peer-reviewed statistical approach, and the veracity of its outputs could potentially be improved by enhancing the data on which they rely. For instance, species occurrences from geolocated fisheries catch databases or trawl surveys within New Zealand EEZ could be used to improve the reliability of AquaX predictions by working directly with the AquaX developers. Likewise, AquaX distributions depend on the vertical distribution of species, so validating species occurrence depths prior to modelling could also enhance the realism of the species distribution estimates.

Alternatively, with multiple estimated distributions per species, an ensemble approach could be adopted, such as averaging or committee averaging; this would help ensure greater reliability and quantify uncertainty in vulnerability estimates from CRIB-NZ. As a preliminary step, the DoC approach would need to be expanded to include missing species (e.g. many invertebrates), and the analysis would benefit from making the data from both MPI and the DoC accessible as a single download. While such investigations are advisable and readily tractable, they are beyond the scope of this work, which was primarily focused on developing the CVA framework and demonstrating its functionality.

5 Interpreting CRIB-NZ outputs

5.1 Climate vulnerability

CRIB-NZ produces empirically rooted, spatially explicit estimates of relative climate vulnerability. The CRIB does not seek to evaluate climate-driven range shifts; Instead, it assesses the likelihood of adverse consequences (IPCC, 2021) at individual locations within species' native geographic distributions to inform conservation and management efforts where they operate. Because the CRIB-NZ does not estimate range expansions, it represents the climate risk to the *in situ* persistence of species and the biotic intactness of their ecosystems. It represents a baseline that can be updated flexibly in response to new data and knowledge.

Vulnerability scores are reported in dimensionless units, allowing species and ecosystems to be scored and ranked on relative, rather than absolute, scales between 0 and 1. This approach helps identify patterns and trends in species' climate vulnerabilities relative to other species assessed in *the same vulnerability analysis.* This can be useful if the objective is to rank or triage species by their relative climate vulnerability.

However, interpreting vulnerability rankings in dimensionless units on relative scales can also be challenging. For instance, a species with a vulnerability score of 0.6 is more vulnerable than one with

a score of 0.5, but what does a score of 0.6 truly mean ecologically? Does 0.6 represent an imminent climate impact of high magnitude or a distant threat of little concern? How would an end user—manager, scientist, policy-maker, or otherwise—understand such information and use it? This challenge could contribute to the limited incorporation of CVAs into management.

5.2 Climate risk

Previous vulnerability studies, or comparably holistic cumulative impact indices, have defined categories of high/low based on the statistical distribution of the dimensionless indices representing them (Halpern et al. 2008; Stortini et al. 2015; Foden et al. 2019; Albouy et al. 2020). In contrast, the CRIB can identify climate risk thresholds that translate climate vulnerability into risk categories based on the ecological interpretation of the 12 climate indices. Despite the challenges of reliably identifying such thresholds (Hillebrand et al. 2020), they are increasingly used to guide conservation strategies and actions (Ficetola & Denoel, 2009; van der Hoek et al. 2015; Arroyo-Rodríguez et al. 2020; Shennan-Farpón et al. 2021). In CRIB, the thresholds are defined in their native units and propagated through the analysis, preserving their meaning and interpretation yet informing the interpretation of the dimensionless vulnerability scores.

The threshold-based approach developed in CRIB is comparable to the definition of extinction risk used by the IUCN Red List Index (RLI) of species (IUCN, 2021), the definition of safe operating space in the planetary boundaries theory (Rockström et al. 2009), and the reasons for concern (RFC) framework adopted to define climate risk by the Intergovernmental Panel on Climate Change (IPCC)(IPCC, 2001, 2014, 2021). However, whereas the RLI assesses extinction risk at the species level and is identical across species' distributions, the climate risk index for biodiversity (CRIB) disaggregates climate risk and its spatial variation across the sites throughout a species' distribution and evaluates risk for both individual species and aggregate ecosystems.

It allows the vulnerability of species and communities to be categorised according to our ecological interpretation of them and is guided rather than defined by their statistical properties. Identifying thresholds to determine risk is notoriously challenging (Hillebrand et al. 2020; Zommers et al. 2020) due to various factors, including a lack of knowledge needed to represent them, uncertainties in climate model projections, and differences in value judgments regarding what constitutes dangerous risk (Fischlin, 2009; Garner et al. 2016; Leemans & Vellinga, 2017; Hillebrand et al. 2020; Zommers et al. 2020).

Despite these challenges, threshold-defined risk assessments have proven highly valuable for communicating risks to a broad audience while supporting public engagement, management, and policy decisions. For instance, since 2001, the IPCC RFC framework has communicated levels of climate risk to humans using thresholds set by expert judgment (e.g. IPCC, 2001). The resulting 'burning embers' diagrams have become widely used tools to communicate the risks stemming from anthropogenic climate change in a clear, intuitive manner that is critical for decision-making (Zommers et al. 2020). For instance, the goal of the Paris Agreement to limit global warming to below 2°C was supported by IPCC reports of increasing risks beyond 1.5°C or 2°C warming (Fischlin, 2009; Leemans and Vellinga, 2017).

The CRIB framework calculates risk categories for each climate index and dimension. Risk thresholds are defined using transparent and, where possible, empirically supported approaches (Swart et al. 2009; Budescu et al. 2012; Oppenheimer et al. 2016). Boyce et al. (2022) describe the CRIB rationale for defining thresholds that denote negligible, moderate, high and critical risk categories. These thresholds serve as waypoints for defining and communicating climate risk and, to the extent possible, are guided by empirical information (Table F3).

To assess risk within CRIB-NZ, the thresholds would need to be updated to reflect the revised climate indices. This work was outside the scope of the current study, but could be considered as part of a future research project to progress the CRIB-NZ framework.

6 Acknowledgements

This work was completed under a provision-of-services agreement between the Ministry for Primary Industries and Wild Ocean Research (agreement number 407326). Thanks to Jean Davis for guiding the project (ZDB2024-04) and to Erik Behrens, Pamela Mace, Gabriel Reygondeau and Yulia Egorova for providing input data. Thanks to the New Zealand Ministry for Primary Industries for providing valuable input across several meetings that shaped this work.

7 References

Aitkenhead, I.; Kuleshov, Y.; Sun, Q.; Choy, S. (2025). Selecting Tailored Risk Indicators for Assessing Marine Heatwave Risk to the Fisheries Sector in Vanuatu. *Climate 13(11):* 225. doi:10.3390/cli13110225.

Albouy, C.; Delattre, V.; Donati, G.; Frölicher, T.L.; Albouy-boyer, S.; Ru, M.; Pellissier, L.; Mouillot, D. (2020). Global vulnerability of marine mammals to global warming. *Scientific reports, 10(1)*, 548. https://doi.org/10.1038/s41598-019-57280-3

Andren, H. (1994). Effects of habitat fragmentation on birds and mammals in landscapes with different proportions of suitable habitat: a review. OIKOS 71(3): 355–366. doi:10.2307/3545823.

Arroyo-Rodríguez, V.; Fahrig, L.; Tabarelli, M.; Watling, J.I.; Tischendorf, L.; Benchimol, M.; Cazetta, E.; Faria, D.; Leal, I.R.; Melo, F.P.L.; Morante-Filho, J.C.; Santos, B.A.; Arasa-Gisbert, R.; Arce-Peña, N.; Cervantes-López, M.J.; Cudney-Valenzuela, S.; Galán-Acedo, C.; San-José, M.; Vieira, I.C.G.; Slik, J.W.F.; Nowakowski, A.J.; Tscharntke, T. (2020). Designing optimal human-modified landscapes for forest biodiversity conservation. *Ecological Letters 23(9)*: 1404–1420. doi:10.1111/ele.13535.

Bak, T.M.; Camp, R.J.; Heim, N.A.; McCauley, D.J.; Payne, J.L.; Knope, M.L. (2023). A global ecological signal of extinction risk in marine ray-finned fishes (class Actinopterygii). *Cambridge Prisms Extinction 1*: e25. doi:10.1017/ext.2023.23.

Ban, N.C.; Alidina, H.M.; Ardron, J.A. (2010). Cumulative impact mapping: Advances, relevance and limitations to marine management and conservation, using Canada's Pacific waters as a case study. *Marine Policy 34(5):* 876–886. doi:10.1016/j.marpol.2010.01.010.

Barrier, N.; Maury, O.; Seferian, R.; Santana-Falcón, Y.; Tidd, A.; Lengaigne, M. (2025). Assessing the Time of Emergence of Marine Ecosystems From Global to Local Scales Using IPSL-CM6A-LR/APECOSM Climate-To-Fish Ensemble Simulations. *Earth's Future 13(2)*. doi:10.1029/2024EF004736.

Bateman, B.L.; Wilsey, C.; Taylor, L.; Wu, J.; LeBaron, G.S.; Langham, G. (2020). North American birds require mitigation and adaptation to reduce vulnerability to climate change. *Conservation Science and Practice 2(8)*. doi:10.1111/csp2.242.

Behrens, E.; Dunn, M.R.; Holmes, S.J.; Cummings, V.J. (2025). Marine heatwaves and fisheries in Aotearoa New Zealand: observed and projected temperature anomalies and potential impacts by fisheries management area. *New Zealand Aquatic Environment and Biodiversity Report 351*: 57 p.

Behrens, E.; Williams, J.; Morgenstern, O.; Sutton, P.; Rickard, G.; Williams, M.J.M. (2020). Local Grid Refinement in New Zealand's Earth System Model: Tasman Sea Ocean Circulation Improvements and Super-Gyre Circulation Implications. *Journal of Advances in Modelling*

Earth Systems 12(7). doi:10.1029/2019MS001996.

Bennett, J.M.; Calosi, P.; Clusella-Trullas, S.; Martínez, B.; Sunday, J.; Algar, A.C.; Araújo, M.B.; Hawkins, B.A.; Keith, S.; Kühn, I.; Rahbek, C.; Rodríguez, L.; Singer, A.; Villalobos, F.; Ángel Olalla-Tárraga, M.; Morales-Castilla, I. (2018). GlobTherm, a global database on thermal tolerances for aquatic and terrestrial organisms. *Scientific Data 5(1)*: 180022. doi:10.1038/sdata.2018.22.

Bennett, J.M.; Sunday, J.; Calosi, P.; Villalobos, F.; Martínez, B.; Molina-Venegas, R.; Araújo, M.B.; Algar, A.C.; Clusella-Trullas, S.; Hawkins, B.A.; Keith, S.A.; Kühn, I.; Rahbek, C.; Rodríguez, L.; Singer, A.; Morales-Castilla, I.; Olalla-Tárraga, M.Á. (2021). The evolution of critical thermal limits of life on Earth. *Nature Communications 12(1)*: 1198. doi:10.1038/s41467-021-21263-8.

Benthuysen, J.A.; Oliver, E.C.J.; Chen, K.; Wernberg, T. (2020). Editorial: Advances in Understanding Marine Heatwaves and Their Impacts. *Frontiers in Marine Science 7*. doi:10.3389/fmars.2020.00147.

Berry, P.; Ogawa-Onishi, Y.; McVey, A. (2013). The Vulnerability of Threatened Species: Adaptive Capability and Adaptation Opportunity. *Biology (Basel). 2(3)*: 872–893. doi:10.3390/biology2030872.

Blueweiss, L.; Fox, H.; Kudzma, V.; Nakashima, D.; Peters, R.; Sams, S. (1978). Relationships between body size and some life history parameters. *Oecologia 37(2)*: 257–272. doi:10.1007/BF00344996.

Boyce, D.; Tittensor, D.P.; Schleit, K.E.; Fuller, S. (2025). Climate vulnerability and risk assessments in marine ecosystems, with a special focus on fisheries in Aotearoa (New Zealand). *New Zealand Aquatic Environment and Biodiversity Report No. 367*: 49 p.

Boyce, D.G.; Cyr, F.; Fuller, S.; Schleit, K.E.; Rideout, R.M. (2026). Exploring the impacts of climate change on fisheries resources within the NAFO Convention Area. *Journal of Atlantic Fisheries Science 57*: 1–33.

Boyce, D.G.; Frank, K.T.; Leggett, W.C. (2015a). From mice to elephants: overturning the 'one size fits all' paradigm in marine plankton food chains. *Ecological Letters 18*: 504–515. doi:10.1111/ele.12434.

Boyce, D.G.; Frank, K.T.; Worm, B.; Leggett, W.C. (2015b). Spatial patterns and predictors of trophic control across marine ecosystems. *Ecological Letters 18(10)*: 1001–1011.

Boyce, D.G.; Fuller, S.; Karbowski, C.; Schleit, K.; Worm, B. (2021). Leading or lagging: How well are climate change considerations being incorporated into Canadian fisheries management? *Canadian Journal of Fisheries and Aquatic Science 78(8)*: 1120–1129. doi:10.1139/cjfas-2020-0394.

Boyce, D.G.; Lewis, M.L.; Worm, B. (2010). Global phytoplankton decline over the past century. *Nature 466(7306)*: 591–596. doi:10.1038/nature09268.

Boyce, D.G.; Lotze, H.K.; Tittensor, D.P.; Carozza, D.A.; Worm, B. (2020a). Future ocean biomass losses may widen socioeconomic equity gaps. *Nature Communications 11(2235)*: 1–11.

Boyce, D.G.; Petrie, B.; Frank, K.T.; Worm, B.; Leggett, W.C. (2017). Environmental structuring of marine plankton phenology. *Nature Ecology & Evolution 1*. doi:10.1038/s41559-017-0287-3.

Boyce, D.G.; Schleit, K.; Fuller, S. (2020b). Incorporating climate change into fisheries management in Atlantic Canada and the Eastern Arctic. Oceans North Report 184 p. Available from www.oceansnorth.org.

Boyce, D.G.; Shackell, N.; Greenar, B. (2024b). A climate risk index for marine life across the Canadian exclusive economic zone. *Canadian Technical Report on Fisheries and Aquatic Sciences 3568*: 46 p.

Boyce, D.G.; Shackell, N.; Greyson, P.; Greenan, B. (2023). A prospective framework to support climate-adaptive fisheries in Canada. *FACETS 8*: 1–15. doi:10.1139/facets-2022-0164.

Boyce, D.G.; Tittensor, D.P.; Fuller, S.; Henson, S.; Kaschner, K.; Reygondeau, G.; Schleit, K.E.; Saba, V.; Shackell, N.; Stanley, R.R.E.; Worm, B. (2024b). Operationalizing climate risk in a global warming hotspot. *npj Ocean Sustainability 3(1)*: 33. doi:10.1038/s44183-024-00067-5.

Boyce, D.G.; Tittensor, D.P.; Garilao, C.; Henson, S.; Kaschner, K.; Kesner-Reyes, K.; Pigot, A.; Reyes, R.B.; Reygondeau, G.; Schleit, K.E.; Shackell, N.L.; Sorongon-Yap, P.; Worm, B. (2022). A climate risk index for marine life. *Nature Climate Change 12(9)*: 854–862. doi:10.1038/s41558-022-01437-y.

Brauer, C.J.; Beheregaray, L.B. (2020). Recent and rapid anthropogenic habitat fragmentation increases extinction risk for freshwater biodiversity. *Evolutionary Applications 13(10)*: 2857–2869. doi:10.1111/eva.13128.

Braun, C.D.; Boyce, D.; Farchadi, N.; Arostegui, M.C.; Alexander, M.; Carroll, G.; Crear, D.P.; Hazen, E.L.; Hoffmayer, E.R.; Kleisner, K.M.; Li, Y.; Lopez, J.; Lucey, S.; McDonnell, L.H.; Napoli, N.; Quinlan, J.A.; Saba, V.S.; Shumchenia, E.; Lewison, R.L. (2026). Identifying the critical elements for a next generation of climate vulnerability assessments for fisheries. *Fisheries 51(7):*298–307. doi:10.1093/fshmag/vuaf133.

Brito-Morales, I.; Molinos, J.G.; Schoeman, D.S.; Burrows, M.T.; Poloczanska, E.S.; Brown, C.J.; Ferrier, S.; Harwood, T.D.; Klein, C.J.; Pandolfi, J.M.; Watson, J.E.M.; Wenger, A.S.; Richardson, A.J. (2018). Climate Velocity Can Inform Conservation in a Warming World Simple Climate Metrics Could Help Conservation in a Changing Climate. *Trends in Ecology and Evolution 33(6):* 1–17. doi:10.1016/j.tree.2018.03.009.

Brito-Morales, I.; Schoeman, D.S.; Molinos, J.G.; Burrows, M.T.; Klein, C.J.; Arafeh-Dalmau, N.; Kaschner, K.; Garilao, C.; Kesner-Reyes, K.; Richardson, A.J. (2020). Climate velocity reveals increasing exposure of deep-ocean biodiversity to future warming. Nature Climate Change 10(6): 576–581. doi:10.1038/s41558-020-0773-5.

Britten, G.L.; Dowd, M.; Minto, C.C.C, Ferretti, F.; Boero, F.; Lotze, H.K. (2014). Predator decline leads to decreased stability in a coastal fish community. *Ecological Letters 17(12)*: 1518–1525. doi:10.1111/ele.12354.

Brown, J.H.; Kodric-Brown, A. 1977. Turnover Rates in Insular Biogeography: Effect of Immigration on Extinction. *Ecology 58(2)*: 445–449. doi:10.2307/1935620.

Bruno, A.; Casiraghi, M.; Bautista, M.; Hajibabaei, M. (2021). Editorial: Stressors Acting on Aquatic Ecosystems: High-Throughput Sequencing Approaches to Shed Light on Human-Nature Interactions. *Frontiers in Ecological Evolution 9*. doi:10.3389/fevo.2021.763442.

Bruno, J.F.; Bates, A.E.; Cacciapaglia, C.; Pike, E.P.; Amstrup, S.C.; Van Hooidonk, R.; Henson, S.A.; Aronson, R.B. (2018). Climate change threatens the world's marine protected areas.

Nature Climate Change 8(6): 499–503. Springer US. doi:10.1038/s41558-018-0149-2.

Bryndum-Buchholz, A.; Tittensor, D.P.; Lotze, H.K. (2021). The status of climate change adaptation in fisheries management: Policy, legislation and implementation. *Fish and Fisheries 22(6)*: 1248–1273. faf.12586. doi:10.1111/faf.12586.

Budescu, D.V.; Por, H.H.; Broomell, S.B. (2012). Effective communication of uncertainty in the IPCC reports. *Climate Change 113(2)*: 181–200. doi:10.1007/s10584-011-0330-3.

Burek, K.A.; Gulland, F.M.D.; O'Hara, T.M. (2008). Effects of climate change on Arctic marine mammal health. *Ecological Applications 18(sp2)*: S126–S134. doi:10.1890/06-0553.1.

Burrows, M.T.; Schoeman, D.S.; Buckley, L.B.; Moore, P.; Poloczanska, E.S.; Brander, K.M.; Brown, C.; Bruno, J.F.; Duarte, C.M.; Halpern, B.S.; Holding, J.; Kappel, C. V, Kiessling, W.; O'Connor, M.I.; Pandolfi, J.M.; Parmesan, C.; Schwing, F.B.; Sydeman, W.J.; Richardson, A.J. (2011). The Pace of Shifting Climate in Marine and Terrestrial Ecosystems. *Science 334*: 652–655. doi:10.1126/science.1210288.

Busch, D.S.; Griffis, R.; Link, J.; Abrams, K.; Baker, J.; Brainard, R.E.; Ford, M.; Hare, J.A.; Himes-Cornell, A.; Hollowed, A.; Mantua, N.J.; McClatchie, S.; McClure, M.; Nelson, M.W.; Osgood, K.; Peterson, J.O.; Rust, M.; Saba, V.; Sigler, M.F.; Sykora-Bodie, S.; Toole, C.; Thunberg, E.; Waples, R.S.; Merrick, R. (2016). Climate science strategy of the US National Marine Fisheries Service. *Marine Policy 74*: 58–67. doi:10.1016/j.marpol.2016.09.001.

Butt, N.; Halpern, B.S.; O'Hara, C.C.; Allcock, A.L.; Polidoro, B.; Sherman, S.; Byrne, M.; Birkeland, C.; Dwyer, R.G.; Frazier, M.; Woodworth, B.K.; Arango, C.P.; Kingsford, M.J.; Udyawer, V.; Hutchings, P.; Scanes, E.; McClaren, E.J.; Maxwell, S.M.; Diaz-Pulido, G.; Dugan, E.; Simmons, B.A.; Wenger, A.S.; Linardich, C.; Klein, C.J. (2022). A trait-based framework for assessing the vulnerability of marine species to human impacts. *Ecosphere 13(2)*. doi:10.1002/ecs2.3919.

Capotondi, A.; Rodrigues, R.R.; Sen Gupta, A.; Benthuysen, J.A.; Deser, C.; Frölicher, T.L.; Lovenduski, N.S.; Amaya, D.J.; Le Grix, N.; Xu, T.; Hermes, J.; Holbrook, N.J.; Martinez-Villalobos, C.; Masina, S.; Roxy, M.K.; Schaeffer, A.; Schlegel, R.W.; Smith, K.E.; Wang, C. (2024). A global overview of marine heatwaves in a changing climate. *Communications on Earth and the Environment 5(1)*: 701. doi:10.1038/s43247-024-01806-9.

Cardinale, B.J.; Duffy, J.E.; Gonzalez, A.; Hooper, D.U.; Perrings, C.; Venail, P.; Narwani, A.; Mace, G.M.; Tilman, D.; Wardle, D.A.; Kinzig, A.P.; Daily, G.C.; Loreau, M.; Grace, J.B.; Larigauderie, A.; Srivastava, D.S.; Naeem, S. (2012). Biodiversity loss and its impact on humanity. *Nature 486(7401)*: 59–67. Nature Publishing Group. doi:10.1038/nature11148.

Carilli, J.; Donner, S.D.; Hartmann, A.C. (2012). Historical Temperature Variability Affects Coral Response to Heat Stress. *PLoS One 7(3)*: e34418. doi:10.1371/journal.pone.0034418.

Carilli, J.E.; Norris, R.D.; Black, B.A.; Walsh, S.M.; McField, M. (2009). Local Stressors Reduce Coral Resilience to Bleaching. *PLoS One 4(7)*: e6324. doi:10.1371/journal.pone.0006324.

Carroll, C.; Lawler, J.J.; Roberts, D.R.; Hamann, A. (2015). Biotic and Climatic Velocity Identify Contrasting Areas of Vulnerability to Climate Change. *PLoS One 10(10)*: e0140486. doi:10.1371/journal.pone.0140486.

Chao, A.; Gotelli, N.J.; Hsieh, T.C.; Sander, E.L.; Ma, K.H.; Colwell, R.K.; Ellison, A.M. (2014). Rarefaction and extrapolation with Hill numbers: a framework for sampling and estimation in species diversity studies. *Ecological Monographs 84(1)*: 45–67. doi:10.1890/13-0133.1.

Chase, J.M.; Blowes, S.A.; Knight, T.M.; Gerstner, K.; May, F. (2020). Ecosystem decay exacerbates biodiversity loss with habitat loss. *Nature 584(7820)*: 238–243. doi:10.1038/s41586-020-2531-2.

Chen, S.; Wu, S.; Ma, M. (2023). Ecological restoration programs reduced forest fragmentation by stimulating forest expansion. *Ecological Indicators 154*: 110855. doi:10.1016/j.ecolind.2023.110855.

Chessman, B.C. (2013). Identifying species at risk from climate change: Traits predict the drought vulnerability of freshwater fishes. *Biological Conservation 160*: 40–49. doi:10.1016/j.biocon.2012.12.032.

Cheung, W.W.L.; Brodeur, R.D.; Okey, T.A.; Pauly, D. (2015). Projecting future changes in distributions of pelagic fish species of Northeast Pacific shelf seas. *Progress in Oceanography 130*: 19–31. doi:10.1016/j.pocean.2014.09.003.

Cheung, W.W.L.; Frolicher, T.L. (2020). Marine heatwaves exacerbate climate change impacts for fisheries in the northeast Pacific. *Science Reports 10(1).* doi:10.1038/s41598-020-63650-z.

Cheung, W.W.L.; Lam, V.W.Y.; Sarmiento, J.L.; Kearney, K.; Watson, R.; Pauly, D. (2009). Projecting global marine biodiversity impacts under climate change scenarios. *Fish and Fisheries 10(3)*: 235–251. doi:10.1111/j.1467-2979.2008.00315.x.

Cheung, W.W.L.; Oyinlola, M.A. (2018). Vulnerability of flatfish and their fisheries to climate change. *Journal of Sea Research 140(January):* 1–10. doi:10.1016/j.seares.2018.06.006.

Cheung, W.W.L.; Pauly, D.; Sarmiento, J.L. (2013). How to make progress in projecting climate change impacts. *ICES Journal of Marine Science 70(6)*: 1069–1074. doi:10.1093/icesjms/fst133.

Cheung, W.W.L.; Watson, R.; Morato, T.; Pitcher, T.J.; Pauly, D. (2007). Intrinsic vulnerability in the global fish catch. *Marine Ecology Progress Series 333*: 1–12.

Chichorro, F.; Juslén, A.; Cardoso, P. (2019). A review of the relation between species traits and extinction risk. *Biological Conservation 237*: 220–229. doi:10.1016/j.biocon.2019.07.001.

Cole, L.E.S.; Bhagwat, S.A.; Willis, K.J. (2014). Recovery and resilience of tropical forests after disturbance. *Nature Communications 5(1)*: 3906. doi:10.1038/ncomms4906.

Comte, L.; Olden, J.D. (2017). Climatic vulnerability of the world's freshwater and marine fishes. *Nature Climate Change 7(10)*: 718–722. doi:10.1038/nclimate3382.

Cook, K.M.; Dunn, M.R.; Behrens, E.; Pinkerton, M.H.; Law, C.; Cummings, V.J.; Cummings, C. (2025). Marine heatwaves and fisheries in Aotearoa New Zealand: review of potential effects on marine ecosystems and fishstocks. *New Zealand Aquatic Environment and Biodiversity Report No. 352*: 53 p.

Copernicus Marine Service. (2023). Global Ocean Physics Reanalysis (Product ID: GLOBAL_MULTIYEAR_PHY_001_030). doi:10.48670/moi-00021.

COSEWIC. (2012). COSEWIC assessment and status report on the Smooth Skate *Malacoraja senta* in Canada. Ottawa, Canada.

Craig, J.K.; Runde, B.J.; Bacheler, N.M.; Burton, M.L.; Muñoz, R.C.; Quinlan, J.A.; Nelson, M.W.; Binion-Rock, S.M.; Kellison, G.T.; Smith, J.W.; Laney, R.W.; Sedberry, G.R.; Morley, J.W.; Poland, S.J.; Brodie, R.; Gentry, L.; Gore, K.; Rock, J.E.; Johnson, M.W.; Flowers, J.; Collier,

C. (2025). Climate vulnerability assessment of fish and invertebrates in the U.S. South Atlantic large marine ecosystem. *PLOS Climate 4(6)*: e0000543. doi:10.1371/journal.pclm.0000543.

Crain, C.M.; Kroeker, K.; Halpern, B.S. (2008). Interactive and cumulative effects of multiple human stressors in marine systems. *Ecological Letters 11(12)*: 1304–1315. doi:10.1111/j.1461-0248.2008.01253.x.

Crooks, K.R.; Burdett, C.L.; Theobald, D.M.; King, S.R.B.; Di Marco, M.; Rondinini, C.; Boitani, L. (2017). Quantification of habitat fragmentation reveals extinction risk in terrestrial mammals. *Proceedings of the National Academy of Science 114(29)*: 7635–7640. doi:10.1073/pnas.1705769114.

Cummings, V.J.; Lundquist, C.J.; Dunn, M.R.; Francis, M.; Horn, P.; Law, C.; Pinkerton, M.H.; Sutton, P.; Tracey, D.; Hansen, L.; Mielbrecht, E. (2021). Assessment of potential effects of climate-related changes in coastal and offshore waters on New Zealand's seafood sector. *New Zealand Aquatic Environment and Biodiversity Report No. 261*. 153 p.

Dahlke, F.T.; Wohlrab, S.; Butzin, M.; Portner, H.-O. (2020). Thermal bottlenecks in the life cycle define climate vulnerability of fish. *Science 369(6499)*: 65–70.

Darling, E.S.; Côté, I.M. (2008). Quantifying the evidence for ecological synergies. *Ecology Letters 11(12)*: 1278–1286. doi:10.1111/j.1461-0248.2008.01243.x.

Davidson, A.D.D.; Boyer, A.G.; Kim, H.; Pompa-Mansilla, S.; Hamilton, M.J.; Costa, D.P.; Ceballos, G.; Brown, J.H. (2012). Drivers and hotspots of extinction risk in marine mammals. *Proceedings of the National Academy of Science 109(9)*: 3395–3400. doi:10.1073/pnas.1121469109.

Davies, S.C.; Thompson, P.L.; Gomez, C.; Nephin, J.; Knudby, A.; Park, A.E.; Friesen, S.K.; Pollock, L.J.; Rubidge, E.M.; Anderson, S.C.; Iacarella, J.C.; Lyons, D.A.; MacDonald, A.; McMillan, A.; Ward, E.J.; Holdsworth, A.M.; Swart, N.; Price, J.; Hunter, K.L. (2023). Addressing uncertainty when projecting marine species' distributions under climate change. *Ecography 2023(11)*. doi:10.1111/ecog.06731.

Davies, T.E.; Maxwell, S.M.; Kaschner, K.; Garilao, C.; Ban, N.C. (2017). Large marine protected areas represent biodiversity now and under climate change. *Science Reports 7(1)*: 1–7. Springer US. doi:10.1038/s41598-017-08758-5.

Dennison, F.; Keeble, J.; Morgenstern, O.; Zeng, G.; Luke Abraham, N.; Yang, X. (2019). Improvements to stratospheric chemistry scheme in the UM-UKCA (v10.7) model: Solar cycle and heterogeneous reactions. *Geoscientific Model Development 12(3)*: 1227 – 1239. doi:10.5194/gmd-12-1227-2019.

Deser, C.; Phillips, A.S.; Alexander, M.A.; Amaya, D.J.; Capotondi, A.; Jacox, M.G.; Scott, J.D. (2024). Future Changes in the Intensity and Duration of Marine Heat and Cold Waves: Insights from Coupled Model Initial-Condition Large Ensembles. *Journal of Climate 37(6)*: 1877–1902. doi:10.1175/JCLI-D-23-0278.1.

Deutsch, C.A.; Tewksbury, J.J.; Huey, R.B.; Sheldon, K.S.; Ghalambor, C.K.; Haak, D.C.; Martin, P.R. (2008). Impacts of climate warming on terrestrial ectotherms across latitude. *Proceedings of the National Acadamy of Science 105(18)*: 6668–6672. doi:10.1073/pnas.0709472105.

de los Ríos, C.; Watson, J.E.M.; Butt, N. (2018). Persistence of methodological, taxonomical, and geographical bias in assessments of species' vulnerability to climate change: A review. *Global Ecology and Conservation 15*. doi:10.1016/j.gecco.2018.e00412.

DFO. (2021). Assessment of the northern contingent of Atlantic mackerel (*Scomber scombrus*) in (2020). *Canadian Science Advisory Secretariat Science Advisory Report 2021/029(July)*: 18.

Dickinson, M.G.; Orme, C.D.L.; Suttle, K.B.; Mace, G.M. (2014). Separating sensitivity from exposure in assessing extinction risk from climate change. *Scientific Reports 4(1)*: 6898. doi:10.1038/srep06898.

Donner, S.D.; Carilli, J. (2019). Resilience of Central Pacific reefs subject to frequent heat stress and human disturbance. *Scientific Reports 9(1)*: 3484. doi:10.1038/s41598-019-40150-3.

Drevillon, M.; Gues, F. (2023). Quality Information Document for Global Ocean Physics Reanalysis (CMEMS-GLO-QUID-001-030, Issue 1.6). Mercator Ocean International.

Ducatez, S.; Shine, R. (2017). Drivers of Extinction Risk in Terrestrial Vertebrates. *Conservation Letters 10(2)*: 186–194. doi:10.1111/conl.12258.

Dulvy, N.K.; Fowler, S.L.; Musick, J.A.; Cavanagh, R.D.; Kyne, P.M.; Harrison, L.R.; Carlson, J.K.; Davidson, L.N.; Fordham, S. V, Francis, M.P.; Pollock, C.M.; Simpfendorfer, C.A.; Burgess, G.H.; Carpenter, K.E.; Compagno, L.J.; Ebert, D.A.; Gibson, C.; Heupel, M.R.; Livingstone, S.R.; Sanciangco, J.C.; Stevens, J.D.; Valenti, S.; White, W.T. (2014). Extinction risk and conservation of the world's sharks and rays. *Elife 3*. doi:10.7554/eLife.00590.

Dunn, D.C.; Maxwell, S.M.; Boustany, A.M.; Halpin, P.N. (2016). Dynamic ocean management increases the efficiency and efficacy of fisheries management. *Proceedings of the National Acadamy of Science 113(3)*: 668–673. doi:10.1073/pnas.1513626113.

Duplisea, D.E.; Roux, M.-J.; Hunter, K.L.; Rice, J. (2020). Resource management under climate change: a risk-based strategy to develop climate-informed science advice. *DFO Canadian Science Advisory Secretariat Research Document 2019/044*: 45 p.

Duplisea, D.E.; Roux, M.-J.; Hunter, K.L.; Rice, J. (2021). Fish harvesting advice under climate change: A risk-equivalent empirical approach. *PLoS One 16(2)*: e0239503. doi:10.1371/journal.pone.0239503.

du Pontavice, H.; Gascuel, D.; Reygondeau, G.; Maureaud, A.; Cheung, W.W.L. (2020). Climate change undermines the global functioning of marine food webs. *Global Change Biology 26(3)*: 1306–1318. doi:10.1111/gcb.14944.

English, P.A.; Ward, E.J.; Rooper, C.N.; Forrest, R.E.; Rogers, L.A.; Hunter, K.L.; Edwards, A.M.; Connors, B.M.; Anderson, S.C. (2022). Contrasting climate velocity impacts in warm and cool locations show that effects of marine warming are worse in already warmer temperate waters. *Fish and Fisheries 23(1)*: 239–255. doi:10.1111/faf.12613.

Estes, J.A.; Tinker, M.T.; Williams, T.M.; Doak, D.F. (1998). Killer Whale Predation on Sea Otters Linking Oceanic and Nearshore Ecosystems. *Science (80-.). 282(5388)*: 473–476. doi:10.1126/science.282.5388.473.

Eyring, V.; Bony, S.; Meehl, G.A.; Senior, C.A.; Stevens, B.; Stouffer, R.J.; Taylor, K.E. (2016). Overview of the Coupled Model Intercomparison Project Phase 6 (CMIP6) experimental design and organization. *Geoscience Model Development 9(5)*: 1937–1958. doi:10.5194/gmd-9-1937-2016.

Eyring, V.; Cox, P.M.; Flato, G.M.; Gleckler, P.J.; Abramowitz, G.; Caldwell, P.; Collins, W.D.; Gier, B.K.; Hall, A.D.; Hoffman, F.M.; Hurtt, G.C.; Jahn, A.; Jones, C.D.; Klein, S.A.; Krasting, J.P.;

Kwiatkowski, L.; Lorenz, R.; Maloney, E.; Meehl, G.A.; Pendergrass, A.G.; Pincus, R.; Ruane, A.C.; Russell, J.L.; Sanderson, B.M.; Santer, B.D.; Sherwood, S.C.; Simpson, I.R.; Stouffer, R.J.; Williamson, M.S. (2019). Taking climate model evaluation to the next level. *Nature Climate Change 9(2)*: 102–110. Springer US. doi:10.1038/s41558-018-0355-y.

Fahrig, L. 2002. Effect of habitat fragmentation on the extinction threshold: A synthesis. *Ecological Applications 12(2)*: 346–353. doi:10.1890/1051-0761(2002)012[0346:eohfot]2.0.co;2.

FAO. (2018). Impacts of climate change on fisheries and aquaculture: synthesis of current knowledge, adaptation and mitigation options. *In* FAO Fisheries and Aquaculture Technical Paper. *Edited by* M. Barange, T. Bahiri, M.C.M. Beveridge, K.L. Cochrane, S. Funge-Smith, and F. Poulain. Rome. p. 628.

Farchadi, N.; Crear, D.; Li, Y.; Alexander, M.; Arostegui, M.; Boyce, D.G.; Carroll, G.; Hazen, E.L.; Hoffmayer, E.; Karp, M.; Kleisner, K.M.; Lopez, J.; McDonnell, L.; Napoli, N.; Quinlan, J.A.; Saba, V.; Shumchenia, E.; Braun, C.D.; Lewison, R.L. (2026). Climate Vulnerability Assessments in Marine Fisheries: Taking Stock and Looking Ahead. *Fish and Fisheries 27 (3)*: 496–505 doi:10.1111/faf.70064.

Fenchel, T. (1974). Intrinsic rate of natural increase: The relationship with body size. *Oecologia 14(4)*: 317–326. doi:10.1007/BF00384576.

Ficetola, G.F.; Denoel, M. (2009). Ecological thresholds: an assessment of methods to identify abrupt changes in species-habitat relationships. *Ecography (Cop.). 32(6)*: 1075–1084. doi:10.1111/j.1600-0587.2009.05571.x.

Firth, B.L.; Drake, D.A.R.; Power, M. (2021). Seasonal and environmental effects on upper thermal limits of eastern sand darter (Ammocrypta pellucida). *Conservation Physiology 9(1).* doi:10.1093/conphys/coab057.

Fischlin, A. (2009). Do We Have Sufficient Safety Margins in Climate Policy? GAIA-Ecological Perspectives on Science and Society 18(3): 193–199. doi:10.14512/gaia.18.3.3.

Foden, W.B.; Butchart, S.H.M.; Stuart, S.N.; Vié, J.-C.; Akçakaya, H.R.; Angulo, A.; DeVantier, L.M.; Gutsche, A.; Turak, E.; Cao, L.; Donner, S.D.; Katariya, V.; Bernard, R.; Holland, R.A.; Hughes, A.F.; O'Hanlon, S.E.; Garnett, S.T.; Şekercioğlu, Ç.H.; Mace, G.M. (2013). Identifying the World's Most Climate Change Vulnerable Species: A Systematic Trait-Based Assessment of all Birds, Amphibians and Corals. *PLoS One 8(6)*: e65427. doi:10.1371/journal.pone.0065427.

Foden, W.B.; Young, B.E.; Akçakaya, H.R.; Garcia, R.A.; Hoffmann, A.A.; Stein, B.A.; Thomas, C.D.; Wheatley, C.J.; Bickford, D.; Carr, J.A.; Hole, D.G.; Martin, T.G.; Pacifici, M.; Pearce-Higgins, J.W.; Platts, P.J.; Visconti, P.; Watson, J.E.M.; Huntley, B. (2019). Climate change vulnerability assessment of species. *WIREs Climate Change 10(1)*: 1–36. doi:10.1002/wcc.551.

Fordham, D.A. (2024). Identifying species traits that predict vulnerability to climate change. *Cambridge Prisms: Extinction 2*: e21. doi:10.1017/ext.2024.24.

Frank, K.T.; Petrie, B.; Fisher, J.A.D.; Leggett, W.C. (2011). Transient dynamics of an altered large marine ecosystem. *Nature 477(7362)*: 86–89. doi:10.1038/nature10285.

Frank, K.T.; Petrie, B.; Shackell, N.L. (2007). The ups and downs of trophic control in continental shelf ecosystems. *Trends in Ecology and Evolution 22(5)*: 236–242. doi:10.1016/j.tree.2007.03.002.

Frank, K.T.; Petrie, B.; Shackell, N.L.; Choi, J.S. (2006). Reconciling differences in trophic control in

mid-latitude marine ecosystems. *Ecology Letters 9(10)*: 1096–1105. doi:10.1111/j.1461-0248.2006.00961.x.

Frank, K.T.; Petrie, B.; Choi, J.S.; Leggett, W.C. (2005). Trophic cascades in a formerly cod-dominated ecosystem. *Science (80-.). 308(5728)*: 1621–1623. doi:10.1126/science.1113075.

Frawley, T.; Provost, M.; Bellquist, L.; Ben-Aderet, N.; Blondin, H.; Brodie, S.; Buil, M.P.; Jacox, M.; Bograd, S.J.; Hazen, E.L.; McGonigal, H.; Ramey, K. (2025). A collaborative climate vulnerability assessment of California marine fishery species. *PLOS Climate 4(2)*: e0000574. doi:10.1371/journal.pclm.0000574.

Froese, R.; Pauly, D. (*Editors*). (2000). FishBase 2000: concepts, design and data sources. Los Banos, Laguna, Philippines.

Froese, R.; Pauly, D. (2014). FishBase. *In* FishBase: World Wide Web electronic publication. www.fishbase.org, version (02/2022). *Edited By* R. Froese and D. Pauly. World Wide Web electronic publication. www.fishbase.org, version (11/2014).

Frölicher, T.L.; Fischer, E.M.; Gruber, N. (2018). Marine heatwaves under global warming. *Nature 560(7718)*: 360–364. Springer US. doi:10.1038/s41586-018-0383-9.

Frye, R. (1986). Variability and management of large marine ecosystems - Sherman, K, Alexander, LM. *Natural Resources Journal 26(3)*: 653–654.

Gallagher, R.V.; Allen, S.; Wright, I.J. (2019). Safety margins and adaptive capacity of vegetation to climate change. *Scientific Reports 9(1)*: 8241. doi:10.1038/s41598-019-44483-x.

Gao, Q.; Yu, M. (2014). Discerning Fragmentation Dynamics of Tropical Forest and Wetland during Reforestation, Urban Sprawl, and Policy Shifts. *PLoS One 9(11)*: e113140. doi:10.1371/journal.pone.0113140.

Garciá Molinos, J.; Halpern, B.S.; Schoeman, D.S.; Brown, C.J.; Kiessling, W.; Moore, P.J.; Pandolfi, J.M.; Poloczanska, E.S.; Richardson, A.J.; Burrows, M.T.; García Molinos, J.; Halpern, B.S.; Schoeman, D.S.; Brown, C.J.; Kiessling, W.; Moore, P.J.; Pandolfi, J.M.; Poloczanska, E.S.; Richardson, A.J.; Burrows, M.T. (2016). Climate velocity and the future global redistribution of marine biodiversity. *Nature Climate Change 6(1)*: 83–88. doi:10.1038/nclimate2769.

Garcia, R.A.; Araujo, M.B.; Burgess, N.D.; Fden, W.B.; Gutsche, A.; Rahbek, C.; Cabeza, M. (2014). Matching species traits to projected threats and opportunities from climate change. *Journal of Biogeography 41*: 724–735.

Garner, G.; Reed, P.; Keller, K. (2016). Climate risk management requires explicit representation of societal trade-offs. *Climate Change 134(4)*: 713–723. doi:10.1007/s10584-016-1607-3.

Gattuso, J.-P.; Magnan, A.; Billé, R.; Cheung, W.L.; Howes, E.L.; Joos, F.; Allemand, D.; Bopp, L.; Cooley, S.R.; Eakin, C.M.; Hoegh-Guldberg, O.; Kelly, R.P.; Pörtner, H.O.; Rogers, A.D.; Baxter, J.M.; Laffoley, D.; Osborn, D.; Rankovic, A.; Rochette, J.; Sumaila, U.R.; Treyer, S.; Turley, C. (2015). Contrasting futures for ocean and society from different anthropogenic CO2 emissions scenarios. *Science (80-.). 349(6243)*: aac4722-1-aac4722-10. doi:10.1126/science.aac4722.

Gebco gridded global bathymetry data. (2009). British Oceanographic Data Centre, Liverpool, UK.

Gonzalez-Suarez, M.; Gomez, A.; Revilla, E. (2013). Which intrinsic traits predict vulnerability to

extinction depends on the actual threatening processes. *Ecosphere 4*: 1–16.

Gove, J.M.; Williams, G.J.; Lecky, J.; Brown, E.; Conklin, E.; Counsell, C.; Davis, G.; Donovan, M.K.; Falinski, K.; Kramer, L.; Kozar, K.; Li, N.; Maynard, J.A.; McCutcheon, A.; McKenna, S.A.; Neilson, B.J.; Safaie, A.; Teague, C.; Whittier, R.; Asner, G.P. (2023). Coral reefs benefit from reduced land–sea impacts under ocean warming. *Nature 621(7979)*: 536–542. doi:10.1038/s41586-023-06394-w.

Greenan, B.J.W.; Shackell, N.L.; Ferguson, K.; Greyson, P.; Cogswell, A.; Brickman, D.; Wang, Z.; Cook, A.; Brennan, C.E.; Saba, V.S. (2019). Climate Change Vulnerability of American Lobster Fishing Communities in Atlantic Canada. *Frontiers in Marine Science 6: 1–18*. Frontiers Media, Lausanne, Switzerland. doi:10.3389/fmars.2019.00579.

Groom, B.; Drupp, M.A.; Freeman, M.C.; Nesje, F. (2022). The Future, Now: A Review of Social Discounting. *Annual Review of Resource Economics 14(1)*: 467–491. doi:10.1146/annurev-resource-111920-020721.

Guest, J.R.; Baird, A.H.; Maynard, J.A.; Muttaqin, E.; Edwards, A.J.; Campbell, S.J.; Yewdall, K.; Affendi, Y.A.; Chou, L.M. (2012). Contrasting Patterns of Coral Bleaching Susceptibility in 2010 Suggest an Adaptive Response to Thermal Stress. *PLoS One 7(3)*: e33353. doi:10.1371/journal.pone.0033353.

Gunderson, A.R.; Armstrong, E.J.; Stillman, J.H. (2016). Multiple Stressors in a Changing World: The Need for an Improved Perspective on Physiological Responses to the Dynamic Marine Environment. *Annual Review of Marine Science 8(1)*: 357–378. doi:10.1146/annurev-marine-122414-033953.

Halpern, B.S.; Frazier, M.; Potapenko, J.; Casey, K.S.; Koenig, K.; Longo, C.; Lowndes, J.S.; Rockwood, R.C.; Selig, E.R.; Selkoe, K.A.; Walbridge, S. (2015). Spatial and temporal changes in cumulative human impacts on the world's ocean. *Nature Communications 6(May)*: 1–7. Nature Publishing Group. doi:10.1038/ncomms8615.

Halpern, B.S.; Longo, C.; Hardy, D.; McLeod, K.L.; Samhouri, J.F.; Katona, S.K.; Kleisner, K.; Lester, S.E.; Oleary, J.; Ranelletti, M.; Rosenberg, A.A.; Scarborough, C.; Selig, E.R.; Best, B.D.; Brumbaugh, D.R.; Chapin, F.S.; Crowder, L.B.; Daly, K.L.; Doney, S.C.; Elfes, C.; Fogarty, M.J.; Gaines, S.D.; Jacobsen, K.I.; Karrer, L.B.; Leslie, H.M.; Neeley, E.; Pauly, D.; Polasky, S.; Ris, B.; St Martin, K.; Stone, G.S.; Rashid Sumaila, U.; Zeller, D.; (2012). An index to assess the health and benefits of the global ocean. *Nature 488(7413)*: 615–620. Nature Publishing Group. doi:10.1038/nature11397.

Halpern, B.S.; Walbridge, S.; Selkoe, K.A.; Kappel, K.V.; Micheli, F.; D'Agrosa, C.; Bruno, J.F.; Casey, K.S.; Ebert, C.; Fox, H.E.; Fujita, R.; Heinemann, D.; Lenihan, H.S.; Madin, E.M.P.; Perry, M.T.; Selig, E.R.; Spalding, M.; Steneck, R.; Watson, R. (2008). A global map of human impact on marine ecosystems. *Science (80-.). 319(5865)*: 948–952. doi:10.1126/science.1149345.

Hare, J.A.; Morrison, W.E.; Nelson, M.W.; Stachura, M.M.; Teeters, E.J.; Griffis, R.B.; Alexander, M.A.; Scott, J.D.; Alade, L.; Bell, R.J.; Chute, A.S.; Curti, K.L.; Curtis, T.H.; Kircheis, D.; Kocik, J.F.; Lucey, S.M.; McCandless, C.T.; Milke, L.M.; Richardson, D.E.; Robillard, E.; Walsh, H.J.; McManus, M.C.; Marancik, K.E.; Griswold, C.A. (2016). A vulnerability assessment of fish and invertebrates to climate change on the northeast U.S. continental shelf. *PLoS One 11(2)*: 1–30. doi:10.1371/journal.pone.0146756.

Hazen, E.L.; Jorgensen, S.; Rykaczewski, R.R.; Bograd, S.J.; Foley, D.G.; Jonsen, I.D.; Shaffer, S.A.; Dunne, J.P.; Costa, D.P.; Crowder, L.B.; Block, B.A. (2013). Predicted habitat shifts of Pacific

top predators in a changing climate. *Nature Climate Change 3(3)*: 234–238. doi:10.1038/nclimate1686.

Healy, K.; Guillerme, T.; Finlay, S.; Kane, A.; Kelly, S.B.A.; McClean, D.; Kelly, D.J.; Donohue, I.; Jackson, A.L.; Cooper, N. (2014). Ecology and mode-of-life explain lifespan variation in birds and mammals. *Proceedings of the Royal Society B Biological Science 281(1784)*: 20140298. doi:10.1098/rspb.2014.0298.

Henson, S.A.; Beaulieu, C.; Ilyina, T.; John, J.G.; Long, M.; Séférian, R.; Tjiputra, J.; Sarmiento, J.L. (2017). Rapid emergence of climate change in environmental drivers of marine ecosystems. *Nature Communications 8(5020)*: 1–9. doi:10.1038/ncomms14682.

Hill, M.F.; Caswell, H. (1999). Habitat fragmentation and extinction thresholds on fractal landscapes. *Ecology Letters 2(2)*: 121–127. doi:10.1046/j.1461-0248.1999.22061.x.

Hill, M.O. (1973). Diversity and Evenness: A Unifying Notation and Its Consequences. *Ecology 54(2)*: 427–432. doi:10.2307/1934352.

Hillebrand, H.; Brey, T.; Gutt, J.; Hagen, W.; Metfies, K.; Meyer, B.; Lewandowska, A. (2018). Climate Change: Warming Impacts on Marine Biodiversity. *In* Handbook on Marine Environment Protection. Springer International Publishing, Cham. pp. 353–373. doi:10.1007/978-3-319-60156-4_18.

Hillebrand, H.; Donohue, I.; Harpole, W.S.; Hodapp, D.; Kucera, M.; Lewandowska, A.M.; Merder, J.; Montoya, J.M.; Freund, J.A. (2020). Thresholds for ecological responses to global change do not emerge from empirical data. *Nature Ecology and Evolution 4(11)*: 1502–1509. doi:10.1038/s41559-020-1256-9.

Hobday, A.J.; Alexander, L.V.; Perkins, S.E.; Smale, D.A.; Straub, S.C.; Oliver, E.C.J.; Benthuysen, J.A.; Burrows, M.T.; Donat, M.G.; Peng, M.; Holbrook, N.J.; Moore, P.J.; Scannell, H.A.; Sen Gupta, A.; Wernberg, T. (2016). A hierarchical approach to defining marine heatwaves. *Progress in Oceanography 141*: 227–238. doi:10.1016/j.pocean.2015.12.014.

Hodapp, D.; Roca, I.T.; Fiorentino, D.; Garilao, C.; Kaschner, K.; Kesner-Reyes, K.; Schneider, B.; Segschneider, J.; Kocsis, Á.T.; Kiessling, W.; Brey, T.; Froese, R. (2023). Climate change disrupts core habitats of marine species. *Global Change Biology 29(12)*: 3304–3317. doi:10.1111/gcb.16612.

Holsman, K.; Ianelli, J.N.; Aydin, K.; Spies, I. (2019). Multi-species supplement: 2019 Climate-enhanced multi-species Stock Assessment for walleye pollock, Pacific cod, and arrowtooth flounder in the Eastern Bering Sea. NPFMC Stock Assess. *Fisheries Evaluation Report Groundfish Resources Bering Sea/Aleutian Islands Region (November)*: 43 p.

Homan, R.N.; Windmiller, B.S.; Reed, J.M. (2004). Critical thresholds associated with habitat loss for two vernal pool-breeding amphibians. *Ecological Applications 14(5)*: 1547–1553. doi:10.1890/03-5125.

Hooper, D.U.; Adair, E.C.; Cardinale, B.J.; Byrnes, J.E.K.; Hungate, B.A.; Matulich, K.L.; Gonzalez, A.; Duffy, J.E.; Gamfeldt, L.; O'Connor, M.I. (2012). A global synthesis reveals biodiversity loss as a major driver of ecosystem change. *Nature 486(7401)*: 105–8. doi:10.1038/nature11118.

WoRMS Editorial Board (2020). World Register of Marine Species. Available from https://www.marinespecies.org at VLIZ. Accessed 2020. doi:10.14284/170

Hunke, E.; Lipscomb, W.; Jones, P.; Turner, A.; Jeffery, N.; Elliott, S. (2017). CICE: The Los Alamos sea ice model. CICE, Los Alamos Sea Ice Model. Available from https://www.scopus.com/inward/record.uri?eid=2-s2.0-85081072888&partnerID=40&md5=83561b4252cf88d3e706ad2203b2dd2f.

Hureau, J.C. (1991). La base de données GICIM: Gestion informatisée des collections ichthyologiques du Muséum. Atlas Préliminaire des Poisson. d'Eau Douce Fr. Cons. Supérieur la Pêche, Ministère l'Environnement, *CEMAGREF Muséum Nationale d'Histoire Naturelle Paris*: 225–227.

IPCC. (2001). Climate Change 2001: Impacts, Adaptation, and Vulnerability. Contribution of Working Group II to the Third Assessment Report of the Intergovernmental Panel on Climate Change (IPCC). *Edited By*J.J. McCarthy, O. Canziani, N.A. Leary, D.J. Dokken, and K.S. White. Cambridge University Press, Cambridge, U.K.

IPCC. (2014). Climate Change 2014: Impacts, Adaptation, and Vulnerability. Part A: Global and Sectoral Aspects. Contribution of Working Group II to the Fifth Assessment Report of the Intergovernmental Panel on Climate Change. *Edited By* C.B. Field, V.R. Barros, D.J. Dokken, K.J. Mach, M.D. Mastrandrea, T.E. Bilir, M. Chatterjee, K.L. Ebi, Y.O. Estrada, R.C. Genova, B. Girma, E.S. Kissel, A.N. Levy, S. MacCracken, P.R. Mastrandrea, and L.L. White. Cambridge University Press, Cambridge, United Kingdom and New York, NY, USA.

IPCC. (2021). Climate Change 2021: The Physical Science Basis. Contribution of Working Group I to the Sixth Assessment Report of the Intergovernmental Panel on Climate Change. *Edited By*V. Masson-Delmotte, P. Zhai, A. Pirani, S.L. Connors, C. Pean, S. Berger, N. Caud, Y. Chen, L. Goldfarb, M.I. Gomis, M. Huang, K. Leitzell, E. Lonnoy, J.B.R. Matthews, T.K. Maycock, T. Waterfield, O. Yelekci, R. Yu, and B. Zhou. Cambridge University Press, Cambridge, U.K. doi:10.1017/9781009157896.

IPCC. (2022). IPCC 2022: Climate Change 2022: Impacts, Adaptation and Vulnerability: Climate Change 2022: Impacts, Adaptation and Vulnerability. Cambridge University Press: 37–118. Available from https://www.ipcc.ch/report/ar6/wg2/.

Irvine, A.L.; Reygondeau, G.; Stanley, R.R.E.; Egorova, Y.; Tittensor, D.P. (2025). Future Climate-Driven Ecological Disruption in a Network of Marine Protected Areas on Canada's East Coast. *Conservation Letters 18(4)*. doi:10.1111/conl.13123.

Isbell, F.; Craven, D.; Connolly, J.; Loreau, M.; Schmid, B.; Beierkuhnlein, C.; Bezemer, T.M.; Bonin, C.; Bruelheide, H.; de Luca, E.; Ebeling, A.; Griffin, J.N.; Guo, Q.; Hautier, Y.; Hector, A.; Jentsch, A.; Kreyling, J.; Lanta, V.; Manning, P.; Meyer, S.T.; Mori, A.S.; Naeem, S.; Niklaus, P.A.; Polley, H.W.; Reich, P.B.; Roscher, C.; Seabloom, E.W.; Smith, M.D.; Thakur, M.P.; Tilman, D.; Tracy, B.F.; van der Putten, W.H.; van Ruijven, J.; Weigelt, A.; Weisser, W.W.; Wilsey, B.; Eisenhauer, N. (2015). Biodiversity increases the resistance of ecosystem productivity to climate extremes. *Nature 526(7574)*: 574–577. doi:10.1038/nature15374.

IUCN. (2012). IUCN Red List Categories and Criteria: Version 3.1. *In* 2nd edition. IUCN, Gland, Switzerland and Cambridge, UK.

IUCN. (2021). The IUCN Red List of Threatened Species. Available from https://www.iucnredlist.org.

Jacox, M.G.; Alexander, M.A.; Bograd, S.J.; Scott, J.D. (2020). Thermal displacement by marine heatwaves. *Nature 584(7819)*: 82–86. doi:10.1038/s41586-020-2534-z.

Jean-Michel, L.; Eric, G.; Romain, B.-B.; Gilles, G.; Angélique, M.; Marie, D.; Clément, B.; Mathieu,

H.; Olivier, L.G.; Charly, R.; Tony, C.; Charles-Emmanuel, T.; Florent, G.; Giovanni, R.; Mounir, B.; Yann, D.; Pierre-Yves, L.T. (2021). The Copernicus Global 1/12° Oceanic and Sea Ice GLORYS12 Reanalysis. *Frontiers of Earth Science 9*. doi:10.3389/feart.2021.698876.

Jenouvrier, S.; Long, M.C.; Coste, C.F.D.; Holland, M.; Gamelon, M.; Yoccoz, N.G.; Sæther, B. (2022). Detecting climate signals in populations across life histories. *Global Change Biology 28(7)*: 2236–2258. doi:10.1111/gcb.16041.

Jiang, D.; Ji, X.; Wang, D.; Liu, P. (2023). Spatiotemporal changes in land use and landscape fragmentation in coastal plain areas—A case study of Yancheng City, China. *Frontiers in Sustainable Food Systems 7*. doi:10.3389/fsufs.2023.1105897.

Jost, L. (2006). Entropy and diversity. *Oikos 113(2)*: 363–375. doi:10.1111/j.2006.0030-1299.14714.x.

Kajtar, J.B.; Holbrook, N.J.; Lyth, A.; Hobday, A.J.; Mundy, C.N.; Ugalde, S.C. (2024). A stakeholder-guided marine heatwave hazard index for fisheries and aquaculture. *Climate Change 177(2)*: 26. doi:10.1007/s10584-024-03684-8.

Kaschner, K.; Kesner-Reyes, K.; Garilao, C.; Segschneider, J.; Rius-Barile, J.; Rees, T.; Froese, R. (2019). Aquamaps: Predicted range maps for aquatic species.

Kaschner, K.; Watson, R.; Trites, A.; Pauly, D. (2006). Mapping world-wide distributions of marine mammal species using a relative environmental suitability (RES) model. *Marine Ecology Progress Series 316*: 285–310. doi:10.3354/meps316285.

Keen, L.; Stortini, C.; Boyce, D.G.; Stanley, R. (2023). Representing Climate Change Vulnerabilities in Canadian Marine Conservation Networks. Submitted.

Keen, L.H.; Stortini, C.H.; Boyce, D.G.; Stanley, R.R.E. (2024). Assessing climate change vulnerability in Canadian marine conservation networks: implications for conservation planning and resilience. *FACETS 9: 1–15*. doi:10.1139/facets-2023-0124.

Keith, D.A.; Mahony, M.; Hines, H.; Elith, J.; Regan, T.J.; Baumgartner, J.B.; Hunter, D.; Heard, G.W.; Mitchell, N.J.; Parris, K.M.; Penman, T.; Scheele, B.; Simpson, C.C.; Tingley, R.; Tracy, C.R.; West, M.; Akçakaya, H.R. (2014). Detecting Extinction Risk from Climate Change by IUCN Red List Criteria. *Conservation Biology 28(3)*: 810–819. doi:10.1111/cobi.12234.

Kroeker, K.J.; Kordas, R.L.; Crim, R.; Hendriks, I.E.; Ramajo, L.; Singh, G.S.; Duarte, C.M.; Gattuso, J.-P. (2013). Impacts of ocean acidification on marine organisms: quantifying sensitivities and interaction with warming. *Global Change Biology 19(6)*: 1884–1896. doi:10.1111/gcb.12179.

Kuo, C.; Ko, C.; Lai, Y. (2022). Assessing warming impacts on marine fishes by integrating physiology-guided distribution projections, life-history changes and food web dynamics. *Methods in Ecology and Evolution 13(6)*: 1343–1357. doi:10.1111/2041-210X.13846.

Lacheheb, M.; Noy, I.; Kahui, V. (2024). Marine heatwaves and commercial fishing in New Zealand. *Science of the Total Environment 954*: 176558. doi:10.1016/j.scitotenv.2024.176558.

Laidre, K.L.; Stirling, I.; Lowry, L.F.; Wiig, O.; Heide-Jorgensen, M.P.; Ferguson, S.H. (2008). Quantifying the sensitivity of Arctic marine mammals to climate-induced habitat change. *Ecological Applications 18*: S97-125.

Lange, R.; Durka, W.; Holzhauer, S.I.J.; Wolters, V.; Diekotter, T. (2010). Differential threshold effects of habitat fragmentation on gene flow in two widespread species of bush crickets. *Molecular Ecology 19(22)*: 4936–4948. doi:10.1111/j.1365-294X.2010.04877.x.

Lavender, E.; Fox, C.J.; Burrows, M.T. (2021). Modelling the impacts of climate change on thermal habitat suitability for shallow-water marine fish at a global scale. *PLoS One 16(10)*: e0258184. doi:10.1371/journal.pone.0258184.

Le Bris, A.; Mills, K.E.; Wahle, R.A.; Chen, Y.; Alexander, M.A.; Allyn, A.J.; Schuetz, J.G.; Scott, J.D.; Pershing, A.J. (2018). Climate vulnerability and resilience in the most valuable North American fishery. *Proceedings of the National Academy of Science USA. 115(8)*: 1831–1836. doi:10.1073/pnas.1711122115.

Le Bris, A.; Pershing, A.J.; Hernandez, C.M.; Mills, K.E.; Sherwood, G.D. (2015). Modelling the effects of variation in reproductive traits on fish population resilience. ICES Journal of Marine Science 72(9): 2590–2599. doi:10.1093/icesjms/fsv154.

Leemans, R.; Vellinga, P. (2017). The scientific motivation of the internationally agreed "well below 2 degrees C" climate protection target: a historical perspective. *Current Opinions on Environmental Sustainability 26–27*: 134–142. doi:10.1016/j.cosust.2017.07.010.

Lehtinen, R.M.; Galatowitsch, S.M.; Tester, J.R. (1999). Consequences of habitat loss and fragmentation for wetland amphibian assemblages. *Wetlands 19(1)*: 1–12. doi:10.1007/BF03161728.

Lettrich, M.D.; Asaro, M.J.; Borggaard, D.L.; Dick, D.M.; Griffis, R.B.; Litz, J.A.; Orphanides, C.D.; Palka, D.L.; Soldevilla, M.S.; Balmer, B.; Chavez, S.; Cholewiak, D.; Claridge, D.; Ewing, R.Y.; Fazioli, K.L.; Fertl, D.; Fougeres, E.M.; Gannon, D.; Garrison, L.; Gilbert, J.; Gorgone, A.; Hohn, A.; Horstman, S.; Josephson, B.; Kenney, R.D.; Kiszka, J.J.; Maze-Foley, K.; McFee, W.; Mullin, K.D.; Murray, K.; Pendleton, D.E.; Robbins, J.; Roberts, J.J.; Rodriguez- Ferrer, G.; Ronje, E.I.; Rosel, P.E.; Speakman, T.; Stanistreet, J.E.; Stevens, T.; Stolen, M.; Moore, R.T.; Vollmer, N.L.; Wells, R.; Whitehead, H.R.; Whitt, A. (2023). Vulnerability to climate change of United States marine mammal stocks in the western North Atlantic, Gulf of Mexico, and Caribbean. *PLoS One 18(9)*: e0290643. doi:10.1371/journal.pone.0290643.

Lettrich, M.D.; Dick, D.M.; Fahy, C.C.; Griffis, R.B.; Haas, H.L.; Jones, T.T.; Kelly, I.K.; Klemm, D.; Lauritsen, A.M.; Sasso, C.R.; Schroeder, B.; Seminoff, J.A.; Upite, C.M.; Allen, C.; Casale, P.; Fuentes, M.M.P.B.; Gaos, A.; Hamann, M.; Kurpita, L.; Liles, M.J.; Martin, S.; Piovano, S.; Possardt, E.; Saba, V.; Swimmer, Y.; Tiwari, M.; Wibbels, T.; Wyneken, J. (2025). A global sea turtle climate vulnerability assessment. *Ecological Indicators 179*: 114143. doi:10.1016/j.ecolind.2025.114143.

Lewis, S.A.; Stortini, C.H.; Boyce, D.G.; Stanley, R.R.E. (2023). Climate change, species thermal emergence, and conservation design: a case study in the Canadian Northwest Atlantic. *FACETS 8*: 1–16. doi:10.1139/facets-2022-0191.

Li, D.; Wu, S.; Liu, L.; Zhang, Y.; Li, S. (2018). Vulnerability of the global terrestrial ecosystems to climate change. *Global Change Biology 24(9)*: 4095–4106. doi:10.1111/gcb.14327.

Liao, J.; Li, Z.; Hiebeler, D.E.; El-Bana, M.; Deckmyn, G.; Nijs, I. (2013). Modelling plant population size and extinction thresholds from habitat loss and habitat fragmentation: Effects of neighbouring competition and dispersal strategy. *Ecological Modelling 268*: 9–17. doi:10.1016/j.ecolmodel.2013.07.021.

Loarie, S.R.; Duffy, P.B.; Hamilton, H.; Asner, G.P.; Field, C.B.; Ackerly, D.D. (2009). The velocity

of climate change. *Nature 462(7276)*: 1052–1056. doi:10.1038/nature08649.

Longhurst, A. (2007). Ecological geography of the sea. Elsevier Inc.; Burlington, MA.

Lotze, H.K.; Tittensor, D.P.; Bryndum-Buchholz, A.; Eddy, T.D.; Cheung, W.W.; Galbraith, E.D.; Barange, M.; Barrier, N.; Bianchi, D.; Blanchard, J.L.; Bopp, L.; Buechner, M.; Bulman, C.; Carozza, D.A.; Christensen, V.; Coll, M.; Dunne, J.; Fulton, E.A.; Jennings, S.; Jones, M.; Mackinson, S.; Maury, O.; Niiranen, S.; Oliveros-Ramos, R.; Roy, T.; Fernandes, J.A.; Schewe, J.; Shin, Y.-J.; Silva, T.A.; Steenbeek, J.; Stock, C.A.; Verley, P.; Volkholz, J.; Walker, N.D. (2019). Ensemble projections of global ocean animal biomass with climate change. *Proceedings of the National Acadamy of Science*: 1–6. doi:doi.org/10.1073/pnas.1900194116.

Lundquist, C.; Stephenson, F.; McCartain, L.; Watson, S.; Brough, T.; Nelson, W.; Neill, K.; Anderson, O.; Bulmer, R.; Gee, E.; Pinkerton, M.; Rowden, A.; Thompson, D. (2020). Evaluating Key Ecological Areas datasets for the New Zealand Marine Environment. *In* NIWA Client Report No. 2020109HN, prepared for the Department of Conservation.

MacKenzie, B.R.; Payne, M.R.; Boje, J.; Hoyer, J.L.; Siegstad, H. (2014). A cascade of warming impacts brings bluefin tuna to Greenland waters. *Global Change Biology 20(8)*: 2484–2491. doi:10.1111/gcb.12597.

MacLean, S.A.; Beissinger, S.R. (2017). Species' traits as predictors of range shifts under contemporary climate change: A review and meta-analysis. *Global Change Biology 23(10)*: 4094–4105. doi:10.1111/gcb.13736.

Madec, G. (2015). NEMO ocean engine. Inst. Pierre-Simon Laplace. Available from https://www.scopus.com/inward/record.uri?eid=2-s2.0-58249090425&partnerID=40&md5=164f30ad07e79ecd9726d450c7c2e6cf.

Mann, K.H.; Lazier, J.R.N. (1991). *Dynamics of marine ecosystems*. Blackwell, Oxford, UK.

Martin, T.G.; Watson, J.E.M. (2016). Intact ecosystems provide best defence against climate change. *Nature Climate Change 6(2)*: 122–124. doi:10.1038/nclimate2918.

Maxwell, S.M.; Hazen, E.L.; Bograd, S.J.; Halpern, B.S.; Breed, G.A.; Nickel, B.; Teutschel, N.M.; Crowder, L.B.; Benson, S.; Dutton, P.H.; Bailey, H.; Kappes, M.A.; Kuhn, C.E.; Weise, M.J.; Mate, B.; Shaffer, S.A.; Hassrick, J.L.; Henry, R.W.; Irvine, L.; McDonald, B.I.; Robinson, P.W.; Block, B.A.; Costa, D.P. (2013). Cumulative human impacts on marine predators. *Nature Communications 4(1)*: 2688. doi:10.1038/ncomms3688.

McClain, C.R.; Heim, N.A.; Knope, M.L.; Monarrez, P.M.; Payne, J.L.; Santos, I.T.; Webb, T.J. (2025). MOBS 1.0: A Database of Interspecific Variation in Marine Organismal Body Sizes. *Global Ecology and Biogeography 34(6)*. doi:10.1111/geb.70062.

McClure, M.M.; Haltuch, M.A.; Willis-Norton, E.; Huff, D.D.; Hazen, E.L.; Crozier, L.G.; Jacox, M.G.; Nelson, Andrews, K.S.; Barnett, L.A.K.; Berger, A.M.; Beyer, S.; Bizzarro, J.; Boughton, D.; Cope, J.M.; Carr, M.; Dewar, H.; Dick, E.; Dorval, E.; Dunham, J.; Gertseva, V.; Greene, C.M.; Gustafson, R.G.; Hamel, O.S.; Harvey, C.J.; Henderson, M.J.; Jordan, C.E.; Kaplan, I.C.; Lindley, S.T.; Mantua, N.J.; Matson, S.E.; Monk, M.H.; Moyle, P.; Nicol, C.; Pohl, J.; Rykaczewski, R.R.; Samhouri, J.F.; Sogard, S.; Tolimieri, N.; Wallace, J.; Wetzel, C.; Bograd, S.J. (2023). Vulnerability to climate change of managed stocks in the California Current large marine ecosystem. *Frontiers in Marine Science 10*. doi:10.3389/fmars.2023.1103767.

McHenry, J.; Welch, H.; Lester, S.E.; Saba, V. (2019). Projecting marine species range shifts from

only temperature can mask climate vulnerability. *Global Change Biology 25(12)*: 4208–4221. doi:10.1111/gcb.14828.

McLeod, E.; Salm, R.; Green, A.; Almany, J. (2009). Designing marine protected area networks to address the impacts of climate change. *Frontiers in Ecology and the Environment 7(7)*: 362–370. doi:10.1890/070211.

Meinshausen, M.; Nicholls, Z.R.J.; Lewis, J.; Gidden, M.J.; Vogel, E.; Freund, M.; Beyerle, U.; Gessner, C.; Nauels, A.; Bauer, N.; Canadell, J.G.; Daniel, J.S.; John, A.; Krummel, P.B.; Luderer, G.; Meinshausen, N.; Montzka, S.A.; Rayner, P.J.; Reimann, S.; Smith, S.J.; van den Berg, M.; Velders, G.J.M.; Vollmer, M.K.; Wang, R.H.J. (2020). The shared socio-economic pathway (SSP) greenhouse gas concentrations and their extensions to 2500. *Geoscience Model Development 13(8)*: 3571–3605. doi:10.5194/gmd-13-3571-2020.

Merino, G.; Arrizabalaga, H.; Arregui, I.; Santiago, J.; Murua, H.; Urtizberea, A.; Andonegi, E.; De Bruyn, P.; Kell, L.T. (2019). Adaptation of North Atlantic Albacore Fishery to Climate Change: Yet Another Potential Benefit of Harvest Control Rules. *Frontiers in Marine Science 6(October)*: 1–14. doi:10.3389/fmars.2019.00620.

Meyer, A.S.; Pigot, A.L.; Merow, C.; Kaschner, K.; Garilao, C.; Kesner-Reyes, K.; Trisos, C.H. (2024). Temporal dynamics of climate change exposure and opportunities for global marine biodiversity. *Nature Communications 15(1)*: 5836. doi:10.1038/s41467-024-49736-6.

Molina, A.N.; García-Huidobro, M.R.; Rezende, E.L.; Carter, M.J. (2025). Chronic Heat Tolerance Reveals Overestimated Thermal Safety Margins and Increased Vulnerability in Marine Fish Populations. *Ecology Letters 28(6)*. doi:10.1111/ele.70165.

Moll, D.; Asmus, H.; Blöcker, A.; Böttcher, U.; Conradt, J.; Färber, L.; Funk, N.; Funk, S.; Gutte, H.; Hinrichsen, H.-H.H.; Kotterba, P.; Krumme, U.; Madiraca, F.; Meier, H.E.M.M.; Meyer, S.; Moritz, T.; Otto, S.A.; Pinto, G.; Polte, P.; Riekhof, M.-C.C.; Sarrazin, V.; Schwermer, H.; Scotti, M.; Voss, R.; Winkler, H.; Möllmann, C. (2024). A climate vulnerability assessment of the fish community in the Western Baltic Sea. *Scientific Reports 14(1)*: 16184. doi:10.1038/s41598-024-67029-2.

Moore, S.E.; Huntington, H.P. (2008). Arctic marine mammals and climate change: impacts and resilience. *Ecological Applications 18(sp2)*: S157–S165. doi:10.1890/06-0571.1.

Mora, C.; Caldwell, I.R.; Caldwell, J.M.; Fisher, M.R.; Genco, B.M.; Running, S.W. (2015). Suitable Days for Plant Growth Disappear under Projected Climate Change: Potential Human and Biotic Vulnerability. *PLoS Biol. 13(6)*: e1002167. doi:10.1371/journal.pbio.1002167.

Mora, C.; Danovaro, R.; Loreau, M. (2014). Alternative hypotheses to explain why biodiversity-ecosystem functioning relationships are concave-up in some natural ecosystems but concave-down in manipulative experiments. *Scientific Reports 4*: 5427. doi:10.1038/srep05427.

Mora, C.; Frazier, A.G.; Longman, R.J.; Dacks, R.S.; Walton, M.M.; Tong, E.J.; Sanchez, J.J.; Kaiser, L.R.; Stender, Y.O.;erson, J.M.; Ambrosino, C.M.; Fernandez-Silva, I.; Giuseffi, L.M.; Giambelluca, T.W. (2013a). The projected timing of climate departure from recent variability. *Nature 502(7470)*: 183+. doi:10.1038/nature12540.

Mora, C.; Wei, C.-L.; Rollo, A.; Amaro, T.; Baco, A.R.; Billett, D.; Bopp, L.; Chen, Q.; Collier, M.; Danovaro, R.; Gooday, A.J.; Grupe, B.M.; Halloran, P.R.; Ingels, J.; Jones, D.O.B.; Levin, L.A.; Nakano, H.; Norling, K.; Ramirez-Llodra, E.; Rex, M.; Ruhl, H. a; Smith, C.R.; Sweetman, A.K.; Thurber, A.R.; Tjiputra, J.F.; Usseglio, P.; Watling, L.; Wu, T.; Yasuhara, M. (2013b). Biotic and human vulnerability to projected changes in ocean biogeochemistry over the 21st

century. *PLoS Biol. 11(10)*: 1–14. doi:10.1371/journal.pbio.1001682.

Morley, S.A.; Hirse, T.; Pörtner, H.-O.; Peck, L.S. (2009). Geographical variation in thermal tolerance within Southern Ocean marine ectotherms. *Comparative Biochemistry and Physiology Part A: Molecular & Integrative Physiology 153(2)*: 154–161. doi:10.1016/j.cbpa.2009.02.001.

Morrison, W.E.; Nelson, M.W.; Griffis, R.B.; Hare, J.A. (2016). Methodology for Assessing the Vulnerability of Marine and Anadromous Fish Stocks in a Changing Climate. *Fisheries 41(7)*: 407–409. doi:10.1080/03632415.2016.1182507.

Morrison, W.E.; Nelson, M.W.; Howard, J.F.; Teeters, E.J.; Hare, J.A.; Griffis, R.B.; Scott, J.D.; Alexander, M.A. (2015). Methodology for assessing the vulnerability of marine fish and shellfish species to a changing climate. *NOAA Technical Memorandum NMFS-OSF-3*: 48 p.

Nadeau, C.P.; Urban, M.C.; Bridle, J.R. (2017). Climates past, present, and yet-to-come shape climate change vulnerabilities. *Trends in Ecology and Evolution 32(10)*: 786–800. doi:10.1016/j.tree.2017.07.012.

Natori, Y.; Haneda, A.; Suzuki, Y. (2006). Vertical and seasonal differences in biogenic silica dissolution in natural seawater in Suruga Bay, Japan: Effects of temperature and organic matter. *Marine Chemistry 102(3–4)*: 230–241. doi:10.1016/j.marchem.2006.04.007.

Newbold, T.; Hudson, L.N.; Arnell, A.P.; Contu, S.; De Palma, A.; Ferrier, S.; Hill, S.L.L.; Hoskins, A.J.; Lysenko, I.; Phillips, H.R.P.; Burton, V.J.; Chng, C.W.T.; Emerson, S.; Gao, D.; Pask-Hale, G.; Hutton, J.; Jung, M.; Sanchez-Ortiz, K.; Simmons, B.I.; Whitmee, S.; Zhang, H.; Scharlemann, J.P.W.; Purvis, A. (2016). Has land use pushed terrestrial biodiversity beyond the planetary boundary? A global assessment. *Science (80-.). 353(6296)*: 288–291. doi:10.1126/science.aaf2201.

Ochoa-Quintero, J.M.; Gardner, T.A.; Rosa, I.; de Barros Ferraz, S.F.; Sutherland, W.J. (2015). Thresholds of species loss in Amazonian deforestation frontier landscapes. *Conservation Biology29(2)*: 440–451. doi:10.1111/cobi.12446.

Ofori, B.Y.; Stow, A.J.; Baumgartner, J.B.; Beaumont, L.J. (2017). Influence of adaptive capacity on the outcome of climate change vulnerability assessment. *Scientific Reports 7(1)*: 12979. doi:10.1038/s41598-017-13245-y.

Ohlemüller, R.;erson, B.J.; Araújo, M.B.; Butchart, S.H..; Kudrna, O.; Ridgely, R.S.; Thomas, C.D. (2008). The coincidence of climatic and species rarity: high risk to small-range species from climate change. *Biology Letters 4(5)*: 568–572. doi:10.1098/rsbl.2008.0097.

Ojoyi, M.M.; Odindi, J.; Mutanga, O.; Abdel-Rahman, E.M. (2016). Analysing fragmentation in vulnerable biodiversity hotspots in Tanzania from 1975 to 2012 using remote sensing and fragstats. *Nature Conservation 16*: 19–37. doi:10.3897/natureconservation.16.9312.

Oliver, E.C.J.; Donat, M.G.; Burrows, M.T.; Moore, P.J.; Smale, D.A.; Alexander, L.V.; Benthuysen, J.A.; Feng, M.; Sen Gupta, A.; Hobday, A.J.; Holbrook, N.J.; Perkins-Kirkpatrick, S.E.; Scannell, H.A.; Straub, S.C.; Wernberg, T. (2018). Longer and more frequent marine heatwaves over the past century. *Nature Communications 9(1)*: 1–12. Springer US. doi:10.1038/s41467-018-03732-9.

Oliver, E.C.J.; O'Kane, T.J.; Holbrook, N.J. (2015). Projected changes to Tasman Sea eddies in a future climate. *Journal of Geophysical Researcy - Oceanography 120(11)*: 7150–7165. doi:10.1002/2015JC010993.

Oliver, T.H. (2016). How much biodiversity loss is too much? *Science (80-.). 353(6296)*: 220–221. doi:10.1126/science.aag1712.

Oppenheimer, M.; Little, C.M.; Cooke, R.M. (2016). Expert judgement and uncertainty quantification for climate change. *Nature Climate Change 6(5)*: 445–451. doi:10.1038/NCLIMATE2959.

Ottersen, G.; Hjermann, D.O.; Stenseth, N.C. (2006). Changes in spawning stock structure strengthen the link between climate and recruitment in a heavily fished cod (*Gadus morhua*) stock. *Fisheries Oceanography 15(3)*: 230–243. doi:10.1111/j.1365-2419.2006.00404.x.

Pacifici, M.; Foden, W.B.; Visconti, P.; Watson, J.E.M.; Butchart, S.H.M.; Kovacs, K.M.; Scheffers, B.R.; Hole, D.G.; Martin, T.G.; Akçakaya, H.R.; Corlett, R.T.; Huntley, B.; Bickford, D.; Carr, J.A.; Hoffmann, A.A.; Midgley, G.F.; Pearce-Kelly, P.; Pearson, R.G.; Williams, S.E.; Willis, S.G.; Young, B.; Rondinini, C. (2015). Assessing species vulnerability to climate change. *Nature Climate Change 5(3)*: 215–225. doi:10.1038/nclimate2448.

Palmeirim, A.F.; Santos-Filho, M.; Peres, C.A. (2020). Marked decline in forest-dependent small mammals following habitat loss and fragmentation in an Amazonian deforestation frontier. *PLoS One 15(3)*: e0230209. doi:10.1371/journal.pone.0230209.

Palomares, M.L.D.; Pauly, D. (2022). SeaLifeBase. World Wide Web Electronic Publication www.sealifebase.org, version (11/2014).

Parker, M.; Mac Nally, R. (2002). Habitat loss and the habitat fragmentation threshold: an experimental evaluation of impacts on richness and total abundances using grassland invertebrates. *Biological Conservation 105(2)*: 217–229. doi:10.1016/S0006-3207(01)00184-7.

Pauly, D.; Christensen, V.; Froese, R.; Longhurst, A.; Platt, T.; Sathyendranath, S.; Sherman, K.; Watson, R. (2000). Mapping fisheries onto marine ecosystems: a consensus approach for regional, oceanic and global integrations. In D. Pauly; T.J. Pitcher, eds. Methods for Evaluating the Impacts on Fisheries on North Atlantic Ecosystems. *Fisheries Centre Research Reports 8(2)*

Payne, M.R.; Kudahl, M.; Engelhard, G.H.; Peck, M.A.; Pinnegar, J.K. (2021). Climate risk to European fisheries and coastal communities. *Proceedings of the National Acadamy of Science U.S.A. 118(40)*: 1–10. doi:10.1073/pnas.2018086118.

Pearson, R.G.; Stanton, J.C.; Shoemaker, K.T.; Aiello-Lammens, M.E.; Ersts, P.J.; Horning, N.; Fordham, D.A.; Raxworthy, C.J.; Ryu, H.Y.; McNees, J.; Akçakaya, H.R. (2014). Life history and spatial traits predict extinction risk due to climate change. *Nature Climate Change 4(3)*: 217–221. doi:10.1038/nclimate2113.

Peters, R.L. (1985). The Greenhouse Effect and Nature Reserves. *Biosciences 35*: 707–717.

Pigot, A.L.; Merow, C.; Wilson, A.; Trisos, C.H. (2023). Abrupt expansion of climate change risks for species globally. *Nature Ecology and Evolution 7(7)*: 1060–1071. doi:10.1038/s41559-023-02070-4.

Pikitch, E.K.; Rountos, K.J.; Essington, T.E.; Santora, C.; Pauly, D.; Watson, R.; Sumaila, U.R.; Boersma, P.D.; Boyd, I.L.; Conover, D.O.; Cury, P.; Heppell, S.S.; Houde, E.D.; Mangel, M.; Plagányi, É.; Sainsbury, K.; Steneck, R.S.; Geers, T.M.; Gownaris, N.; Munch, S.B.(2014). The global contribution of forage fish to marine fisheries and ecosystems. *Fish and Fisheries 15(1):* 43–64. doi:10.1111/faf.12004.

Pinnegar, J.K.; Engelhard, G.H.; Norris, N.J.; Theophille, D.; Sebastien, R.D.; Hidalgo, M. (2019). Assessing vulnerability and adaptive capacity of the fisheries sector in Dominica: Long-term

climate change and catastrophic hurricanes. *ICES Journal of Marine Science 76(5)*: 1353–1367. doi:10.1093/icesjms/fsz052.

Pinsky, M.L.; Eikeset, A.M.; McCauley, D.J.; Payne, J.L.; Sunday, J.M. (2019). Greater vulnerability to warming of marine versus terrestrial ectotherms. *Nature 569*: 108–111. doi:10.1038/s41586-019-1132-4.

Pinsky, M.L.; Fenichel, E.; Fogarty, M.; Levin, S.; McCay, B.; St. Martin, K.; Selden, R.L.; Young, T. (2021). Fish and fisheries in hot water: What is happening and how do we adapt? *Population Ecology 63(1):* 17–26. doi:10.1002/1438-390X.12050.

Pinsky, M.L.; Mantua, N.J. (2014). Emerging Adaptation Approaches for Climate-Ready Fisheries Management. *Oceanography 27(4, SI)*: 146–159. doi:10.5670/oceanog.2014.93.

Pinsky, M.L.; Worm, B.; Fogarty, M.J.; Sarmiento, J.L.; Levin, S.A. (2013). Marine Taxa Track Local Climate Velocities. S*cience (80-.). 341(6151)*: 1239–1242. doi:10.1126/science.1239352.

Poloczanska, E.S.; Burrows, M.T.; Brown, C.J.; Garcia Molinos, J.; Halpern, B.S.; Hoegh-Guldberg, O.; Kappel, C.V, Moore, P.J.; Richardson, A.J.; Schoeman, D.S.; Sydeman, W.J. (2016). Responses of Marine Organisms to Climate Change across Oceans. *Frontiers of Marine Science 3(May)*: 62. doi:10.3389/fmars.2016.00062.

Portner, H.O.; Farrell, A.P. (2008). Physiology and climate change. *Science (80-.). 322(5902)*: 690–692. doi:10.1126/science.1163156.

R Core Team; R Team. (2024). R: A language and environment for statistical computing. *In* R Foundation for Statistical Computing. R Foundation for Statistical Computing, Vienna, Austria. Available from https://www.r-project.org/.

Rae, J.G.L.; Hewitt, H.T.; Keen, A.B.; Ridley, J.K.; West, A.E.; Harris, C.M.; Hunke, E.C.; Walters, D.N. (2015). Development of the Global Sea Ice 6.0 CICE configuration for the Met Office Global Coupled model. *Geoscience Model Development 8(7)*: 2221 – 2230. doi:10.5194/gmd-8-2221-2015.

Reddin, C.J.; Aberhan, M.; Raja, N.B.; Kocsis, Á.T. (2022). Global warming generates predictable extinctions of warm- and cold-water marine benthic invertebrates via thermal habitat loss. *Global Change Biology 28(19)*: 5793–5807. doi:10.1111/gcb.16333.

Rehm, E.M.; Olivas, P.; Stroud, J.; Feeley, K.J. (2015). Losing your edge: climate change and the conservation value of range-edge populations. *Ecology and Evolution 5(19)*: 4315–4326. doi:10.1002/ece3.1645.

Reygondeau, G.; Egorova, Y.; Boerder, K.; Tittensor, D.P.; Kaschner, K.; Kesner-Reyes, K.; Bailly, N.; Cheung, W.W.L. (2026). AquaX: An enhanced and revised AquaMaps framework to model marine species distributions and biodiversity. *PLoS One 21(2)*: e0335823. doi:10.1371/journal.pone.0335823.

Reynolds, R.W.; Smith, T.M.; Liu, C.; Chelton, D.B.; Casey, K.S.; Schlax, M.G. (2007). Daily high-resolution-blended analyses for sea surface temperature. *Journal of Climate 20(22)*: 5473–5496. doi:10.1175/2007jcli1824.1.

Riahi, K.; van Vuuren, D.P.; Kriegler, E.; Edmonds, J.; O'Neill, B.C.; Fujimori, S.; Bauer, N.; Calvin, K.; Dellink, R.; Fricko, O.; Lutz, W.; Popp, A.; Cuaresma, J.C.; Samilr, K.C.; Leimbach, M.; Jiang, L.; Kram, T.; Rao, S.; Emmerling, J.; Ebi, K.; Hasegawa, T.; Havlik, P.; Humpenöder, F.;

Da Silva, L.A.; Smith, S.; Stehfest, E.; Bosetti, V.; Eom, J.; Gernaat, D.; Masui, T.; Rogelj, J.; Strefler, J.; Drouet, L.; Krey, V.; Luderer, G.; Harmsen, M.; Takahashi, K.; Baumstark, L.; Doelman, J.C.; Kainuma, M.; Klimont, Z.; Marangoni, G.; Lotze-Campen, H.; Obersteiner, M.; Tabeau, A.; Tavoni, M. (2017). The Shared Socioeconomic Pathways and their energy, land use, and greenhouse gas emissions implications: An overview. *Global Environmental Change 42*: 153–168. doi:10.1016/j.gloenvcha.2016.05.009.

Ripple, W.J.; Wolf, C.; Newsome, T.M.; Hoffmann, M.; Wirsing, A.J.; McCauley, D.J. (2017). Extinction risk is most acute for the world's largest and smallest vertebrates. *Proceedings of the National Acadamy of Science 114(40)*: 10678–10683. doi:10.1073/pnas.1702078114.

Robinson, N.M.; Nelson, W.A.; Costello, M.J.; Sutherland, J.E.; Lundquist, C.J. (2017). A Systematic Review of Marine-Based Species Distribution Models (SDMs) with Recommendations for Best Practice. *Frontiers in Marine Science 4*. doi:10.3389/fmars.2017.00421.

Rockström, J.; Steffen, W.; Noone, K.; Persson, Å.; Chapin, F.S.; Lambin, E.F.; Lenton, T.M.; Scheffer, M.; Folke, C.; Schellnhuber, H.J.; Nykvist, B.B.; de Wit, C.A.; Hughes, T.; van der Leeuw, S.; Rodhe, H.; Sörlin, S.; Snyder, P.K.; Costanza, R.; Svedin, U.; Falkenmark, M.; Karlberg, L.; Corell, R.W.; Fabry, V.J.; Hansen, J.; Walker, B.; Liverman, D.; Richardson, K.; Crutzen, P.; Foley, J.A.; Rockstrom, J.; Steffen, W.; Noone, K.; Persson, A.; Chapin III, F.S.; Lambin, E.F.; Lenton, T.M.; Scheffer, M.; Folke, C.; Schellnhuber, H.J.; Nykvist, B.B.; de Wit, C.A.; Hughes, T.; van der Leeuw, S.; Rodhe, H.; Sorlin, S.; Snyder, P.K.; Costanza, R.; Svedin, U.; Falkenmark, M.; Karlberg, L.; Corell, R.W.; Fabry, V.J.; Hansen, J.; Walker, B.; Liverman, D.; Richardson, K.; Crutzen, P.; Foley, J.A. (2009). A safe operating space for humanity. *Nature 461(7263)*: 472–475. doi:10.1038/461472a.

Rogan, J.E.; Lacher, T.E. (2018). Impacts of Habitat Loss and Fragmentation on Terrestrial Biodiversity. *In* Reference Module in Earth Systems and Environmental Sciences. Elsevier. doi:10.1016/B978-0-12-409548-9.10913-3.

Rogers-Bennett, L.; Catton, C.A. (2019). Marine heat wave and multiple stressors tip bull kelp forest to sea urchin barrens. *Scientific Reports 9(1)*: 15050. doi:10.1038/s41598-019-51114-y.

Rogers, L.A.; Salomon, A.K.; Connors, B.; Krkošek, M. (2018). Collapse, Tipping Points, and Spatial Demographic Structure Arising from the Adopted Migrant Life History. *American Naturalist 192(1)*: 000–000. doi:10.1086/697488.

Rompre, G.; Boucher, Y.; Belanger, L.; Cote, S.; Robinson, W.D. (2010). Conserving biodiversity in managed forest landscapes: The use of critical thresholds for habitat. *Forestry Chronical 86(5):* 589–596. doi:10.5558/tfc86589-5.

Rosset, V.; Oertli, B. (2011). Freshwater biodiversity under climate warming pressure: Identifying the winners and losers in temperate standing waterbodies. *Biological Conservation 144:* 2311–2319.

Rueda, M.; Hawkins, B.A.; Morales-Castilla, I.; Vidanes, R.M.; Ferrero, M.; Rodríguez, M.Á. (2013). Does fragmentation increase extinction thresholds? A European-wide test with seven forest birds. *Global Ecology and Biogeography 22(12)*: 1282–1292. doi:10.1111/geb.12079.

Runge, C.A.; Tulloch, A.; Hammill, E.; Possingham, H.P.; Fuller, R.A. (2015). Geographic range size and extinction risk assessment in nomadic species. *Conservation Biology29(3)*: 865–876. doi:10.1111/cobi.12440.

Safaie, A.; Silbiger, N.J.; McClanahan, T.R.; Pawlak, G.; Barshis, D.J.; Hench, J.L.; Rogers, J.S.; Williams, G.J.; Davis, K.A. (2018). High frequency temperature variability reduces the risk of coral bleaching. *Nature Communications 9(1)*: 1671. Springer US. doi:10.1038/s41467-018-

04074-2.

Salinger, M.J.; Trenberth, K.E.; Diamond, H.J.; Behrens, E.; Fitzharris, B.B.; Herold, N.; Smith, R.O.; Sutton, P.J.; Trought, M.C.T. (2024). Climate Extremes in the New Zealand Region: Mechanisms, Impacts and Attribution. *International Journal of Climatology 44(16)*: 5809–5824. doi:10.1002/joc.8667.

Scheffers, B.R.; De Meester, L.; Bridge, T.C.L.L.; Hoffmann, A.A.; Pandolfi, J.M.; Corlett, R.T.; Butchart, S.H.M.M.; Pearce-Kelly, P.; Kovacs, K.M.; Dudgeon, D.; Pacifici, M.; Rondinini, C.; Foden, W.B.; Martin, T.G.; Mora, C.; Bickford, D.; Watson, J.E.M.M. (2016). The broad footprint of climate change from genes to biomes to people. *Science (80-.). 354*:6313. doi:10.1126/science.aaf7671.

Scholes, R.J.; Biggs, R. (2005). A biodiversity intactness index. *Nature 434(7029)*: 45–49. doi:10.1038/nature03289.

Sein, D. V.; Koldunov, N. V.; Danilov, S.; Sidorenko, D.; Wekerle, C.; Cabos, W.; Rackow, T.; Scholz, P.; Semmler, T.; Wang, Q.; Jung, T. (2018). The Relative Influence of Atmospheric and Oceanic Model Resolution on the Circulation of the North Atlantic Ocean in a Coupled Climate Model. *Journal of Advances in Modelling Earth Systems 10(8)*: 2026–2041. doi:10.1029/2018MS001327.

Shackell, N.L.; Ricard, D.; Stortini, C. (2014). Thermal Habitat Index of Many Northwest Atlantic Temperate Species Stays Neutral under Warming Projected for 2030 but Changes Radically by 2060. *PLoS One 9(3)*. doi:10.1371/journal.pone.0090662.

Shah, A.A.; Gill, B.A.; Encalada, A.C.; Flecker, A.S.; Funk, W.C.; Guayasamin, J.M.; Kondratieff, B.C.; Poff, N.L.; Thomas, S.A.; Zamudio, K.R.; Ghalambor, C.K. (2017). Climate variability predicts thermal limits of aquatic insects across elevation and latitude. *Functional Ecology 31(11)*: 2118–2127. doi:10.1111/1365-2435.12906.

Shennan-Farpón, Y.; Visconti, P.; Norris, K. (2021). Detecting ecological thresholds for biodiversity in tropical forests: Knowledge gaps and future directions. *Biotropica 53(5)*: 1276–1289. btp.12999. doi:10.1111/btp.12999.

Shin, M. (2023). Freshwater Climate Risk Index for Biodiversity (FW-CRIB): Using Climate Change Vulnerability and Risk Assessments (CCVA/CCRA) to Guide Freshwater Management in Canada's Maritime Provinces. Dalhousie University.

Smale, D.A.; Wernberg, T.; Oliver, E.C.J.; Thomsen, M.; Harvey, B.P.; Straub, S.C.; Burrows, M.T.; Alexander, L. V.; Benthuysen, J.A.; Donat, M.G.; Feng, M.; Hobday, A.J.; Holbrook, N.J.; Perkins-Kirkpatrick, S.E.; Scannell, H.A.; Sen Gupta, A.; Payne, B.L.; Moore, P.J. (2019). Marine heatwaves threaten global biodiversity and the provision of ecosystem services. *Nature Climate Change 9(4)*: 306–312. doi:10.1038/s41558-019-0412-1.

Spencer, P.D.; Hollowed, A.B.; Sigler, M.F.; Hermann, A.J.; Nelson, M.W. (2019). Trait-based climate vulnerability assessments in data-rich systems: An application to eastern Bering Sea fish and invertebrate stocks. *Global Change Biology 25(11)*: 3954–3971. doi:10.1111/gcb.14763.

Stanton, J.C.; Shoemaker, K.T.; Pearson, R.G.; Akçakaya, H.R. (2015). Warning times for species extinctions due to climate change. *Global Change Biology 21(3)*: 1066–1077. doi:10.1111/gcb.12721.

Staude, I.R.; Navarro, L.M.; Pereira, H.M. (2020). Range size predicts the risk of local extinction

from habitat loss. *Global Ecology and Biogeography 29(1):* 16–25. doi:10.1111/geb.13003.

Stelzenmüller, V.; Lee, J.; South, A.; Rogers, S. (2010). Quantifying cumulative impacts of human pressures on the marine environment: a geospatial modelling framework. *Marine Ecology Progress Series 398*: 19–32. doi:10.3354/meps08345.

Storm, Z. (2025). Home is where your heat is: local conditions forge a fish's temperature tolerance. *Conservation Physiology 13(1)*. doi:10.1093/conphys/coaf021.

Stortini, C.H.C.H.; Shackell, N.L.N.L.; Tyedmers, P.; Beazley, K. (2015). Assessing marine species vulnerability to projected warming on the Scotian Shelf, Canada. *ICES Journal of Marine Science 72(6)*: 1731–1743. doi:10.1093/icesjms/fsv022.

Stuart-Smith, R.D.; Edgar, G.J.; Barrett, N.S.; Kininmonth, S.J.; Bates, A.E. (2015). Thermal biases and vulnerability to warming in the world's marine fauna. *Nature 528(7580)*: 88+. doi:10.1038/nature16144.

Sumaila, U.R.; Tai, T.C. (2020). End Overfishing and Increase the Resilience of the Ocean to Climate Change. *Frontiers in Marine Science 7*. doi:10.3389/fmars.2020.00523.

Sunday, J.M.; Bates, A.E.; Dulvy, N.K. (2011). Global analysis of thermal tolerance and latitude in ectotherms. *Proceedings of the Royal Society B Biological Science 278(1713)*: 1823–1830. doi:10.1098/rspb.2010.1295.

Sunday, J.M.; Bates, A.E.; Dulvy, N.K. (2012). Thermal tolerance and the global redistribution of animals. *Nature Climate Change 2(9)*: 686–690. doi:10.1038/nclimate1539.

Sunday, J.M.; Bates, A.E.; Kearney, M.R.; Colwell, R.K.; Dulvy, N.K.; Longino, J.T.; Huey, R.B. (2014). Thermal-safety margins and the necessity of thermoregulatory behavior across latitude and elevation. *Proceedings of the National Acadamy of Science U.S.A. 111(15)*: 5610–5615. doi:10.1073/pnas.1316145111.

Swart, R.; Bernstein, L.; Ha-Duong, M.; Petersen, A. (2009). Agreeing to disagree: uncertainty management in assessing climate change, impacts and responses by the IPCC. *Climate Change 92(1–2)*: 1–29. doi:10.1007/s10584-008-9444-7.

Swift, T.L.; Hannon, S.J. (2010). Critical thresholds associated with habitat loss: a review of the concepts, evidence, and applications. *Biological Reviews 85(1)*: 35–53. doi:10.1111/j.1469-185X.2009.00093.x.

Thurman, L.L.; Stein, B.A.; Beever, E.A.; Foden, W.; Geange, S.R.; Green, N.; Gross, J.E.; Lawrence, D.J.; LeDee, O.; Olden, J.D.; Thompson, L.M.; Young, B.E. (2020). Persist in place or shift in space? Evaluating the adaptive capacity of species to climate change. *Frontiers in Ecology and the Environment 18(9)*: 520–528. doi:10.1002/fee.2253.

Tittensor, D.P.; Beger, M.; Boerder, K.; Boyce, D.G.; Cavanagh, R.D.; Cosandey-Godin, A.; Crespo, G.O.; Dunn, D.C.; Ghiffary, W.; Grant, S.M.; Hannah, L.; Halpin, P.N.; Harfoot, M.; Heaslip, S.G.; Jeffery, N.W.; Kingston, N.; Lotze, H.K.; McGowan, J.; McLeod, E.; McOwen, C.J.; O'Leary, B.C.; Schiller, L.; Stanley, R.R.E.; Westhead, M.; Wilson, K.L.; Worm, B. (2019). Integrating climate adaptation and biodiversity conservation in the global ocean. *Science Advances 5(11)*: 1–16. doi:10.1126/sciadv.aay9969.

Trisos, C.H.; Merow, C.; Pigot, A.L. (2020). The projected timing of abrupt ecological disruption from climate change. *Nature 580(7804)*: 496–501. doi:10.1038/s41586-020-2189-9.

Turk, D.; Wang, H.; Hu, X.; Gledhill, D.K.; Wang, Z.A.; Jiang, L.; Cai, W.-J. (2019). Time of Emergence of Surface Ocean Carbon Dioxide Trends in the North American Coastal Margins in Support of Ocean Acidification Observing System Design. *Frontiers in Marine Science 6*. doi:10.3389/fmars.2019.00091.

van der Hoek, Y.; Zuckerberg, B.; Manne, L.L. (2015). Application of habitat thresholds in conservation: Considerations, limitations, and future directions. *Global Ecology and Conservation 3*: 736–743. doi:10.1016/j.gecco.2015.03.010.

Vinagre, C.; Dias, M.; Cereja, R.; Abreu-Afonso, F.; Flores, A.A.V.; Mendonça, V. (2019). Upper thermal limits and warming safety margins of coastal marine species – Indicator baseline for future reference. *Ecological Indicators 102*: 644–649. doi:10.1016/j.ecolind.2019.03.030.

Voldoire, A.; Saint-Martin, D.; Sénési, S.; Decharme, B.; Alias, A.; Chevallier, M.; Colin, J.; Guérémy, J. -F.; Michou, M.; Moine, M. -P.; Nabat, P.; Roehrig, R.; Salas y Mélia, D.; Séférian, R.; Valcke, S.; Beau, I.; Belamari, S.; Berthet, S.; Cassou, C.; Cattiaux, J.; Deshayes, J.; Douville, H.; Ethé, C.; Franchistéguy, L.; Geoffroy, O.; Lévy, C.; Madec, G.; Meurdesoif, Y.; Msadek, R.; Ribes, A.; Sanchez-Gomez, E.; Terray, L.; Waldman, R. (2019). Evaluation of CMIP6 DECK Experiments With CNRM-CM6-1. *Journal of Advances in Modelling Earth Systems 11(7)*: 2177–2213. doi:10.1029/2019MS001683.

Walters, A.W.; Mandeville, C.P.; Rahel, F.J. (2018). The interaction of exposure and warming tolerance determines fish species vulnerability to warming stream temperatures. *Biology Letters 14(9)*: 20180342. doi:10.1098/rsbl.2018.0342.

Walters, D.; Baran, A.J.; Boutle, I.; Brooks, M.; Earnshaw, P.; Edwards, J.; Furtado, K.; Hill, P.; Lock, A.; Manners, J.; Morcrette, C.; Mulcahy, J.; Sanchez, C.; Smith, C.; Stratton, R.; Tennant, W.; Tomassini, L.; Van Weverberg, K.; Vosper, S.; Willett, M.; Browse, J.; Bushell, A.; Carslaw, K.; Dalvi, M.; Essery, R.; Gedney, N.; Hardiman, S.; Johnson, B.; Johnson, C.; Jones, A.; Jones, C.; Mann, G.; Milton, S.; Rumbold, H.; Sellar, A.; Ujiie, M.; Whitall, M.; Williams, K.; Zerroukat, M. (2019). The Met Office Unified Model Global Atmosphere 7.0/7.1 and JULES Global Land 7.0 configurations. *Geoscience Model Development 12(5)*: 1909 – 1963. doi:10.5194/gmd-12-1909-2019.

Warren, M.S.; Hill, J.K.; Thomas, J.A.; Asher, J.; Fox, R.; Huntley, B.; Toy, D.B.; Telfer, M.G.; Jeffcoate, S.; Harding, P.; Jeffcoate, G.; Willis, S.G.; Greatorex-Daview, J.N.; Moss, D.; Thomas, C.D. (2001). Rapid responses of British butterflies to opposing forces of climate and habitat change. *Nature 414*: 65–69.

Williams, J.; Morgenstern, O.; Varma, V.; Behrens, E.; Hayek, W.; Oliver, H.; Dean, S.; Mullan, B.; Frame, D. (2016). Development of the New Zealand Earth System Model: NZESM. *Weather and Climate 36*: 25–44. Available from https://www.scopus.com/inward/record.uri?eid=2-s2.0-85068874990&partnerID=40&md5=fb822b910a3b4e8087fc69ffb659ca0b.

Worm, B.; Barbier, E.B.; Beaumont, N.; Duffy, J.E.; Folke, C.; Halpern, B.S.; Jackson, J.B.C.; Lotze, H.K.; Micheli, F.; Palumbi, S.R.; Sala, E.; Selkoe, K.A.; Stachowicz, J.J.; Watson, R. (2006). Impacts of biodiversity loss on ocean ecosystem services. *Science (80-.). 314(5800)*: 787–90. doi:10.1126/science.1132294.

Worm, B.; Duffy, J.E. (2003). Biodiversity, productivity, and stability in real food webs. *Trends in Ecology and Evolution 18(12)*: 628–632.

Worm, B.; Lotze, H.K.; Hillebrand, H.; Sommer, U. (2002). Consumer versus resource control of species diversity and ecosystem functioning. *Nature 417*: 848–851.

Xu, C.; Kohler, T.A.; Lenton, T.M.; Svenning, J.-C.; Scheffer, M. (2020). Future of the human climate niche. *Proceedings of the National Acadamy of Science 117(21)*: 11350–11355. doi:10.1073/pnas.1910114117.

Xu, Y.; Shen, Z.-H.; Ying, L.-X.; Ciais, P.; Liu, H.-Y.; Piao, S.; Wen, C.; Jiang, Y.-X. (2016). The exposure, sensitivity and vulnerability of natural vegetation in China to climate thermal variability (1901–2013): An indicator-based approach. *Ecological Indicators 63*: 258–272. doi:10.1016/j.ecolind.2015.12.023.

Yin, D.; Leroux, S.J.; He, F. (2017). Methods and models for identifying thresholds of habitat loss. *Ecography 40(1)*: 131–143. doi:10.1111/ecog.02557.

Yool, A.; Popova, E.E.; Anderson, T.R. (2013). MEDUSA-2.0: An intermediate complexity biogeochemical model of the marine carbon cycle for climate change and ocean acidification studies. *Geoscience Model Development **6**(5)*: 1767 – 1811. doi:10.5194/gmd-6-1767-2013.

Zommers, Z.; Marbaix, P.; Fischlin, A.; Ibrahim, Z.Z.; Grant, S.; Magnan, A.K.; Pörtner, H.-O.; Howden, M.; Calvin, K.; Warner, K.; Thiery, W.; Sebesvari, Z.; Davin, E.L.; Evans, J.P.; Rosenzweig, C.; O'Neill, B.C.; Patwardhan, A.; Warren, R.; van Aalst, M.K.; Hulbert, M. (2020). Burning embers: towards more transparent and robust climate-change risk assessments. *Nature Reviews Earth and Environment, 1(10)*, 516–529. https://doi.org/10.1038/s43017-020-0088-0

Appendix A: Vulnerability across life stages

The overarching purpose and benefit of CVAs is to provide vulnerability rankings across a large number of species or stocks to synoptically identify those most at risk. Thus, any framework for assessing the vulnerability of early life stages must also be capable of providing climate-impact information for many species or stocks. Presently, Fisheries New Zealand manages ~98 species and ~642 stocks. The CRIB-NZ framework can assess vulnerability for most of these species at the adult life stage, and, to be equally effective, any CVA for early life stages would require input data or information from a similar proportion of species and stocks. Two avenues for achieving this were explored:

1. **CRIB analysis:** The most straightforward way to assess the vulnerability of species' early life stages would be to conduct an independent CRIB-NZ analysis specific to larvae and/or juveniles. This would require several life-stage-specific input data layers, including estimates of distribution, thermal niches, conservation status, vertical habitat use, and size, along with corresponding climate time series. Global species distribution modelling initiatives such as AquaMaps (Kaschner et al. 2019) and AquaX (Reygondeau et al. 2026) provide estimates of the present-day distributions of more than 30 000 marine species, but do not produce such estimates for larvae or juveniles due to data limitations. NABIS contains estimates of the annual geographic distribution for 47 species at the juvenile stage and 39 species at the spawning (larval) life stage in New Zealand waters (NABIS Layer Index). These distributions are produced by first constructing distributional maps of where juveniles are captured in research bottom trawl records available between October 1, 1961 and August 25, 2005. Subsequently, expert scientists integrate this information with literature data (e.g. New Zealand fishing news, unpublished electronic bibliographies, scientific papers and abstracts) and their expert judgment to produce hand-drawn distributional maps, which are then digitised. Thus, the distributions are subject to shifts in the distribution of fishing effort and in research trawl survey data, as well as to the expert assessor's judgment. However, these distributional estimates are only available for less than half of the ~98 harvested species in New Zealand and are thus not yet a viable option.

   In the CRIB analysis for adults, species thermal niches are publicly available from AquaMaps and have been validated against independent estimates from studies and experiments. However, to date, publicly available databases of thermal niche for a large number of species at the larval or juvenile stages do not exist. Although more labour-intensive, we also explored the feasibility of deriving thermal tolerances from scientific studies. We searched the published literature in SCOPUS and Google Scholar for studies on thermal tolerance and preferences for the species of interest at early life stages, but could not locate any information. However, even if this route were fruitful, extracting thermal niche information from published studies for 98 species would be time-consuming and likely beyond the scope of the work.

   In addition to the lack of crucial distributional and thermal niche information for juveniles, other requisite information for their conservation status, body size, and vertical habitat preferences was also lacking. In light of this, applying a separate CRIB analysis to early life stages is impossible until this information becomes more widely available.

Expert assessment: As an alternative, we also explored an expert-assessment approach to evaluate species vulnerability during early life stages. Expert assessment approaches benefit from not relying on the availability of input data; however, they still require studies, reports, and analyses to support the expert assessments, as well as a clear, structured approach to assessment. We searched the published literature in SCOPUS and Google Scholar for studies using the keywords “climate”, “temperature”, and “New Zealand”, combined with the name of our species of interest. Even omitting the key search terms “larvae”, “juvenile”, or “spawning”, our search returned few results, indicating a limited understanding of climate impacts on marine species in New Zealand, particularly those at early life stages. Lacking such baseline information and given the time required for experts to

complete assessments for 97 species, an expert-assessment CVA was outside the scope of this work but could be explored in the future, especially if additional information became available.

Appendix B: Extended data

B.1 Species geographic distributions

Occurrence data undergo extensive preprocessing, including coordinate cleaning, removal of impossible locations, duplicate resolution, and the application of quality flags that reconcile the reliability indicators of AquaMaps, OBIS, and GBIF. Ecological and life-history traits—for example, depth range, habitat preferences, pelagic versus benthic affinity, and vertical occupancy—are compiled from FishBase and SeaLifeBase and used to populate the D3-Ocean System, which characterises species' three-dimensional habitat affinities. These traits, combined with biogeographical information from the Pelagic Provinces of the World (PPOW), Benthic Provinces of the World (BPOW), and the Circumpolar Biodiversity Monitoring Program (CBMP) Arctic units, are used to generate spatially realistic species-specific range maps.

When International Union for Conservation of Nature (IUCN) expert range maps (ERMs) exist, they are buffered, clipped to ocean basins, and intersected with land masks to define biogeographical (BR) and potential (PR) ranges, which in turn serve as constraints for SDM training. For species lacking ERMs, AquaX derives bounding boxes from cleaned occurrence data, removes remaining spatially implausible records, and further refines them using ecological traits, thinning procedures, and biogeographical filtering. Spatial and environmental thinning procedures ensure that the training set captures the full breadth of ecological conditions while minimizing bias from uneven sampling effort.

To construct the modelling dataset, verified occurrences within the BR are matched to corresponding Bio-ORACLE v3.0 environmental variables at 0.05° resolution, selecting appropriate depth layers based on whether a species is pelagic or benthic. For species with limited observations within ERMs, pseudo-occurrences are generated across environmentally plausible portions of the range to reduce niche truncation and improve model calibration. Pseudo-absences are produced differently for pelagic and benthic species, using a Surface Range Envelope approach for pelagic taxa and a distance-based habitat-informed method for benthic taxa, with all absences restricted to each species' PR.

Species distribution model predictions employ an ensemble of 10 algorithms—Generalised Linear Model (GLM), Generalised Additive Model (GAM), Random Forests (RF), Artificial Neural Networks (ANN), Flexible Discriminant Analysis (FDA), Classification Tree Analysis (CTA), Gradient Boosting Machine (GBM), Maximum Entropy (MaxNet), Extreme Gradient Boosting (XGBoost), and Multivariate Adaptive Regression Splines (MARS); each method is optimised separately for each species. Cross-validation is conducted in environmental space rather than geographic space, generating up to 300 individual model runs per species and ensuring that evaluation reflects ecological gradients rather than spatial sampling patterns. Model performance is assessed using threshold-dependent (TSS, CSI) and threshold-independent area under the curve (AUC) metrics, with only models achieving TSS > 0.6 retained for ensemble formation. Ensemble outputs include mean suitability, committee averaging, and the coefficient of variation, enabling quantification of spatial uncertainty and model agreement. Environmental extrapolation is mapped to identify locations where projected conditions fall outside the training domain, further enhancing interpretability.

Of critical value to the CRIB, the AquaX process can empirically determine species presence/absence using species-specific thresholds calculated within the modelling framework. These thresholds are derived during model calibration and evaluation using model performance criteria implemented in the ensemble species distribution models, allowing the suitability cutoff to vary among species based on model performance and species-specific environmental relationships. Consequently, species presence was inferred only in grid cells where predicted habitat suitability exceeded the species-specific optimised threshold.

All outputs are rendered at 0.05° resolution, representing a ten-fold improvement over the resolution of traditional AquaMaps products and enabling ecologically meaningful mapping in coastal and topographically complex regions. Multiple validation layers—occurrence quality filtering, range-based exclusion of implausible points, environmental thinning, cross-validation, and ensemble-level uncertainty estimates—ensure high-confidence predictions for each species. These quality-control steps collectively reduce common SDM biases such as sampling heterogeneity, basin-mirror artifacts, and environmentally suitable but ecologically impossible projections. Compared with earlier AquaMaps approaches, AquaX incorporates a richer taxonomic backbone, integrates expert-verified ERMs, and uses a much broader set of ecologically relevant environmental predictors. It also incorporates biogeographical boundaries to ecologically constrain projections, eliminating spurious predictions across realms, basins, and depth strata. The ensemble machine-learning design captures more complex nonlinear species–environment relationships than the previously used trapezoidal environmental envelopes. This results in substantially improved predictive accuracy, as demonstrated through case studies comparing AquaX outputs with expert maps, high-resolution coral richness datasets, and AquaMaps products. The AquaX framework is transparent, reproducible, and based on open-source data, thereby advancing global marine biodiversity research.

Appendix C: Extended methods

C.1 Climate Sensitivity

C.1.1 Thermal safety margins

The standardization function allowed climate sensitivity to increase exponentially as the TSM declined as

$$S\,TSM_{s,c} = e^{-\lambda TSM_{s,c}}, \quad \text{Equation 1}$$

where $TSM_{s,c}$ is the thermal safety margin (°C) for species *s* in grid cell *c,* and λ is the rate parameter (0.33).

C.1.2 Vertical habitat use

The indices were calculated according to the specifications outlined by Boyce et al. (Boyce et al. 2022, 2024; Boyce et al. 2024b), whereby climate sensitivity to ocean warming declined exponentially, with both the maximum distance of the species occupancy to surface or bottom warming, respectively, and the vertical range of each species as

$$S\,VR_s = e^{-\lambda VR_s} \quad \text{Equation 2}$$

$$S\,Mdep_s = e^{-\lambda Mdep_s} \quad \text{Equation 3}$$

where VR_s is the total realised vertical range for species *s* in meters and $Mdep_s$ is the realised proximity of species *s* to the sea surface (for surface-associated species) or to the sea bottom (for bottom-associated species) in meters. λ is the rate parameter (0.05). Estimates of the minimum and maximum depths of occupancy, associated vertical habitat range, and vertical habitat categorization were retrieved from AquaMaps (Kaschner et al. 2019) and FishBase (Froese & Pauly, 2014).

For vertically mobile surface-associated species (e.g. tuna, herring, etc.), $Mdep_s$ was set to the lesser of the minimum occupancy depth or 100 m. For vertically immobile, bottom-associated species $Mdep_s$ was set to 0 for sessile species (e.g. tunicates, etc.), or 0.5 m for non-sessile species (e.g. crabs, lobsters, etc.). For vertically mobile bottom-associated species (e.g. cod, halibut, etc.), $Mdep_s$ was set according to the vertical habitat classification of each species as follows:

1. Benthic: 2 m
2. Reef-associated: 5 m
3. Demersal: 2 m
4. Bathydemersal: 5 m
5. Benthopelagic: 10 m
6. Bathypelagic: 100 m

For vertically mobile species, VR_s is calculated as the difference between the deepest and shallowest occupancy depth of the species. For vertically immobile bottom-associated species VR_s was set to 0 for sessile species or 1 for non-sessile species.

VR_s and $Mdep_s$ were truncated by the maximum bathymetry in each grid cell within each species' native geographic distribution to obtain realised rather than theoretical estimates. Bathymetry values were extracted from the Copernicus Marine Data Store at the same resolution as the analysis. Cumulative climate sensitivity was then calculated as the mean of the species' standardised vertical range (Equation 2) and the maximum depth of occupancy (Equation 3) indices. Refer to Boyce et al. (Boyce et al. 2022) for an evaluation of how the vulnerability calculations are affected by the specification of λ.

The rate parameter, λ, corresponds to the rate of decline in climate sensitivity over depth range and proximity to the sea surface or bottom and was empirically derived as the exponential rate of change in the difference between surface and subsurface temperatures across depths between 0 and 1000 m globally.

C.1.3 Cumulative impacts

Climate sensitivity as a function of HII was standardised, as

$$S\,HII_c = 1 - e^{-\lambda HII_c}, \qquad \text{Equation 4}$$

where HII_c is the HII in cell *c,* and λ is the rate parameter, set to 0.6. The equation standardises the index (0–1), normalises its distribution and ensures that $S\,HII_c$ falls between 0 and 1 and is nearly uniform for values above 5 (Figure 18). Refer to Boyce et al. (2022) for an evaluation of how the vulnerability calculations are affected by the specification of λ.

C.2 Climate Exposure

C.2.1 Time of climate emergence

The ToEs were standardised according to

$$E\,ToE_{s,c} = e^{-\lambda ToE_{s,c}}, \qquad \text{Equation 5}$$

where $ToE_{s,c}$ is the ensemble projected year of climate emergence from the thermal niche for species *s* in grid cell *c,* and λ is the rate parameter (0.033). The equation was chosen to ensure that $E\,ToE_{s,c}$ ranges between 0 and 1, and increases more rapidly as it approaches 0 and declines more slowly as it increases (Figure 20). Maximal exposure occurs for species inhabiting waters that are already thermally hazardous (e.g. ToE=0). Refer to Boyce et al. (2022) for an evaluation of how the vulnerability calculations are affected by the specification of λ.

C.2.2 Ecosystem disruption

Ecosystem disruption was standardised according to

$$E\,ToEE_c = 1 - e^{-\lambda ToEE_c}, \quad \text{Equation 6}$$

where $ToEE_c$ is the proportion of all species in grid cell *c* that emerge from their thermal niche by 2100, and λ is the rate parameter, set at 4. The equation was chosen to standardise the index (0–1), normalise its distribution, and ensure that a species' exposure increases asymptotically with the fraction of species lost in its ecosystem, with the greatest exposure occurring for species inhabiting ecosystems with the greatest loss of species. Refer to Boyce et al. (2022) for an evaluation of how the vulnerability calculations are affected by the specification of λ. $ToEE_c$ was estimated individually for each ESM using the approach described in Trisos et al. (2020) and then averaged across all ensemble models.

C.2.3 Loss of suitable thermal habitat

Thermal habitat loss was standardised according to

$$E\,THL_s = 1 - e^{-\lambda THL_s}, \quad \text{Equation 7}$$

where THL_s is the proportion of all grid cells across the native geographic distribution of species s that are projected to become thermally hazardous by 2100, and λ is the rate parameter, set at 5. The equation standardises the index (0–1) and specifies that a species' exposure increases asymptotically with the fraction of thermal habitat loss, with the most significant exposure occurring for species that lose all of their present-day suitable thermal habitat. The maximum exposure occurs for species projected to lose all suitable habitats. Refer to Boyce et al. (2022) for an evaluation of how the vulnerability calculations are affected by the specification of λ. THL_s was estimated individually for each ESM and then averaged across all ensemble models.

C.2.4 Marine heatwaves

Methods for calculating MHW properties—frequency, duration, and intensity—vary, yet the use of daily temperature observations is exceedingly common (Hobday et al. 2016). For instance, operational systems, such as the NOAA National Centers for Environmental Information, use daily SST products at high spatial resolutions to evaluate MHWs globally[6]. Yet, the requirement for daily observations creates computational challenges when calculating MHW indices over long projection horizons (e.g. to 2100) and/or at high spatial resolutions (e.g. 0.08 degrees), as considered here. However, Oliver et al. (2018) tested eight candidate monthly proxies against daily-based MHW metrics derived from high-resolution satellite and *in situ* temperature series. They found that the number of months with anomalously warm temperatures (NT) closely predicted the annual *frequency* of daily MHWs, whereas the maximum annual difference between the monthly mean temperature and the average monthly temperature (TAX) was the best predictor of MHW *duration*; both indices (NT and TAX) exhibited strong, statistically significant correlations across multiple long-term global stations. These findings suggest that monthly proxies can approximate key MHW characteristics when daily data are unavailable and that while daily data remain ideal for detecting short, transient events, monthly proxies can capture longer, large-scale variability in marine heatwaves and trends.

Accordingly, a climate exposure index ($EMHW_{s,c}$) as a function of the duration and magnitude of species exposure to hazardous temperature was calculated using projected monthly sea surface and bottom temperatures as

[6] Marine Heatwaves | National Marine Ecosystem Status

$$EMHW_{s,c} = \frac{Duration_{s,c} + Magnitude_{s,c}}{2}$$ Equation 8

In this formulation, $Duration_{s,c}$ is a standardised measure of the proportion of time a species is exposed to hazardous temperatures in each cell, calculated as

$$Duration_{s,c} = \frac{1}{N_m}\sum_{t=1}^{N} I\left(T_{s,c,m} > Tmax_s\right)$$ Equation 9

where $T_{s,c,m}$ is the monthly temperature experienced by species *s* in grid cell *c* at month *m*, $Tmax_s$ is the maximum temperature tolerance for species *s*, N_m is the number of non-missing months in the temperature series for cell *c*, and *I* is the indicator function.

$Magnitude_{s,c}$ is a standardised analogue to Oliver et al.'s TAX, calculated as

$$Magnitude_{s,c} = \frac{1}{R_s}\frac{\sum_{t=1}^{N}(T_{s,c,m} - Tmax_s}{\sum_{t=1}^{N} I\left(T_{s,c,m} > Tmax_s\right)}$$ Equation 10

Where $T_{s,c,y}$ is the monthly mean temperature experienced by species *s* in cell *c* and month *m*, $Tmax_s$, and $Trange_s$ are the maximum thermal tolerance and range for species *s*, and R_s is the species-specific thermal niche range.

C.3 Adaptive capacity

C.3.1 Geographic range extent

Adaptivity to climate change increased exponentially with the geographic range area of each species as

$$AC\ Rarea_s = 1 - e^{-\lambda Rarea_s},$$ Equation 11

where $Rarea_s$ is the geographic range area (km^2) of species *s,* and λ is the rate parameter, set at 20. The equation standardises the index (0–1), normalises its distribution and specifies that adaptivity increases asymptotically with geographic range area, with the greatest adaptivity occurring for species with the largest geographic range areas. Adaptivity was virtually uniformly high among species inhabiting >20% of the global ocean area. Refer to Boyce et al. (2022) for an evaluation of how the vulnerability calculations are affected by the specification of λ.

The latitude range of species was calculated as the difference between the highest and lowest latitude occupied by a species across its native geographic distribution. The ranges were standardised on a 0–1 scale by the maximum possible latitude range (90 degrees) as

$$AC\ Lrange_s = \frac{Lrange_s}{90},$$ Equation 12

A standardised index of adaptivity as a function of the geographic range extent ($AC\ Grange_s$) was then calculated for each species as the mean of the standardised geographic range area ($AC\ Rarea_s$) and latitude spanned ($AC\ Lrange_s$).

C.3.2 Habitat fragmentation

The extent of geographic habitat fragmentation for each species across the spatial domain here (*i.e.* the New Zealand EEZ) was calculated from their native geographic distribution. Habitat fragmentation was calculated using the largest patch index (LPI) as

$$LPI_s = 1 - \frac{LPA_s}{TOA_s}, \quad \text{Equation 13}$$

where LPA_s is the area of the largest patch in the geographic distribution of species *s*, and TOA_s is the total occupied geographic distribution of species *s*. Patches were identified as distinct clusters of occupied grid cells, where patches must be connected in eight directions (queen's case=8 cells surrounding). LPI values of 0 represent contiguous habitat (e.g. one patch) and those near 1 represent highly fragmented habitat. Using the LPI, a standardised habitat fragmentation index was then calculated as

$$AC\ Hfrag_s = e^{-\lambda LPI_s}, \quad \text{Equation 14}$$

where $Hfrag_s$ is the geographic habitat fragmentation of species *s,* and λ is the rate parameter, set to 8. The equation standardises the index (0–1), normalises its distribution and specifies that adaptivity due to habitat fragmentation declines asymptotically with geographic range fragmentation, with the lowest adaptivity occurring for species with highly fragmented habitats. Adaptivity was uniformly low across species in which a single large patch comprised <50% of their present-day distribution. Refer to Boyce et al. (2022) for an evaluation of how the vulnerability calculations are affected by the specification of λ.

C.3.3 Thermal habitat variability and use

Historical thermal habitats were characterised using monthly sea temperature data from GLORYS (1993–2025). For each grid cell, a count ($count_i$) of the frequency of SST values in each 0.2°C bin was obtained; each temperature distribution (Tdist) characterises the range and frequency of historical temperatures at each location across the species geographic range. For each species *s* in each grid cell *c*, the environmental temperature distribution was restricted to bins within the species' thermal niche. Let $count_{i,c,s}$ denote the number of observations in bin *i* within the species niche, and $Tcount_{c,s}$ the total number of observations within the niche. The relative frequency of temperatures within the niche is then:

$$p_{i,s,c} = \frac{count_{i,s,c}}{Tcount_{s,c}} \quad \text{Equation 15}$$

The distribution of temperatures within the niche was quantified using Shannon entropy:

$$H_{s,c} = \sum_{i=1}^{N_s} p_{i,c,s} \ln(p_{i,s,c}) \quad \text{Equation 16}$$

Entropy was exponentiated to obtain an interpretable measure of effective niche breadth; this transformation yields the effective number of temperature bins occupied, equivalent to the number of equally frequent bins that would produce the observed distribution (Hill, 1973; Jost, 2006). To standardise this metric across species with different niche widths, the effective number of occupied bins was divided by the total number of bins in the species' niche:

$$TNC_{s,c} = \frac{\exp(H_{s,c})}{N_s}$$ Equation 17

Equation 17 produces a dimensionless index bounded between 0–1 that captures both the breadth of temperatures experienced within a species' niche and the evenness of exposure across that range. When $TNC_{s,c}$ is close to 1, temperatures are broadly and evenly distributed across the species' niche, indicating high thermal niche coverage and strong potential for thermal pre-adaptation. Low $TNC_{s,c}$ means that temperatures are concentrated in a narrow portion of the niche, indicating limited exposure to the full range of thermal conditions (reduced evidence for pre-adaptation). A standardised adaptivity index was then calculated as

$$AC\ TNC_{s,c} = 1 - e^{-3TNC_{s,c}},$$ Equation 18

The equation specifies that adaptivity due to thermal habitat pre-adaptation increases with the proportion of the thermal niche covered by the environment and the evenness of that coverage. Species that inhabit thermal habitats that occupy a greater proportion of their thermal niche are, theoretically, more pre-adapted to climate change than those that inhabit less.

The variability of a species' thermal environment is another crucial characteristic of pre-adaptation. Species inhabiting more thermally variable environments are believed to be more adaptable to thermal environmental changes. Accordingly, the temperature variability experienced by each species at each location across its geographic range was calculated as

$$AC\ Trange_c = Tmax_c - Tmin_c,$$ Equation 19

Where $Tmax_c$ and $Tmax_c$ are the maximum and minimum monthly temperatures in grid cell c over the previous 32 years (1993–2025).

C.3.4 Maximum body length

A standardised index of adaptivity as a function of the maximum possible body length of each species was calculated as

$$AC\ Mlen_s = 1 - MlenSTD_s,$$ Equation 20

where $MlenSTD_s$ is calculated as

$$MlenSTD_s = \frac{log10(Mlen_s+1)}{log10(3000+1)},$$ Equation 21

$Mlen_s$ is the maximum estimated length of species *s* (cm), and 3000 is a scaling factor corresponding to the approximate maximum length that the largest oceanic species (*i.e.* blue whale) could conceivably reach.

C.4 Discount rates

Discount rates are calculated as

$$\partial = \frac{Years}{100\theta} + \frac{Models}{-20\theta} + \vartheta,$$ Equation 22

where $Years$ is the number of years in the climate projection, $Models$ is the number of climate projections in the ensemble, θ is a scaling factor set to 40, and ϑ is 0.026 to yield a maximum discount rate of 5% when projections are made for ≥100 years from a single projection, and are 0% when projections are made for <5 years from >19 projections. The case study presented here evaluated climate projections from 3 models over 80 years, yielding a discount rate of 4.1%. To conserve the vulnerability scaling to between zero and one, discounts applied to exposure are credited to sensitivity (e.g. the current state), such that the maximum total adjustment is 10%.

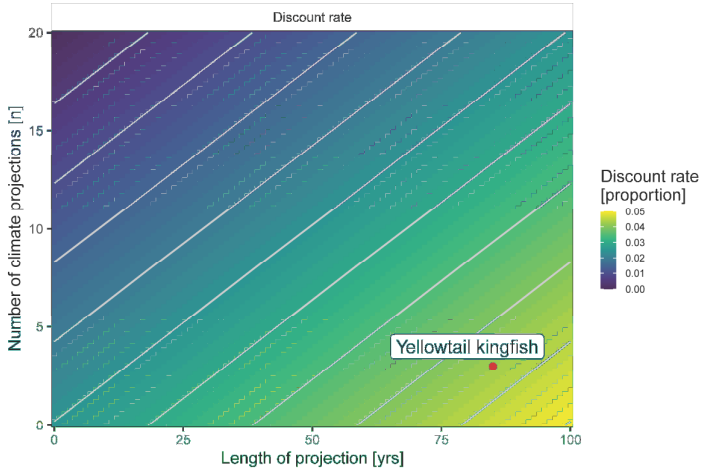


Figure C1: Discount rates. The discount rate on future exposure, credited to the present state, is a function of the length of the climate projection(s) and the size of the climate ensemble.

For each species within each grid cell across its native geographic distribution, the discount rate was applied to the estimated exposure and sensitivity as

$$\breve{E}_{s,c} = [(1 - \partial)(E_{s,c})]\,, \qquad \text{Equation 23}$$

$$\breve{S}_{s,c} = [(1 + \partial)(S_{s.c})]\,, \qquad \text{Equation 24}$$

Where $\breve{S}_{s,c}$ and $\breve{E}_{s,c}$ are the discounted sensitivity and exposure estimates for species s within cell c. Through this equation, the future exposure of species to climate change was discounted relative to their current sensitivity. The discounting was applied to sensitivity, rather than adaptivity, as there is a broad consensus that it is better understood (e.g. Thurman et al. 2020).

C.5 Spatially explicit vulnerability

Unweighted vulnerability is calculated as the average of adaptivity, discounted sensitivity, and discounted exposure, providing a simple, straightforward interpretation of vulnerability.

Alternatively, weighted climate vulnerability was calculated from adaptivity, discounted sensitivity and exposure as

$$V_{s,c} = \frac{\left[\check{S}_{s,c} \times \omega S_{s,c}\right] + \left[\check{E}_{s,c} \times \omega E_{s,c}\right] + \left[\left(1 - AC_{s,c}\right) \times \omega AC_{s,c}\right]}{\omega S_{s,c} + \omega E_{s,c} + \omega AC_{s,c}} \quad \text{Equation 25}$$

where $V_{s,c}$ is the vulnerability, $\check{S}_{s,c}$ and $\check{E}_{s,c}$ are the discounted sensitivity and exposure, respectively, and $AC_{s,c}$ is adaptivity for species s within cell c. $\omega S_{s,c}$, $\omega E_{s,c}$, and $\omega AC_{s,c}$ are the statistical reliability weights for the estimated sensitivity, exposure, and adaptivity, calculated from their scaled variances. For example, the weights for estimated sensitivities were calculated as the inverse of their coefficients of variation as

$$\omega S_{s,c} = \left(\frac{\sigma S_{s,c}}{\mu S_{s,c}}\right)^{-1} \quad \text{Equation 26}$$

where

$$\mu S_{s,c} = \frac{1}{n}\sum_{i=1}^{n} S_{s,c,i} \quad \text{Equation 27}$$

and

$$\sigma S_{s,c} = \sqrt{\frac{\sum_{i=1}^{n}\left(S_{s,c,i} - \mu S_{s,c}\right)^2}{NS_{s,c}}} \quad \text{Equation 28}$$

where $\omega S_{s,c}$ is the reliability weight and $\sigma S_{s,c}$ and $\mu S_{s,c}$ are the standard deviation and mean, respectively, of the four indices, i, that define sensitivity for species s within cell c. $NS_{s,c}$ is the number of climate indices, i, that define sensitivity for species s within cell c.

C.6 Spatially implicit vulnerability

Alternatively, weighted vulnerability for each species was calculated as a variance-weighted mean of the vulnerabilities in each grid cell across its geographic distribution as

$$V_s = \frac{\sum_{c=1}^{n} \omega V_{s,c}\, V_{s,c}}{\sum_{c=1}^{n} \omega V_{s,c}} \quad \text{Equation 29}$$

while their variance-weighted standard deviations were calculated as

$$\sigma V_s = \sqrt{\frac{v_1}{{v_1}^2 - v_2}\sum_{c=1}^{N} \omega V_{s,c}(V_{s,c} - \mu V_{s,c})^2} \quad \text{Equation 30}$$

where,

$$V_1 = \sum_{c=1}^{N} \omega V_{s,c} \quad \text{Equation 31}$$

and

$$V_2 = \sum_{c=1}^{N} \omega V_{s,c}{}^2 \qquad \text{Equation 32}$$

and

$$\omega V_{s,c} = \left(\frac{\sigma D_{s,c}}{\mu D_{s,c}}\right)^{-1}, \qquad \text{Equation 33}$$

In this manner, greater statistical weight is given to vulnerability estimates in grid cells where their variance (e.g. across the indices used to calculate them) is lower, and vice versa. Species vulnerability estimates will be more variable when vulnerability differs more across the grid cells that comprise its geographic distribution, and vice versa.

Appendix D: Practical applications of vulnerability from Canada

The CRIB and CRIB-NZ operate hierarchically, providing climate vulnerability information that can be tailored to a spectrum of users, from those who seek high-level summary information (e.g. rankings and scores of overall vulnerability or risk) as well as those wanting more detailed technical information about how and why species are at high or low risk (e.g. spatially resolved climate vulnerability and risk indices). In this section, case studies illustrate how different output types from the CRIB can inform pathways to climate resilience in marine fisheries and spatial planning.

D.1 Marine fisheries

(Boyce et al. 2024) used the CRIB to estimate climate vulnerability and risk for 90 fish stocks across Atlantic Canada under contrasting emission scenarios to 2100. In this study, the 4T southern Gulf of St. Lawrence (sGSL) smooth skate stock, a bycatch fishery, had the highest climate vulnerability. This fishery is at high risk because it is critically exposed to projected climate change, is highly sensitive to it, and has moderate adaptability. Smooth skate is globally endangered (IUCN, 2021), and the Committee on the Status of Endangered Wildlife in Canada (COSEWIC) has assessed populations in the Laurentian-Scotian region, including the 4T stock, as a species of special concern (COSEWIC, 2012).

When determining which Atlantic Canadian stocks most require climate adaptation, 4T smooth skate would be a high priority. Resources that could further climate adaptation could potentially include pragmatic approaches that integrate climate change considerations into stock assessments, harvest advice, and decision-making (Pinsky & Mantua, 2014; Boyce et al. 2020b; Duplisea et al. 2020; Boyce et al. 2021). Such approaches can range from using climate risk as a modifier of harvest advice to more detailed quantitative integration of climate variables into the stock assessment process (Holsman et al. 2019; Duplisea et al. 2021). For instance, management strategy evaluations (MSE) can find candidate management strategies that are potentially robust to future climate scenarios, population and ecosystem dynamics and other uncertainties (M. A. Haltuch et al. 2019; Melissa A. Haltuch et al. 2019; Merino et al. 2019), whereas dynamic management can set harvest rates based on climate forecasts or respond in real-time to changing conditions (Dunn et al. 2016). Adaptation resources could also include instituting flexible spatial protections where the stock is particularly at risk (Tittensor et al. 2019), targeted ecosystem monitoring for changes in climate vulnerability, and addressing factors affecting the sensitivity and adaptivity of smooth skate (e.g. reducing directed and ecosystem overfishing, bycatch, habitat destruction, and pollution); (Bryndum-Buchholz et al. 2021). Since high natural mortality in the GSL is also thought to impair species recovery (COSEWIC, 2012), understanding the influence of bycatch on their mortality and reducing any fisheries-induced mortality through bycatch reduction (e.g. targeted gear regulations and/or seasonal fishery closures, protected

areas) could improve the climate adaptivity potential for 4T smooth skate, and species with similar climate risk.

Alternatively, the sole Canadian Atlantic mackerel (*Scomber scombrus*) stock is at moderate climate risk, rendering it a medium priority for climate adaptation. However, because the stock is climate-sensitive, it also has high latent climate risk, meaning it is likely to become at risk, particularly as its exposure increases. Mackerel is in the critical zone of Canada's Precautionary Approach Framework (DFO, 2021) and is of high ecological importance, supporting numerous dependent species, including valuable upper-trophic fisheries (Pikitch et al. 2014). Thus, reducing its latent climate risk would enhance ecosystem resilience. Monitoring the stock's environment for any changes in climate exposure that could push its cumulative climate risk to high or critical could be undertaken, for instance, by tracking species' thermal safety margins over time or its projected year of climate emergence. Additional actions could be taken to reduce the stock's high climate sensitivity, such as developing and prioritizing interventions that minimise abatable stressors (e.g. directed and ecosystem overfishing, bycatch, pollution, habitat or ecosystem disruption) or through fisheries closures or climate-integrated marine spatial planning (Tittensor et al. 2019). For example, in 2022, commercial and bait fisheries for Atlantic Mackerel and spring-spawning Atlantic herring in the southern GSL were placed under a moratorium to allow stocks to recover from decades-long declines and current low abundance. These measures can reduce stress and promote the recovery of these species, serving as one example of interventions to mitigate stressors.

The 12 indices that define CRIB risk can also be helpful. For example, the timing of climate emergence from species' thermal niches (Trisos et al. 2020; Xu et al. 2020) can provide a chronology of when a stock will first become exposed to hazardous climate conditions across its management area. While the 4T smooth skate stock is projected to be exposed to a hazardous climate in 32 years (by 2052) on average (range=0-80 yrs.), the ATLSA3-4 Atlantic mackerel stock is not expected to be exposed for another 75 years (by 2095) on average (range: 41-80 yrs.). Such information can aid the proactive development of timelines for implementing adaptation measures before those impacts occur and help assess the pace of climate change on fisheries.

D.2 Conservation and marine spatial planning

The CRIB can also be used to assess climate risk in marine spatial planning. Lewis et al. (2023) used the CRIB to predict the Time of Emergence (ToE) for 30 species in the draft network of conservation areas on the Scotian Shelf–Bay of Fundy. The study revealed a strong latitudinal gradient in climate impacts, with species associated with colder waters experiencing earlier ToEs—especially in more southwesterly areas. With high emissions, 51% of the habitat and up to 42% of the species were projected to be lost.

The study highlighted that the ability of marine protected areas (MPAs) to safeguard biodiversity will likely be undermined by climate change—even with strong mitigation efforts—and that significant impacts are expected within 30 to 50 years. Climate change is expected to reduce the effectiveness of the proposed network of conservation areas and influence conservation priorities for species on the Scotian Shelf, a region projected to warm considerably.

This means planning and managing sites, particularly in the southern region, should integrate climate change adaptation into their design, management, and monitoring. Adaptation strategies could include, for instance, setting flexible conservation goals and objectives that can be revised over time; conducting climate vulnerability or risk assessments to identify how sites might be affected in the future; designing the network to account for climate risks by prioritizing lower-risk sites, areas with high carbon sequestration potential, and locations that are projected to provide future habitat for high-risk species.

Sites expected to undergo rapid shifts in species composition could benefit from flexible boundary design or even a reconfiguration of the network. This is because the current distribution of priority

species may not align with future conditions, potentially reducing long-term conservation effectiveness (Tittensor et al. 2019). Incorporating climate change projections into the planning of conservation areas in the Scotian Shelf–Bay of Fundy Bioregion can help improve network design and make it more resilient—or "future-proofed"—in the face of ongoing environmental change.

In another study, Keen et al. (2024) used the CRIB to assess the climate vulnerability of marine ecosystems within the Canadian Marine Conservation Network (CMCN). Their study found that climate risk representativity across Canada's marine protected area network was highly variable across space. In particular, MPAs with lower climate vulnerability were disproportionately overrepresented in the network. However, the broad-scale geographic targets used in the Scotian Shelf–Bay of Fundy network planning process achieved over 90% representativity of climate vulnerabilities. This highlights the importance of including habitat diversity and broad geographic coverage in conservation planning to build climate resilience—even when climate was not an explicit priority.

The study suggested that prioritizing protection in currently underrepresented, climate-vulnerable regions could strengthen the CMCN's resilience to climate change. Using the CRIB, the study offers practical guidance for Canadian marine conservation practitioners on incorporating climate resilience into planning. Placing greater emphasis on biogeographic representativity—particularly by improving protection for vulnerable coastal and shelf ecosystems- could enhance the effectiveness of the CMCN under climate change. CRIB's vulnerability data can also support site-level design, where areas with higher climate vulnerability could be given stronger protective measures to boost resilience to change.

Appendix E: CRIB-NZ technical workflow

The CRIB-NZ analysis is conceptually and statistically straightforward, yet the workflow is moderately complex due to the multiple input data layers, their volume, and the analysis's hierarchical nature. Figure E1 illustrates the technical workflow for implementing CRIB-NZ for the case study species presented here. Several of the input data layers are pre-processed to format them. Following this, the 12 climate indices are calculated using a separate R script; the exception is 09_E_ToESpecies_NZ.r, which calculates 3 separate exposure indices. R files are named according to the indices they calculate: AC=adaptivity, S=sensitivity, and E=exposure. The 12 indices are saved as separate files (one per index), which are then imported into 11_Comb_indices_NZ.r, where they are combined, standardised, and used to calculate vulnerability and its dimensions. This script also calculates species-level vulnerability. The function of each of the individual R scripts is described below (Statistical computing and R code section) and the files themselves are extensively annotated to enhance reproducibility. The order of operations is specified numerically in the file naming.

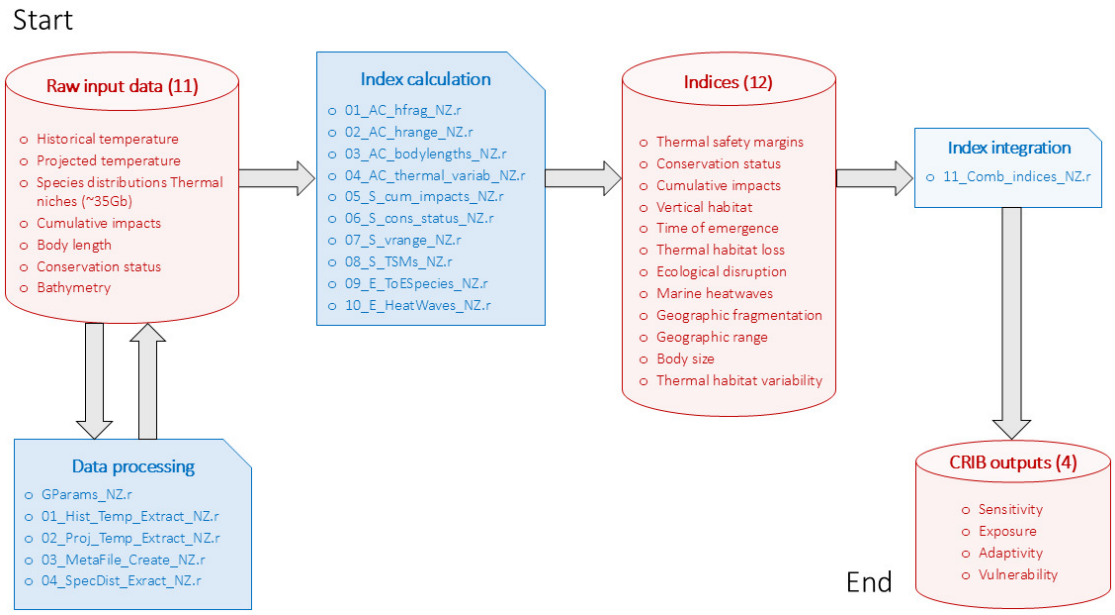


Figure E1: Overview of the CRIB-NZ technical workflow. Red depicts input and output data layers, and blue the R code files used to process them. Arrows show the ordering of the workflow from raw input data to index calculation to the final integration and calculation of the vulnerability outputs.

E.1 Data extractions

E.1.1 AquaX species traits and distributions

Species distribution estimates and associated trait information (thermal niches and vertical habitats) from AquaX were provided by G. Reygondeau. The methodology is described in Reygondeau et al. (2026) and the data therein are available on Figshare (https://doi.org/10.6084/m9.figshare.30754358). The code used to generate the AquaX ensemble habitat suitability projections can be requested directly through the AquaMaps website (https://www.aquamaps.org) in accordance with their data-use and code-access policies. For each species, the current geographic distributions were imported into R, converted to binary presence-absence values using the empirical threshold values, harmonised to a global 0.08° grid, and clipped to the New Zealand EEZ; distributions for all species inhabiting the EEZ were then exported as individual TIFF files and consolidated into a 3D raster object.

E.1.2 GLORYs temperature data

Monthly temperature estimates for the surface and bottom between 1992 and 2025 were extracted from GLORYS on a global 0.083° grid using the Copernicus Marine Toolbox in Python[7]. These data were then imported into R, and for each time step, surface and bottom temperature values were extracted over New Zealand's EEZ. For thermal safety margin calculations, the maximum daily temperature in each grid cell over the past decade (2015–2025) was computed separately for surface and bottom temperatures. For thermal variability calculations, we computed the frequency of temperature occurrences in each 0.2 °C temperature bin between -3° and 40°C for each cell, from 1993 to 2025.

[7] Copernicus Marine Toolbox API - Subset | Copernicus Marine Help Center

E.1.3 CMIP 6 temperature projections

Monthly temperature projections under SSP2-4.5 and SSP3-7.0 between 2015 and 2100 were extracted from the Earth System Grid Federation (ESGF) web platform[8] using GNU Wget software[9]. Projections were extracted at 25 km^2 resolution and harmonised to the template 0.08° grid using inverse distance weighting. Sea surface temperatures were extracted using CMIP6 variable ID=tos (CF standard name=sea_surface_temperature). Sea bottom temperatures were extracted using CMIP6 variable ID=thetao (CF standard name=sea_water_potential_temperature). Sea water potential temperatures were downloaded as 3D potential temperature profiles and processed by first calculating the maximum depth at which temperature was estimated, then extracting the potential temperature at that depth.

E.2 Statistical computing and R code

CRIB-NZ is a quantitative workflow implemented in the R statistical computing environment. The case study analyses were conducted in R version 4.5.0 running on a Dell Workstation with 256 GB of RAM, dual-core (2.60 GHz) processors, and 56 logical cores. Much of the R code is optimised for this hardware, but can be adapted to other systems. The output variables produced by the code are described in Table F4. The following R code files are used in the CRIB-NZ case study analyses.

00_GParams_NZ.r: Contains code required across most code files. Loads required set of R packages, defines file paths to input/output data files, and reads a New Zealand candidate species list that is then joined to a metadata table to attach AphiaIDs and drop unmatched species. It loads and cleans a New Zealand EEZ polygon (including a dateline-safe "0–360" version). It defines multiple transformation/standardization functions for vulnerability index components (sensitivity, exposure, adaptivity, etc.) as well as a discount-rate function. Finally, it constructs lookup tables that map internal index variable names to human-readable labels for both standardised and raw metrics.

01_Hist_Temp_Extract_NZ.r: Extracts and formats historical monthly sea surface and bottom temperatures from high-resolution GLORYS ocean reanalysis NetCDF datasets for the New Zealand region at the native 1/12° (~0.08°) spatial resolution. It establishes the New Zealand analysis domain by creating a 0.083° template raster at the scale of the GLORYS temperature data and saving it for regridding other input data layers. For each monthly time step, the workflow reads surface and bottom temperature fields, converts coordinates to a 0–360° longitude system, crops the data to the New Zealand domain, and writes compressed GeoTIFF layers for efficient storage and downstream processing. The script then stacks all monthly rasters, calculates cell-wise maximum temperatures for selected time periods, and exports spatial summaries as both raster products and tabular datasets, each linked to a unique grid-cell identifier. In addition, it computes full temperature-frequency distributions for every grid cell across the historical time series, producing high-resolution histograms of thermal exposure conditions through time. The workflow is heavily optimised for large-data processing using parallel computation, on-disk raster operations, compressed outputs, and high-memory hardware to efficiently manage several hundred gigabytes of global ocean climate data.

02_Proj_Temp_Extract_NZ.r: Extracts and formats projected monthly sea surface and bottom ocean temperatures from multiple CMIP6 and NZESM climate models for the New Zealand region under SSP2-4.5 and SSP3-7.0 climate scenarios. For each model and time step, the workflow reads large NetCDF temperature outputs, identifies bottom temperatures where needed by selecting the deepest valid water layer, converts longitudes to a 0–360° coordinate system, and regrids the data to a common 0.08° spatial template using nearest-neighbour or inverse-distance interpolation. The

[8] ESGF MetaGrid

[9] Wget - GNU Project - Free Software Foundation

resulting rasters are masked to the New Zealand EEZ, written as compressed GeoTIFF files, and then combined into multilayer monthly raster stacks. The script subsequently converts monthly projections into annual maximum-temperature datasets and exports them as compact raster and R data objects for downstream climate vulnerability and exposure analyses. The workflow is highly optimised for large-data processing using extensive parallelization, temporary scratch storage, memory management, and tiled compressed raster outputs to efficiently handle multi-decadal climate projections on high-performance desktop hardware.

03_MetaFile_Create_NZ.r: Creates the primary species metadata database used for the New Zealand AquaX climate vulnerability assessment by integrating thermal niche estimates, species distribution model outputs, taxonomy, habitat classifications, and biological trait information into a unified analytical framework. The workflow imports multiple thermal niche datasets derived from pelagic and seafloor temperature environments, links them to species with valid SDM outputs, retrieves and standardises common names from FishBase, SeaLifeBase, and WoRMS, and classifies species as surface- or bottom-associated based on habitat, taxonomy, and depth-use characteristics. It then selects the most appropriate thermal niche estimates for each species, calculates thermal ranges and representative depth-use metrics, and derives estimates of vertical habitat position relative to the sea surface or seafloor for use in climate exposure analyses. Additional processing identifies strictly bottom-associated taxa using ecological keywords and higher-level taxonomy, corrects problematic metadata values for selected species, and assigns species-specific depth-use rules for benthic, demersal, pelagic, and bathypelagic organisms. The workflow is designed for large-scale marine biodiversity analysis and uses parallelised data import and memory-efficient data.table operations, and standardised spatial templates to efficiently process thousands of marine species and associated environmental datasets.

04_SpecDist_Extract_NZ.r: Extracts and processes AquaX species distribution model (SDM) outputs to generate standardised marine species distribution datasets for the New Zealand region on a common 0.08° spatial grid. For each species with valid SDM predictions, the workflow loads habitat suitability outputs, converts them to binary presence/absence rasters using species-specific thresholds, masks them to the New Zealand EEZ, aligns them to a common template raster, and exports both compressed raster files and flat tabular representations of occupied grid cells. The script then combines thousands of individual species rasters into a multilayer raster stack and merges all species occurrence records into a single cell-by-species database linked to habitat-association and thermal-niche metadata. Additional processing assigns unique spatial cell identifiers, summarises species richness across the region, and filters distributions to species with known vertical habitat associations for downstream climate vulnerability analyses. The workflow is highly optimised for large-scale biodiversity data processing through parallel computation, compressed on-disk raster operations, and memory-efficient flat-file storage, enabling efficient handling of tens of thousands of marine species distributions.

01_AC_hfrag_NZ.r: Calculates habitat fragmentation metrics for marine species distributions across the New Zealand region using high-resolution AquaX species distribution rasters on a common 0.08° grid. For each species, the workflow identifies occupied habitat cells, estimates the total occupied area, delineates spatially connected habitat patches, and quantifies fragmentation characteristics, including the number of fragments, the largest patch index, and the effective number of habitat patches. It then standardises fragmentation relative to occupied area and cell counts to create comparable habitat-fragmentation indicators suitable for adaptive capacity and climate vulnerability analyses. The script combines outputs from all species into a consolidated metadata table linked to species identifiers and common names, and generates exploratory summaries and visualizations of fragmentation patterns. The workflow is optimised for large-scale biodiversity analyses through parallelised raster processing, on-disk storage of species rasters, and memory-efficient spatial calculations, enabling efficient processing of thousands of marine species distributions.

02_AC_hrange_NZ.r: Calculates geographic range-size and latitudinal distribution metrics for marine species occurring within the New Zealand region using high-resolution AquaX species

distribution rasters aligned to a common 0.08° grid. For each species, the workflow estimates the total occupied area in square kilometres, standardises range size relative to the total ocean area within the New Zealand EEZ, and calculates the minimum and maximum latitudes and the overall latitudinal span from occupied grid cells. The script constructs ocean masks from global land polygons, aligns all calculations to a standardised raster framework, and processes thousands of species simultaneously from a multilayer raster stack. The resulting range-size and latitude-span metrics are exported as adaptive-capacity indicators for downstream climate vulnerability analyses. The workflow is optimised for large-scale spatial biodiversity processing using efficient raster-based calculations and standardised geospatial templates.

03_AC_bodylengths_NZ.r: Compiles a species-level maximum body-size database for marine species included in the New Zealand AquaX climate vulnerability analysis by integrating observed and imputed body-length datasets from multiple sources. The workflow imports and combines large-body-size records from the global MOBS database, standardises taxonomy and AphiaID identifiers, averages duplicate body-length records for individual species, and supplements missing values with imputed body-size estimates from Boyce et al. (2022). It then matches body-length data to AquaX species metadata using crosswalk tables linking AphiaIDs and AquaMaps species identifiers, retaining only accepted taxa relevant to the New Zealand analysis. Additional filtering removes duplicate species entries and prioritises directly observed measurements, where available, before constructing a final species-level body-length dataset. The workflow produces a standardised maximum-length database used as an adaptive-capacity trait metric for downstream marine climate vulnerability analyses.

04_AC_thermal_variab_NZ.r: Calculates thermal habitat variability and thermal niche-coverage metrics for marine species across the New Zealand region by combining species-specific thermal tolerance limits with long-term GLORYS ocean temperature-frequency distributions on a 0.08° grid. For each species and occupied grid cell, the workflow evaluates how local environmental temperatures overlap with the species' realised thermal niche, quantifies local thermal variability, and calculates multiple niche-coverage metrics, including temperature-range occupancy, weighted niche breadth, Shannon entropy, and effective thermal-bin occupancy. Separate analyses are conducted for surface- and bottom-associated species using the corresponding GLORYS surface and bottom temperature climatologies, while species distributions and thermal limits are linked via cell-level occurrence databases. The script uses parallel processing to efficiently evaluate thousands of species-by-cell combinations, exporting standardised metrics that describe local thermal habitat suitability, environmental variability, and thermal niche representation for downstream adaptive-capacity and climate-vulnerability analyses. Additional diagnostic routines generate exploratory plots and quality-control summaries to identify species and locations where environmental temperature distributions poorly overlap with estimated species thermal niches.

05_S_cum_impacts_NZ.r: Processes the Halpern et al. cumulative human impacts dataset to generate a standardised Human Impact Index layer aligned to the New Zealand climate-vulnerability analysis grid. The workflow imports the global cumulative human impacts raster, converts it to a consistent WGS84 geographic coordinate system and 0–360° longitude framework, crops the data to the New Zealand region, and resamples it to the project's common 0.08° spatial template using area-weighted averaging. It then converts the raster to a tabular format with associated longitude, latitude, and unique grid-cell identifiers for integration with species-level vulnerability datasets. The resulting Human Impact Index values provide a spatially explicit measure of anthropogenic pressure used in downstream sensitivity and climate-risk analyses. The workflow is optimised for efficient large-scale spatial processing using terra-based raster operations and standardised geospatial templates shared across the broader New Zealand climate-vulnerability framework.

06_S_cons_status_NZ.r: Creates a spatially explicit fisheries stock-status sensitivity layer for New Zealand marine species by integrating fisheries stock-assessment data, quota management area (QMA) polygons, species taxonomy, and species distribution datasets. The workflow cleans and

standardises fisheries stock-status tables from the New Zealand Ministry for Primary Industries, resolves inconsistencies in stock-area and species naming conventions, links common names to accepted scientific names and AphiaIDs, and assigns overfishing likelihood categories to individual fish stocks. It then converts stock-management polygons into raster layers aligned to the project's 0.08° GLORYS-based analysis grid, producing spatially explicit stock-status surfaces for each managed stock across the New Zealand EEZ. These stock-level overfishing estimates are merged with species distribution data to generate species-by-cell sensitivity metrics representing local fisheries pressure and stock depletion risk. The workflow combines extensive spatial raster processing, polygon rasterization, taxonomy harmonization, and cell-level joins to efficiently integrate fisheries management information into the broader marine climate vulnerability assessment framework.

07_S_vrange_NZ.r: Calculates vertical habitat and depth-related sensitivity metrics for marine species across the New Zealand region by integrating species distribution data, species-specific depth limits, habitat classifications, and high-resolution GLORYS bathymetry on a common 0.08° analysis grid. The workflow extracts and formats bathymetry from Copernicus GLORYS static fields, links local seafloor depth to each occupied species grid cell, and estimates species-specific vertical positioning metrics, such as minimum depth occupancy, maximum vertical extent, and realised vertical habitat range, relative to either the sea surface or the seafloor. Different calculation rules are applied for pelagic, benthic, demersal, reef-associated, bathypelagic, and sessile organisms to account for differences in mobility and habitat association, while all depth estimates are constrained by local bathymetry. The script also develops standardised transformation functions describing how vertical habitat depth and vertical range contribute to species sensitivity and adaptive capacity under climate change. Additional diagnostic analyses and exploratory plots are used throughout the workflow to identify biologically unrealistic depth relationships, evaluate bathymetric truncation effects, and refine vertical habitat assumptions for thousands of marine species and spatial grid cells.

08_S_TSMs_NZ.r: Calculates thermal safety margins (TSMs) for marine species across the New Zealand region by comparing species-specific upper thermal tolerance limits with recent historical ocean temperatures derived from GLORYS surface and bottom temperature climatologies. The workflow imports AquaX species distribution data and corresponding maximum historical sea surface and bottom temperatures from 2015–2025, then links these environmental temperatures to each occupied species grid cell using a common 0.08° spatial framework. For each species-by-cell combination, it computes the remaining thermal buffer between observed environmental temperatures and the species' upper thermal limit, truncating values to zero where local temperatures already exceed the species' tolerance thresholds. Separate analyses are conducted for surface-associated and bottom-associated species so that pelagic and benthic organisms are evaluated against the most ecologically relevant temperature layer. The resulting thermal safety margin datasets provide spatially explicit measures of present-day thermal sensitivity and exposure for downstream climate vulnerability analyses.

09_E_ToESpecies_NZ.r: Calculates species-level and ecosystem-level climate exposure metrics based on the projected time of emergence (ToE) of ocean temperatures beyond species-specific thermal tolerance limits across the New Zealand region. The workflow combines AquaX species distributions and thermal maxima with annual maximum sea surface and bottom temperature projections from multiple CMIP6 climate models and emissions scenarios, then identifies the first year in which local temperatures exceed each species' upper thermal limit for consecutive years within occupied grid cells. For each species and climate model, the script estimates projected native-range loss over time and calculates ecosystem-level species-loss metrics that represent the proportion of species projected to experience thermal exceedance in each spatial grid cell. Separate analyses are conducted for surface-associated and bottom-associated species using ecologically appropriate surface and bottom temperature projections under SSP2-4.5 and SSP3-7.0 climate scenarios. The workflow is heavily parallelised across species and climate models using distributed processing and memory-efficient list-based operations to efficiently analyze thousands of species distributions and multi-decadal ocean climate projections on a high-resolution 0.08° spatial grid.

10_E_HeatWaves_NZ.r: Calculates marine heatwave exposure metrics for marine species across New Zealand by comparing projected monthly ocean temperatures with species-specific upper thermal tolerance limits within occupied habitat cells. The workflow combines AquaX species distributions and thermal niche estimates with monthly sea surface and bottom temperature projections from multiple climate models and emissions scenarios, then identifies the proportion of months in which local temperatures exceed each species' thermal maximum. For each species-by-cell combination, it estimates both marine heatwave duration (frequency of exceedance) and heatwave magnitude (severity of thermal exceedance, scaled relative to the species' thermal niche width), separately for surface-associated and bottom-associated organisms. Results from multiple climate projections are averaged to produce spatially explicit exposure metrics that describe chronic thermal stress and extreme-warming risk across species ranges on a common 0.08° analysis grid. The workflow is heavily optimised for large-scale climate exposure analysis using parallelised species-level computations, memory-efficient raster-to-matrix processing, and multi-model aggregation to efficiently evaluate thousands of marine species under future ocean warming scenarios.

11_Comb_indices_NZ: Combines all standardised adaptive-capacity, sensitivity, and exposure indicators into final spatially explicit climate-vulnerability indices for marine species across the New Zealand region under multiple climate-change scenarios. The workflow imports and joins species distributions with a large suite of environmental, ecological, and fisheries-related metrics—including thermal safety margins, marine heatwave exposure, time-of-emergence projections, habitat fragmentation, body size, human impacts, stock status, and projected ecosystem change—using a common 0.08° analysis grid. It then applies custom transformation functions to standardise all component indicators onto comparable scales, calculates dimension-level adaptive capacity, sensitivity, and exposure scores with associated uncertainty estimates, and derives multiple vulnerability metrics, including discounted, weighted, and unweighted vulnerability indices. Additional processing incorporates uncertainty-weighted averaging using inverse coefficients of variation, quantifies missing-data completeness across species ranges, and combines outputs across SSP2-4.5 and SSP3-7.0 climate scenarios into a final formatted vulnerability database linked to species taxonomy and common names. The workflow is highly optimised for large-scale biodiversity and climate-risk analysis using memory-efficient data.table joins, parallelised preprocessing routines, standardised spatial templates, and modular integration of thousands of species-level and cell-level climate exposure metrics.

Appendix F: Supplementary Tables

Table F1: Indices used in the CRIB framework (Boyce et al. 2022, 2024)**.**

Index	Description	Data	Rationale	References
Sensitivity (S)				
Thermal safety margin	The difference between the maximum environmental temperature and the species' upper temperature tolerance.	AquaMaps, Reynolds daily OISST	Species inhabiting waters at their upper thermal limits are more vulnerable to further warming. The thermal safety margin has been extensively used in climate vulnerability assessments to measure species sensitivity and tolerance to further warming.	(Deutsch et al. 2008; Sunday et al. 2012; Sunday et al. 2014; Pearson et al. 2014; Stuart-Smith et al. 2015; Comte and Olden, 2017; Walters et al. 2018; Vinagre et al. 2019; Gallagher et al. 2019; Pinsky et al. 2019, 2021; Dahlke et al. 2020; Payne et al. 2021; Molina et al. 2025; Storm, 2025)
Conservation status	Assessed species extinction risk (categorical).	IUCN Red List status	Climate effects on species can be more severe when species are or have been impacted by additional stressors (e.g. fishing, pollution, and nutrient loading) and are at low conservation status.	(Ohlemüller et al. 2008; IUCN, 2012; Berry et al. 2013; Pearson et al. 2014; KEITH et al. 2014; Stanton et al. 2015; Morrison et al. 2016; Hare et al. 2016; Foden et al. 2019; Bateman et al. 2020; McClure et al. 2023; Craig et al. 2025; Frawley et al. 2025; Lettrich et al. 2025)
Cumulative impacts	Multivariate index of human impacts.	Human impact index	Species exposed to multiple impacts are more sensitive to additional stressors, tipping points, and synergistic impacts.	(Worm et al. 2002, 2006; Worm & Duffy, 2003; Ottersen et al. 2006; Crain et al. 2008; Darling & Côté 2008; Halpern et al. 2008, 2012, 2015; Carilli et al. 2009; Ban et al. 2010; Stelzenmüller et al. 2010; Maxwell et al. 2013; Kroeker et al. 2013; Le Bris et al. 2018; Rogers-Bennett & Catton, 2019; Sumaila & Tai, 2020; Butt et al. 2022; Gove et al. 2023)
Vertical habitat variability and use	A bivariate function of maximum depth of occupancy and vertical range of species.	AquaMaps FishBase SeaLifeBase	Habitat generalist species are more adapted to climate variability and change than are specialist species due to their ability to occupy a greater variety of habitats. Species inhabiting the upper ocean and having narrow vertical habitat ranges are more sensitive to upper-ocean warming.	(Peters, 1985; Natori et al. 2006; Laidre et al. 2008; Rosset & Oertli, 2011; Guest et al. 2012; Garcia et al. 2014; Spencer et al. 2019; Firth et al. 2021; Lettrich et al. 2023; McClure et al. 2023; Moll et al. 2024)

Index	Description	Data	Rationale	References
Adaptivity (AC)				
Geographic range extent	A bivariate function of the global present-day geographic habitat area and the latitude span occupied by the species.	AquaMaps	Broadly distributed species are less susceptible to adverse climate change events over parts of their geographic distributions. Greater opportunity for favourable habitat (e.g. climate refugia) within larger distributions.	(Cheung et al. 2007; Burek et al. 2008; Laidre et al. 2008; Ohlemüller et al. 2008; Ficetola & Denoel, 2009; Davidson et al. 2012; Gonzalez-Suarez, Gomez and Revilla, 2013; Pearson et al. 2014; Dickinson et al. 2014; Garcia et al. 2014; Runge et al. 2015; Ofori et al. 2017; Ducatez & Shine, 2017; Chichorro et al. 2019; Albouy et al. 2020; Staude et al. 2020; Chase et al. 2020)
Geographic habitat fragmentation	The proportion of species native geographic distribution that is fragmented.	AquaMaps	Species with less fragmented habitat ranges have greater access to potentially favourable habitats (e.g. climate refugia), migration corridors, and larval dispersal. Consequently, studies in terrestrial and marine systems have reported that species with fragmented geographic ranges are more sensitive to and less resilient to climate change impacts	(Brown & Kodric-Brown, 1977; Lehtinen et al. 1999; Warren et al. 2001; Fahrig, 2002; Kaschner et al. 2006; Moore & Huntington, 2008; Rueda et al. 2013; Gonzalez-Suarez, Gomez and Revilla, 2013; Pearson et al. 2014; MacLean & Beissinger, 2017; Crooks et al. 2017; Rogan & Lacher, 2018; Rogers et al. 2018; Albouy et al. 2020; Brauer & Beheregaray, 2020; Palmeirim et al. 2020; Chase et al. 2020; Fordham, 2024)
Maximum body length	The maximum body length reached globally.	FishBase SeaLifeBase	The maximum size is a predictor of several life-history traits (e.g. generation length, time to maturity, intrinsic rate of population increase) that cumulatively define a species' potential reproductive capacity and population growth rate. The maximum size (length or mass) reached by species has been commonly used as a proxy of extinction risks and vulnerability of species to climate change. Smaller species that tend to be r-selected are viewed as more resilient than larger, K-selected ones.	(Fenchel, 1974; Blueweiss et al. 1978; Cheung et al. 2007; Davidson et al. 2012; Gonzalez-Suarez, Gomez and Revilla, 2013; Chessman, 2013; Cheung et al. 2013; Healy et al. 2014; Pearson et al. 2014; Dulvy et al. 2014; Ripple et al. 2017; Cheung & Oyinlola, 2018; Foden et al. 2019; Donner & Carilli, 2019; Albouy et al. 2020; Kuo et al. 2022; Bak et al. 2023; Fordham, 2024)
Thermal habitat variability and use	A bivariate function of the fraction of total historical temperature habitat within the species recorded thermal preference and the total temperature	Reynolds daily OISST	Species inhabiting more variable thermal environments, such as at the range-edges of their geographic distributions, are thought to have a greater capacity to adapt to climate change and are believed to be less sensitive to it	(Morley et al. 2009; Sunday et al. 2011; Carilli et al. 2012; Guest et al. 2012; Cole et al. 2014; Mora et al. 2014; Rehm et al. 2015; Xu et al. 2016; Shah et al. 2017; Nadeau et al. 2017; Safaie et

Index	Description	Data	Rationale	References
	range experienced by the species across its global present-day geographic range.			al. 2018; Donner & Carilli, 2019; Albouy et al. 2020; Bennett et al. 2021)
Exposure (E)				
Projected climate velocity	The ratio of projected temporal and spatial change in thermal isotherms within the species geographic distribution.	CMIP6 monthly SST	The velocity of climate change (VoCC) represents climatic isotherms' geographic movement over time and is a widely used measure of climate exposure	(Loarie et al. 2009; Burrows et al. 2011; IPCC, 2014; Garciá Molinos et al. 2016; Brito-Morales et al. 2018, 2020; Li et al. 2018; English et al. 2022)
Projected ecosystem disruption	For each grid cell across the focal species' native geographic distribution, the proportion of all species projected to exceed their thermal tolerances.	CMIP6 monthly SST	Individual species will be impacted by climate-driven ecosystem restructuring via altered predation, prey availability, and competition.	(Frank et al. 2006; Frank et al. 2018; Cardinale et al. 2012; Boyce et al. 2015; Boyce et al. 2015a; Martin & Watson, 2016; Hillebrand et al. 2018; du Pontavice et al. 2020; Trisos et al. 2020; Irvine et al. 2025)
Projected time of climate emergence from species' thermal niche	The year when the projected temperature first exceeds the thermal tolerance of the focal species for at least three years in a row.	AquaMaps CMIP6 monthly SST	The timing of climate emergence from pre-industrial temperature variability has been widely used as a proxy for the timing of climate change. The time of climate emergence from a species' thermal tolerance range has recently been developed as an index of when a species is exposed to dangerous climate conditions.	(Mora, Frazier, et al. 2013; Henson et al. 2017; Bruno et al. 2018; Turk et al. 2019; Xu et al. 2020; Trisos et al. 2020; Jenouvrier et al. 2022; Lewis et al. 2023; Pigot et al. 2023; Meyer et al. 2024; Barrier et al. 2025)
Projected loss of suitable thermal habitat	For each focal species, the proportion of its native geographic distribution is lost due to projected climate change.	AquaMaps CMIP6 monthly SST	Species that are projected to lose more of their thermal habitat are more vulnerable.	(Cheung et al. 2009, 2015; Pinsky et al. 2013; Hazen et al. 2013; Shackell et al. 2014; MacKenzie et al. 2014; Ochoa-Quintero et al. 2015; Pacifici et al. 2015; Stortini et al. 2015; Davies et al. 2017; Foden et al. 2019; McHenry et al. 2019; Lavender et al. 2021; Reddin et al. 2022; Hodapp et al. 2023; Meyer et al. 2024)

Table F2: Data sources used in the global CRIB run (Boyce et al. 2022)**.**

Variable	Type	Source	Temporal	Spatial	References
Species native geographic distribution	Taxonomic, spatial	AquaMaps	2000-2014	0.5°	(Kaschner et al. 2019)
Conservation status	Taxonomic	IUCN Red List	-	-	(IUCN, 2021)
Vertical habitat variability and use	Taxonomic	FishBase, SeaLifeBase, AquaMaps	-	-	(Froese & Pauly, 2000; Kaschner et al. 2019; Palomares & Pauly, 2022)
Maximum body length	Taxonomic	FishBase, SeaLifeBase	-	-	(Froese & Pauly, 2000; Palomares & Pauly, 2022)
Thermal niche	Taxonomic	AquaMaps	2000-2014	-	(Kaschner et al. 2019)
Species taxonomy	Taxonomic	World Register of Marine Species	-	-	(WoRMS Editorial Board 2020)
Cumulative impacts	Spatial	Cumulative human impact index	-	1km^2	(Halpern et al. 2008, 2012, 2015)
Bathymetry	Spatial	General Bathymetric Chart of the Oceans (GEBCO)	-	4km^2	(*Gebco gridded global bathymetry data*, 2009)
Sea surface temperature	Spatiotemporal	NOAA daily Optimum Interpolation Sea Surface Temperature dataset	1981-2020	0.25°	(Reynolds et al. 2007)
Projected sea surface temperature	Spatiotemporal	Coupled Model Intercomparison Project Phase 6 (CMIP6)	1850-2100	1°	(Eyring et al. 2016)

Table F3: Thresholds used to define climate risk categories.

Index	Tlow	Tmed	Thigh	Rationale	References
Sensitivity					
Thermal safety margin	5°C	2°C	1°C	Guided by warming rates. 1°C and 2°C compare to the rates of Warming over the past 50 and 100 years, respectively(Boyce et al. 2010). 5° to projected warming (Gattuso et al. 2015).	(Boyce et al. 2010; Gattuso et al. 2015; Stuart-Smith et al. 2015; Gallagher et al. 2019; Pinsky et al. 2019)
Conservation status	LC	LC	V, E, CR	Defined by the IUCN RedList categories and criteria(IUCN, 2021): any category at or above 'vulnerable' is considered at high risk.	(IUCN, 2021)
Cumulative impacts	0.6	1.4	2	Guided by (Halpern et al. 2008).	(Halpern et al. 2008; Butt et al. 2022)
Vertical habitat variability and use					
Maximum depth	200m	50m	20m	Standard pelagic biogeochemical divisions within the euphotic zone categorise variation, e.g. mixing, nutrients, photosynthetically active radiation, and primary production.	(Hare et al. 2016; Morrison et al. 2016; Pinnegar et al. 2019)
Vertical range	200m	50m	20m	Standard biogeochemical divisions within the euphotic zone are used to categorise variation, e.g. mixing, nutrients, photosynthetically active radiation, and primary production.	(Hare et al. 2016; Morrison et al. 2016; Pinnegar et al. 2019)
Exposure					
Projected climate velocity	6km yr^{-1}	15km yr^{-1}	30km yr^{-1}	Guided by the quantiles of the statistical distribution.	(Loarie et al. 2009; Burrows et al. 2011; Carroll et al. 2015)

Index	Tlow	Tmed	Thigh	Rationale	References
Projected time of climate emergence from the thermal niche	75yrs	50yrs	25yrs	Guided by the IUCN RedList assessment criteria(IUCN, 2021).	(Trisos et al. 2020; IUCN, 2021)
Projected loss of suitable thermal habitat	5%	10%	20%	Guided by (Homan et al. 2004; Lange et al. 2010; Swift & Hannon, 2010; Yin et al. 2017; Arroyo-Rodríguez et al. 2020).	(Parker & Mac Nally, 2002; Homan et al. 2004; Lange et al. 2010; Rompre et al. 2010; Swift & Hannon, 2010; Liao et al. 2013; Ochoa-Quintero et al. 2015; Yin et al. 2017; Arroyo-Rodríguez et al. 2020; Shennan-Farpón et al. 2021).
Projected ecosystem disruption	5%	10%	20%	Guided by thresholds in (Hooper et al. 2012; Newbold et al. 2016; Trisos et al. 2020).	(Scholes & Biggs, 2005; Hooper et al. 2012; Newbold et al. 2016; Oliver, 2016; Chase et al. 2020; Trisos et al. 2020; Shennan-Farpón et al. 2021)
Adaptivity					
Geographic range extent					
Latitude span	20°	45°	60°	Based on oceanographic and ecological domains that vary by latitude and are defined by biogeographic patterns in e.g. seasonality, ocean circulation, and climate (Mann & Lazier, 1991; Longhurst, 2007; Boyce et al. 2017)	(Mann & Lazier, 1991; Longhurst, 2007; Rompre et al. 2010; Boyce et al. 2017)
Total geographic area	0.04%	1%	4%	Referenced to the size spectrum of large marine ecosystems (Frye, 1986).	(Frye, 1986; Parker & Mac Nally, 2002; Homan et al. 2004; Rompre et al. 2010; Swift & Hannon, 2010; Liao et al. 2013; Yin et al. 2017; Arroyo-Rodríguez et al. 2020; Chase et al. 2020; Staude et al. 2020)
Geographic habitat	20%	10%	1%	Guided by and comparable to those defined in (Albouy et al.	(Andren, 1994; Hill & Caswell, 1999; Fahrig, 2002; Parker &

Index	Tlow	Tmed	Thigh	Rationale	References
fragmentation				2020) for the vulnerability of cetaceans.	Mac Nally, 2002; Lange et al. 2010; Rompre et al. 2010; Rueda et al. 2013; Albouy et al. 2020; Arroyo-Rodríguez et al. 2020; Chase et al. 2020)
Maximum body length	100cm	30cm	10cm	Empirically guided by the relationship with the intrinsic rate of population increase.	(Fenchel, 1974; Blueweiss et al. 1978; Ripple et al. 2017)
Thermal habitat variability and use					
Thermal habitat occupancy	8%	95%	99%	Guided by the quantiles of the statistical distributions	(Carilli et al. 2012; Donner & Carilli, 2019)
Thermal habitat variability	5°C	10°C	15°C	Comparable to those defined in (Albouy et al. 2020) for the vulnerability of cetaceans.	(Carilli et al. 2012; Guest et al. 2012; Xu et al. 2016; Nadeau et al. 2017; Donner & Carilli 2019; Albouy et al. 2020)

Table F4: Output variables produced in the CRIB-NZ framework for the case study species.

Variable	Type	Units	Description
aphiaid	Character	None	WoRMS AphiaID uniquely identifying the marine species.
CRIBthab	Integer	0=surface-associated; 1=bottom-associated	Habitat classification used to determine whether climate indices are calculated from sea-surface or bottom temperatures.
cell	Integer	Grid cell ID	Unique identifier for the 0.083° spatial grid cell.
lon	Numeric	Decimal degrees (°E)	Longitude of the grid cell centroid.
lat	Numeric	Decimal degrees (°N)	Latitude of the grid cell centroid.
sens.sd	Numeric	Standardised score	Standard deviation among the four sensitivity indices, representing variability among sensitivity indicators.
expo.sd	Numeric	Standardised score	Standard deviation among the four exposure indices, representing variability among exposure indicators.
adcap.sd	Numeric	Standardised score	Standard deviation among the four adaptive capacity indices, representing variability among adaptive capacity indicators.
S.HII	Numeric	Standardised index (0–1)	Anthropogenic stressor index derived from the cumulative human impact index. Higher values indicate greater human pressures and greater climate sensitivity.
S.rlstatus	Numeric	Standardised index (0–1)	Conservation or stock-status index based on Fisheries New Zealand estimates of overfishing risk. Higher values indicate poorer conservation status and greater climate sensitivity.
S.TSMr	Numeric	Standardised index (0–1)	Thermal Safety Margin index measuring proximity to the species' upper thermal tolerance. Higher values indicate smaller safety margins and greater climate sensitivity.
S.vind	Numeric	Standardised index (0–1)	Vertical habitat use index describing the degree to which species occupy thermally variable surface waters. Higher values indicate greater climate sensitivity.
E.nrchng	Numeric	Standardised index (0–1)	Ecosystem disruption index describing projected changes in thermal habitat composition. Higher values indicate greater climate exposure.
E.plost	Numeric	Standardised index (0–1)	Thermal habitat loss index representing the projected loss of suitable thermal habitat. Higher values indicate greater exposure.
E.mhw	Numeric	Standardised index (0–1)	Marine heatwave index describing projected duration and intensity of marine heatwaves. Higher values indicate greater exposure.
E.toe	Numeric	Standardised index (0–1)	Time of emergence index describing when climate change exceeds historical natural variability. Higher values indicate earlier emergence and greater exposure.
AC.hrange	Numeric	Standardised index (0–1)	Geographic range extent index. Higher values indicate larger geographic ranges and greater adaptive capacity.
AC.hfrag	Numeric	Standardised index (0–1)	Habitat fragmentation index describing the continuity of occupied habitat. Higher values indicate less fragmented habitat and greater adaptive capacity.
AC.lmax	Numeric	Standardised index (0–1)	Maximum body length index used as a proxy for life-history characteristics influencing adaptive capacity. Higher values indicate greater adaptive capacity.

Variable	Type	Units	Description
AC.tvar	Numeric	Standardised index (0–1)	Thermal habitat variability index describing the range of temperatures naturally experienced by the species. Higher values indicate greater adaptive capacity.
sens	Numeric	Standardised score (0–1)	Mean of the four standardised sensitivity indices. Higher values indicate greater climate sensitivity.
expo	Numeric	Standardised score (0–1)	Mean of the four standardised exposure indices. Higher values indicate greater climate exposure.
adcap	Numeric	Standardised score (0–1)	Mean of the four standardised adaptive capacity indices. Higher values indicate greater adaptive capacity (lower vulnerability).
vuln.uw	Numeric	Standardised score (0–1)	Unweighted climate vulnerability score calculated as the arithmetic mean of sensitivity, exposure, and reversed adaptive capacity. Higher values indicate greater climate vulnerability.
vulnsd.uw	Numeric	Standardised score	Standard deviation among the three vulnerability dimensions used to calculate the unweighted vulnerability score.
vuln.w	Numeric	Standardised score (0–1)	Weighted climate vulnerability score in which dimensions with lower relative uncertainty receive greater weight. Higher values indicate greater climate vulnerability.
vulnsd.w	Numeric	Standardised score	Weighted standard deviation among the three vulnerability dimensions, representing uncertainty in the weighted vulnerability estimate.
ssp	Character	SSP scenario	Shared Socioeconomic Pathway climate scenario used to generate future climate projections (e.g. SSP2-4.5, SSP5-8.5).
cname	Character	None	Common name of the species.